PhD degree in Molecular Medicine

European School of Molecular Medicine (SEMM),

University of Milan and University of Naples "Federico II"

Faculty of Medicine

Settore disciplinare: BIO/11

Terminating Replication at *TER*s at Eukaryotic Chromosomes

Joanna Niska

IFOM-IEO Campus, Milan

Matricola n. R08903

Supervisor: Prof. Marco Foiani

IFOM-IEO Campus, Milan

Anno accademico 2012-2013

Table of contents:

Page:

1 Acknowledgments

The writing of this dissertation has been one of the most significant academic challenges I have ever had to face. I would like to express my sincere gratitude to my supervisor, **Prof. Marco Foiani**, for the contagious passion, being an example of the greatest attitude toward science, caring, having faith in me and providing a wonderful atmosphere for doing research.

I would never have been able to finish my dissertation without the guidance of my committee members. I would like to thank **Dr. Dana Branzei** and **Prof. John Rouse** for supervising my work for the past four years.

I would like to thank **Dr. Giordano Liberi** for the bright ideas, always-helpful suggestions, scientific support and being there for me.

I owe special thanks to my admirable lab friends: **Ghadeer Shubassi**, **Chiara Lucca**, **Mong Sing Lai**, **Mery Piña**, **Yathish Achar**, **Elisa Ferrari**, **Marco Fumasoni** and all the **Foiani research group members** for a stimulating and welcoming social environment, laughter, everyday big smiles on their faces and being a monster tower of strength.

I would like to thank my soul mate, **Alan Blakie**, for all his love and encouragement. His quiet patience was undeniably the bedrock in the most intense, AND THE BEST, time of my life.

Above all, I owe a very special word of thanks to my **Wonderful Parents** for their unconditional support, love and understanding.

2 List of Abbreviations

2D-gel Two Dimensional Agarose Gel Electrophoresis

BSA Bovine Serum Albumin

BrdU 5-bromo-2'-deoxyuridine

BPB Bromophenol blue

CTAB cetyltrimethylammonium bromide

DAPI 4',6-diamidino-2-phenylindole

ddH_2O double-distilled H_2O

DMSO Dimethyl Sulfoxide

dsDNA double-stranded DNA

DTT Dithiothreitol

DSB Double Strand Break

EDTA Ethylen Diammino Tetraacetic Acid

Gal Galactose

Glu Glucose

G418 Geneticin

GIP Genomic ImmunoPrecipitation

HR Homologous Recombination

HU Hydroxyurea

IP ImmunoPrecipitation

kDa kiloDalton

MOPS 3-morpholinopropane-1-sulfonic acid

mRNA messenger RNA

O/N Overnight

ORF Open Reading Frame

PEG Polyethylene glycol

rcf relative centrifugal force

rpm revolutions per minute

RNAPII RNA polymerase II

RT Room Temperature

SDS Sodium Dodecyl Sulphate

SDS-PAGE SDS-Poly-Acrylamide Gel Electrophoresis

SSC Saline-Sodium Citrate

ssDNA single-stranded DNA

SUP Supernatant

TBS Tris-buffered saline

TBST TBS + Tween 20 0.1%

TdT Terminal deoxynucleotidyl transferase

TE Tris-EDTA

TER Termination zone

Triton X-100 polyethylene glycol p-(1,1,3,3-tetramethylbutyl)-phenyl ether

Tween 20 Polyoxyethylene (20) sorbitan monolaurate

YNB Yeast Nitrogen Base

YPD (YEPD) Yeast Extract Peptone Dextrose

YPG (YEPG) Yeast Extract Peptone Galactose

3 Figures Index

Page:

4 Abstract

Faithful transmission of genetic material is challenged by the presence of natural impediments affecting replication fork progression that jeopardize genome integrity. Transcription, which competes with DNA replication for the same template, is a common barrier to replication in both prokaryotes and higher eukaryotes. Multiple mechanisms minimize the consequences of DNA replication and transcription collisions in order to prevent torsional stress accumulation that occurs when replication fork encounters the transcription machinery. Defects in resolving topological problems during chromosome replication lead to fork reversal, R loop formation and recombination-induced genome rearrangements. Our interest is focused on the processes that coordinate replication with transcription at *TER*s (termination sites) and on the molecular pathways involved in termination of DNA replication. We investigated the roles of Rrm3, a DNA helicase that assists replication fork progression, and of Sen1, a DNA/RNA helicase that resolves the conflicts between replication and transcription. We found that Rrm3 and Sen1 mediate replication termination at specific *TER*s, preventing aberrant events ultimately leading to chromosome fragility. Our results contribute to the elucidation of mechanisms coordinating replication and transcription at *TER* zones in eukaryotes.

5 Introduction

5.1 DNA replication challenging genome integrity

DNA replication is an essential process that needs to occur accurately, rapidly and only once during the cell cycle. Thus, faithful transmission of genetic material is crucial to maintain genome stability. Despite well-orchestrated mechanisms preventing mutations and chromosome rearrangements, obstacles that affect replication fork integrity continuously challenge replication fork progression. The enzymatic processes of DNA replication such as leading- and lagging- strand unwinding, template stabilization, daughter strand synthesis and replication fork fusion need to be tightly coordinated. Despite errors that occur during chromosome replication and obstacles, which might destabilize the replisome, chromatin dynamics during S phase affects DNA replication and DNA repair. If the progression of DNA replication fork is impaired, aberrant DNA structures and DNA damage might be generated. Therefore, replication-associated stress is a big contributor to genetic damage and genome instability that leads to tumour formation.

5.1.1 Origin firing and S phase dynamics

Prokaryotes possess only one sequence-specific replication initiation site (Mott and Berger, 2007), from which two replication forks originate and replicate the genome with a speed of 60 kb min^{-1}. In contrary, eukaryotic genome is scattered with numerous replication origins (ORIs). The human genome is 700-

fold bigger than in Prokaryotes but the replication forks progress 20-fold slower (2-3 kb min^{-}1).

ORIs are selected in the G1 phase of the cell cycle by sequential recruitment of the pre-replicative complex (pre-RC). The pre-RC is composed by initiator proteins: origin recognition complex (ORC) (Bell and Stillman, 1992), Cdc6, Cdt1, the MCM complex and Cdc7-Dbf4 (Mechali, 2010). ORC is a six-protein complex, Orc1-6, and all proteins are present in an equal stoichiometry. The complex is conserved throughout evolution but the sequence of all subunits is very different among eukaryotic organisms. The ORC remains bound to the replication origin during the entire cell cycle (Aparicio et al., 1997; Liang and Stillman, 1997). Cyclin-dependent kinases (CDKs) mediate the phosphorylation of the ORC subunits in a cell cycle dependent manner preventing the re-replication of the genetic material during the same cell cycle (Nguyen et al., 2001). Cdc6 is present only during the G1 phase of the cell cycle and its synthesis and degradation is tightly regulated. Cdt1 was first found and characterized in *Schizosaccharomyces pombe* (Hofmann and Beach, 1994) and together with Cdc6 is required for the pre-RC assembly and loading the six MCM proteins onto the chromatin. Cdt1 is a stable protein. In late M and G1 phase is localized in the nucleus, whereas during S and early M phase it displays a cytoplasmic localization (Tanaka and Diffley, 2002). The MCM complex (Mini-Chromosome Maintenance) consists of six proteins, MCM2-7, which are very conserved throughout evolution (Maine et al., 1984). MCM proteins are essential for both initiation and elongation processes in DNA replication. Absence or inactivation of any MCM subunit during G1 phase prevents the entry into S phase. By analogy, MCM protein inactivation during S phase impairs the replication fork progression

(Labib et al., 2000). The MCM proteins can form different complexes. The Mcm4-Mcm6-Mcm7 sub-complex in mammalian cells shows non-processive 3'-5' helicase activity (Ishimi, 1997), suggesting that MCMs could function as replicative helicases. Still it remains elusive how the MCM complex is loaded onto DNA. Several scenarios as the rolling mechanism, the ssDNA embracing and the DNA pumping are considered as potential modes of action of MCM complexes (Mendez and Stillman, 2003). Cdc7 is a protein kinase associated to the chromatin during all the cell cycle (Weinreich and Stillman, 1999) but is active only at the G1-S transition. Its activity depends on the interaction with a regulatory protein, Dbf4, which is transcribed in a cell cycle dependent manner (Jackson et al., 1993) and binds to the chromatin only at the G1-S phase transition and throughout the entire S phase (Weinreich and Stillman, 1999).

It has been shown that 30,000-50,000 of origins are active at each cell cycle, but not all of them are activated at the same time. First genome-wide studies in mammalian cells (Cadoret et al., 2008; Sequeira-Mendes et al., 2009) have argued the correlation between the unmethylated CpG islands, which could be a mark of replication origins, and promoter regions. Transcription levels at replication initiation sites correlate with replication timing and divide ORIs into two classes: those firing in early S phase and associated with moderate/high transcription levels (≥1 RNA copy/cell) mapped to transcription start sites (TSSs) of coding RNAs; and those firing throughout entire S phase and associated with low transcription levels (<1 RNA copy/cell) mapped to TSSs of non-coding RNAs (Dellino et al., 2013).

In fission yeast *Schizosaccharomyces pombe*, replication origins are not determined by a specific sequence but the presence of 384 A+T-rich islands up to

1 kb long (Segurado et al., 2003). The absence of consensus elements in those replication initiation regions indicates that different sequences target the ORC to distinct ORIs.

In *Saccharomyces cerevisiae* the replication origins are well characterized. The budding yeast ORI's were identified by discovering their ability to support the replication of the plasmid. Thus, they were named Autonomously Replicating Sequences (ARS) elements (Hsiao and Carbon, 1979). Each budding yeast replication origin consists of two domains: a short domain A (~11 bp) with an essential DNA sequence recognized and bound by the replication initiation proteins, called the ARC consensus sequence (ACS); and lacking a specific consensus sequence domain B, divided into three variable subdomains: B1, B2 and B3. The B1 subdomain is crucial for binding the replication initiation proteins and when mutated, reduces the origin activity (Bell and Stillman, 1992).

The recent genome-wide studies have confirmed 429 replication origins in *Saccharomyces cerevisiae*, among which 332 are considered as active (Raghuraman et al., 2001; Wyrick et al., 2001). The range of inter-origin space varies between 10 and 200 kb with an average distance between active replication origins of 40 kb. Activation of inactive origins might provide an alternative option to allow completion of DNA replication when forks, initiated at efficiently fired origins, become inactive due to an obstacle encountered ahead (Newlon and Theis, 2002).

In all of the eukaryotic genomes, at each cell cycle, only a subset of replication origins fire. The active origins might be divided into different classes based on their activation time throughout S phase. Those, which become active at the beginning of S phase are called "early", while those that fire at the end are

known as “late”. The inactive origins are considered “dormant”, although they are able to support plasmid replication.

The selection of an active replication origin along the numerous potential ones is regulated by chromatin architecture. Ideally, the replication origin should be positioned in an open chromatin domain, facilitating the preRC assembly. If the origins are located within the heterochromatin region, they become either late or dormant (Ferguson and Fangman, 1992; Stevenson and Gottschling, 1999). Histone acetylation, associated with higher chromatin accessibility, favours origin activation. Mutation of the histone deacetylase (HDAC), Rpd3, induces chromatin hyperacetylation leading to late origins activation (Vogelauer et al., 2002). Origin activity state may change during development, suggesting that the replication initiation sites selection is regulated by epigenetics (Aggarwal and Calvi, 2004). The nuclear envelope can also regulate origin activity by maintaining high level of activators and inhibitors of DNA replication (Walter et al., 1998). Perturbation in nuclear envelope formation blocks replication both in *Xenopus laevis* (Newport, 1987) and *Saccharomyces cerevisiae* (Pasero et al., 1997). Interestingly, studies done in *Xenopus* egg extracts show that both nucleo-cytosolic ratio and nuclear structure play important but different roles in replication initiation regulation. While the number of origins depends on nucleo-cytosolic ratio, changes in nuclei dictate which, among numerous initiation sites, will become an active origin (Dimitrova and Gilbert, 1998).

The selection of replication origins in Eukaryotes involves multiple mechanisms. The choice of active origins must adapt to changes in chromatin structure combined with cell differentiation and development.

5.1.2 DNA synthesis

The successful DNA synthesis is based on the unperturbed progression of a replication fork with its associated replication protein complex. The required replication fork integrity maintenance must coordinate processes advancing replication fork movement across obstacles, stabilizing the replisome and in case of damage, triggering the adequate mechanisms that arrange the replication proteins re-association. Unwinding, replicating and rewinding DNA strands is a challenging task that involve multiple helicases opening the DNA helix ahead of the replication fork. The coordinated activities of helicases expose the unpaired DNA nucleotides, allowing base pairing catalysed by DNA polymerases (Bessman et al., 1958; Lehman et al., 1958). Faithful DNA copying shares conserved features from Prokaryotes to Eukaryotes and is known as semiconservative DNA replication (Meselson and Stahl, 1958).

5.1.2.1 DNA replication initiation

Prior to DNA double helix unwinding, the pre-RC complex is disassembled and replaced by set of proteins initiating DNA synthesis process that form pre-Initiation Complex (pre-IC). The transition between Pre-RC and Pre-IC is mediated by the displacement of Cdc6 and Cdt1, which is followed by the recruitment of replication initiation proteins: Mcm10, Cdc45, Sld3, Dpb11 and GINS.

Mcm10 has been found in the same screen together with MCM2-MCM7 genes in *Saccharomyces cerevisiae*. Mcm10 is tightly associated with the nuclear chromatin and the MCM complex (Merchant et al., 1997). The *mcm10* mutation

impairs replication initiation at the *ARS1* origin and induces the pausing of replication forks coming from the adjacent origins (Homesley et al., 2000). The timing when Mcm10 is recruited and bound to the chromatin differs among organisms. In *Saccharomyces cerevisiae* Mcm10 acts as a pre-RC component and anchors the Mcm2-Mcm7 complex to the replication origin during G1 phase (Homesley et al., 2000). In contrary, in *Xenopus laevis* the Mcm10 recruitment occurs after the MCM complex loading onto DNA.

Cdc45 is essential for cell viability and is required for DNA replication initiation in yeast (Zou et al., 1997). Cdc45 associates with pre-RC in G1 phase and binds to the MCM complex (Aparicio et al., 1997). Its stable association with total chromatin is connected with S-CDKs activation at the G1/S transition (Zou and Stillman, 1998). Cdc45 physically interacts with Mcm2 and serves as a linker between the pre-RC and the pre-IC. The loadings of Cdc45p and DNA Polα onto late origins are inhibited in a Rad53-dependent manner (Aparicio et al., 1999). The association of RPA with late origins is similarly blocked (Tanaka and Nasmyth, 1998).

Throughout the cell cycle in *Saccharomyces cerevisiae*, Cdc45 forms a complex with Sld3 and this interaction is essential for its association with the MCM complex (Kamimura et al., 2001). Sld3-Cdc45 binds to ORIs through Mcm proteins and the complex is crucial for origin unwinding in the initiation step of DNA replication (Kamimura et al., 2001).

Dpb11 suppresses mutations of two essential subunits in DNA polymerase II (ε) in budding yeast. It senses stalled replication forks in S phase and transmits the signals to the checkpoint machinery (Araki et al., 1995).

Another component of the pre-IC is GINS complex, which is composed of four proteins: Psf1, Psf2, Psf3 and Sld5. This multi-protein complex is required during replication initiation and most probably during DNA synthesis (Takayama et al., 2003). GINS complex affects Sld3-Cdc45, Dpb11 and Pol ε binding onto DNA. These proteins assembling occur in a mutually dependent manner to initiate DNA duplex synthesis.

5.1.2.2 Leading- and lagging-DNA strand synthesis

Antiparallel orientation of the leading- and the lagging-strand in DNA duplex challenge highly conserved principles of DNA replication. The DNA template unwinding and polymerization of the daughter strands are the main processes that DNA replication is based on. The enzymes responsible for uncoupling the DNA duplex are helicases, whereas the DNA strand synthesis reaction is carried by DNA replicative polymerases. The DNA unwinding generates ssDNA, which is immediately bound by RPA proteins (Tanaka and Nasmyth, 1998). RPA complex is composed of three subunits: Rfa1, Rfa2 and Rfa3. RPA mediates binding of Dpb11 protein, which is essential for DNA polymerases loading onto DNA. Thus, the coordinated action between DNA helicases and polymerases allows the generation of two copies of the parental genome.

DNA polymerases are highly specialized enzymes that proceed along a single-stranded DNA molecule and recruit free dNTPs to hydrogen bond with their complementary dNTP on the single DNA strand. In Eukaryotes, the main players in the canonical mode of DNA synthesis are five DNA polymerases: α, β,

δ, ε and γ. Polymerase γ is responsible for the mitochondrial DNA synthesis while the others are located in the nucleus and are essential in the nuclear DNA amplification. Because DNA polymerases require a primer from which the DNA synthesis reaction initiates, polymerase α (Pol α) functions as a replicative primase (Fisher et al., 1979) and it is the only eukaryotic polymerase that can start DNA synthesis *de novo*. Pol α is composed of four subunits that create a complex, which is essential in the DNA replication initiation and Okazaki fragments synthesis on the lagging strand of the replication fork. The P180 subunit is required for the polymerase activity, P58 and P48 control the primase activity and the forth B subunit plays an essential role at the early stages of DNA replication (Foiani et al., 1995; Foiani et al., 1997). The primase synthesizes a primer containing a short ~10-nucleotide RNA stretch onto which the DNA polymerase adds 10 to 20 DNA bases (Nethanel et al., 1992). This priming process occurs both during replication initiation of the leading-strand synthesis and at the 5' end of each Okazaki fragment formation on the lagging strand. The RNA stretches priming Okazaki fragments are degraded, and extended DNA segments are linked to form a continuous DNA fragment. The process is called "Okazaki fragments maturation" and is mediated by RPA protein binding, stabilizing DNA:RNA primers and stimulating Dna2 and Fen1 endonuclease activity. By extent of the strand displacement, maturation proceeds by the short or long flap processing pathway. Fen1 and Dna2 degrade initiator RNA in a short and long flap pathway, respectively (Burgers, 2009; Garg et al., 2004).

Although Pol α is indispensable in priming DNA synthesis both on the leading- and the lagging strand, it is not able to continue DNA replication. After polymerase switch, Pol ε completes the leading strand replication. Pol δ generates

Okazaki fragments during lagging-strand synthesis (Nick McElhinny et al., 2008; Pursell et al., 2007).

Replication forks are encircled by specialized clamps, which are called PCNA (Proliferating Cell Nuclear Antigen). PCNA loading does not occur frequently on the leading strand due to continuous DNA replication since its initiation. In contrary, constant initiation of Okazaki fragment synthesis on the lagging strand requires continual PCNA loading. Replication factor C (RF-C) serves as a clamp loader and consists of five subunits forming a stable ATP-dependent complex with PCNA (Tsurimoto and Stillman, 1989, 1990). RF-C recognizes the primer-template junctions, where it loads PCNA. Importantly, when replication must be terminated, clamp loaders unload PCNA from DNA (Yao et al., 2006).

The faithful synthesis of leading- and lagging-strand relies on coordinated action and stable association of DNA polymerases with replication forks. Despite its role in genetic information duplication, DNA synthesis is also needed during DNA repair processes including recombination and lesions-bypass at the damaged DNA site. Thus, the polymerases involved in DNA amplification face the immense task to keep the genome intact.

5.1.3 Genome duplication termination

DNA replication is a well-programmed process that initiates at specific sites, ORIs, and terminates at specialized regions called replication termini (*Ter*), which cause orientation-dependent fork arrest. As a consequence of bi-directionally moving forks, termination processes are spatially dissociated from

the replication initiation. In higher Eukaryotes, DNA replication termination is still poorly understood.

It the simian virus 40 (SV40), the DNA replication termination does not involve a specific nucleotide sequence but it occurs when two replication forks meet (Lai and Nathans, 1975).

In *Escherichia coli* replication termination takes place within specialized complexes in a sequence-specific manner (Neylon et al., 2005). After the unique origin firing, the replication forks move bi-directionally and meet at the replication terminus at a site approximately opposed from the origin. The replication terminus is composed of multiple *Ter* sites, which are recognized and bound by Tus protein that counteracts helicase activity (Coskun-Ari and Hill, 1997). Tus-*Ter* complex arrests the replication fork in an orientation-dependent way (Hill, 1992; Hill et al., 1987). The polarity of replication termination allows the replication fork to pass through the "permissive face" of the DNA-protein terminating complex and blocks it at its "un-permissive face" (Khatri et al., 1989; Lee et al., 1989). The stalled fork is resolved when the other comes from the opposite direction. Interestingly, at the terminus region of *Escherichia coli*, frequent hyperrecombination events occur and involve nucleoid organization and its remodelling after replication (Louarn et al., 1994).

In Eukaryotes, the DNA replication termination is different. Replication fork termination is an event that occurs by fusion of replication forks emanating from the closest fired origins (Edenberg and Huberman, 1975). Along eukaryotic chromosomes numerous replication termination sites are present and ensure the appropriate replication fork convergence. *Schizosaccharomyces pombe* genome contains a genetically programmed replication termination site 1 (*RTS1*) near the

mating-type (*mat1*) locus. The terminating region is involved in mating type switching. The *RTS1* ensures that *mat1* is replicated in the correct direction by optimizing mating-type switching that is a replication-coupled recombination event (Dalgaard and Klar, 1999, 2001). The Pol α gene, Swi7, is required for recombination initiation at the *mat1* locus. Moreover, the Swi1 and Swi3 genes are involved in replication fork arrest at *RTS1* (Dalgaard and Klar, 2000; Krings and Bastia, 2004), which involves several cis-acting sequences and trans-acting proteins (Codlin and Dalgaard, 2003). Interestingly, *RTS1* displays similar features to mammalian rDNA replication fork barriers.

In eukaryotic genomes, there are numerous programmed replication fork barriers (RFBs) that arrest the replication fork in an orientation-dependent manner. Certain barriers prevent the collisions between replication fork and transcribed RNA. One of the best-known RFB is located in the non-transcribed spacer 3' of the 35S ribosomal RNA gene (rDNA) in budding yeast (Linskens and Huberman, 1988). In *Saccharomyces cerevisiae* the rDNA locus on chromosome XII consists of an array of 100-200 repeats, each 9.1 kb in length. The repeats are highly transcribed to produce ribosomes that are essential for translation. An origin of replication (rARS) is present at the non-transcribed spacer 2 (NTS2). Replication initiates from approximately one in five rARS per cell cycle. RFB is present at NTS1 and functions through binding of the non-histone protein Fob1 (Kobayashi and Horiuchi, 1996). The leftward moving from rARS replication fork arrests at RFB in a polar way that is independent from transcription (Brewer et al., 1992).

In *Saccharomyces cerevisiae*, Tof1 and Csm3 proteins, homologs of Swi1 and Swi3 in fission yeast, respectively, contribute in controlling replication termination together with Rrm3 helicase at rDNA (Mohanty et al., 2006). Tof1

and Csm3, together with Fob1, ensure stable fork pausing by counteracting Rrm3 helicase, which displaces Fob1 to facilitate fork progression.

Excluding rDNA regions, recent observations implicate the DNA helicase Rrm3 as an important mediator of replication termination in budding yeast (Fachinetti et al., 2010) that occurs within a zone of 5 kb (Zhu et al., 1992). Rrm3 belongs to Pif1 family helicases and was identified in a screen of genes affecting rDNA recombination (Keil and McWilliams, 1993). Rrm3 is a stable component of the replisome due to its interaction with the catalytic subunit of DNA Polymerase ε, Pol2, the leading strand DNA polymerase (Azvolinsky et al., 2006). Although the deletion of *RRM3* is not lethal, the Rrm3-sensitive sites exhibit increased pausing, aberrant termination intermediates (Fachinetti et al., 2010), spontaneous lesions' accumulation (Torres et al., 2004) and DNA breakage.

In eukaryotes, sequence-specific replication termini are not present within every replication unit. Instead, the termini are found at specialized locations containing replication pausing elements at centromeres, tRNA genes (Pol III) and regions where collision between transcription and DNA replication occurs (Pol II) (Fachinetti et al., 2010). Replication termination is a complex process and the mechanisms that contribute to the appropriate fork fusion are the guardians of genome integrity.

5.2 Cellular roles of DNA topoisomerases

The DNA double helix contorts and supercoils when is unwound by helicases (Schvartzman et al., 2013; Schvartzman and Stasiak, 2004) and various topological constraints act on replicating DNA molecules (Postow et al., 2001).

The replicating DNA generates precatenanes (+), which intertwine the daughter DNA, and positive supercoils ahead of the replication fork. If those structures are not resolved, the physical link between sister chromatids is established that impedes the accurate chromosome segregation during mitosis (Postow et al., 2004).

DNA topoisomerases are specialized enzymes, highly conserved in all Eukaryotes, which alter the DNA topology. Those enzymes tightly control supercoiling, precatenation, catenation and knotting interplay during DNA replication, recombination, transcription and chromosome condensation. (Bermejo et al., 2007; Liu and Wang, 1987; Wang, 1996). Thus, DNA topoisomerases' activity is essential for chromosomal stability and cell survival.

DNA topoisomerases are classified into two categories: type I and type II enzymes. Type I enzymes transiently break DNA strands one at a time, which changes the DNA *Lk* (linking number), a constant that measures number of times two strands of the double helix wind around each other. In contrary, type II enzymes generate nicks in both strands in concert and catalyse the ATP-dependent passage of the intact DNA double helix through another that is transiently broken (Nitiss, 1998). The two types are divided into four subfamilies: IA, IB, IIA and IIB. Despite no sequence homology, topoisomerases of the same subfamily are structurally and functionally similar, while those of different subfamilies do not share neither structural nor mechanistic relation (Champoux, 2001).

Type IA enzymes introduce a transient break in a single-strand DNA region and catalyse the DNA strand passage by forming an 'enzyme-bridge' holding two DNA ends created by the breakage. Type IA topoisomerase (budding

yeast Top3) has an activity toward negatively supercoiled DNA, but not positively supercoiled DNA (Kim and Wang, 1992). The type IB enzymes (budding yeast Top1) relax both positively and negatively supercoiled DNA. The type IB topoisomerase, differently from the type IA, creates a nick in a dsDNA segment (Champoux, 2001).

Type II A enzymes (budding yeast Top2) have the strong capacity to create nicks in both DNA strands and relax the over-wound DNA, positively supercoiled, by reducing the torsional stress. Another subclass of the type II enzymes, called type IIB, was identified in the archaeon *Sulfolobus shibatae* and shares similar catalytic activity with the type IIA enzyme (Bergerat et al., 1994).

The DNA topology alters with the torsional constraints arising during replication and transcription processes that use the same substrate, DNA, as a template. Replication forks and transcription bubbles move along the DNA and accumulate positive supercoils ahead. Both DNA polymerases (DNAPs) and RNA polymerases (RNAPs) are able to rotate along the double helix (Doksani et al., 2009; Harada et al., 2001; Reyes-Lamothe et al., 2008). The rotation along its axis forms precatenanes, which are the intertwinings of replicated chromatids that move the torsional stress backward. The positive supercoils accumulate ahead of both replication fork and transcription machinery and are the substrate for type IB and type II topoisomerases.

The process of fork fusion creates tremendous topological constraints and aberrant torsional stress resolution may challenge chromosome integrity (Wang, 2002). *In vivo* and *in vitro* studies have shown the implication of both types topoisomerases: IB (Top1) and II (Top2) in replication termination (Baxter and Diffley, 2008; Bermejo et al., 2007). The two topoisomerases travel with the

replication forks presumably for precatenanes resolution behind the fork (Top2) and positive supercoiling downstream of the fork (Top1). However, at the very last step of termination the positive supercoils, in between two approaching forks, are not resolved by Top1. Top2 is known to resolve the last DNA helix overwinds, approximately 1 kb in length, allowing the replication to terminate (Fachinetti et al., 2010).

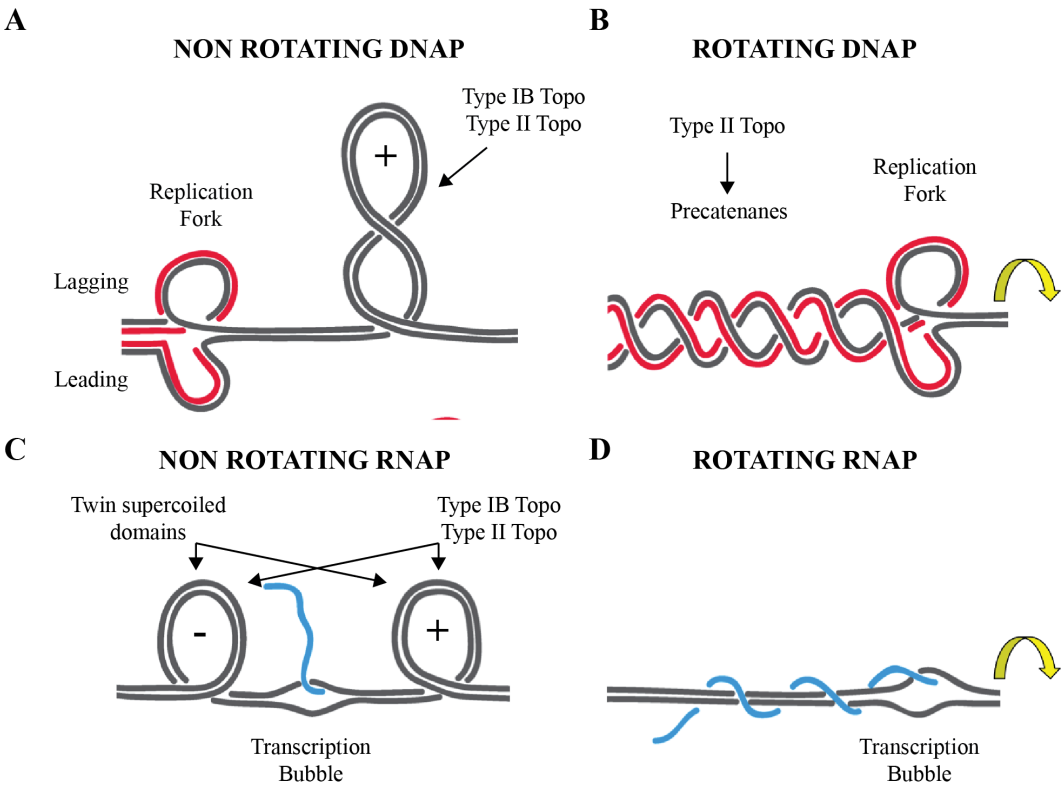

Model 1. The DNA topological transitions resulting from DNAP and RNAP rotations. Adapted from (Bermejo et al., 2012)

(A) When the DNAP machinery does not rotate, DNA helix overwinds ahead of the fork.

(B) When the DNAP rotates, the positive supercoils are redistributed behind the fork and form precatenanes.

(C) Nonrotating RNAP machinery accumulates positive supercoils ahead and negative supercoils behind the transcription bubble, called twin supercoiled domains.
(D) The RNAP rotation results in the nascent RNA entanglement around the double helix behind the transcription bubble.

5.3 Natural impediments to DNA replication

Numerous factors with exogenous, genetic and/or intrinsic origin hinder the replication fork passage along the genome and can jeopardize its integrity.

Exogenous factors interfering with DNA replication are the source of DNA damage and/or nucleotide pools depletion. In the first matter, DNA replication is blocked at the sites of damage caused by, for example, UV light irradiation, DNA-damaging agents or topoisomerase inhibitors. In the second matter, replication fork progression is impaired by the lack of the deoxynucleoside triphosphates (dNTPs) essential for DNA amplification. Hydroxyurea is one of the drugs that affect the dNTPs pool.

Mutations of genes that inhibit replication fork progression by affecting S phase dynamics, the replisome components or factors contributing in nucleotide pool control are a genetic threat that affect the accurate replication of the whole genome.

The integrity of S phase processes is threatened by the intrinsic factors that are the natural impediments to DNA replication. Those hindrances can be classified into five main replication-threatening groups: transcription, recombination and DNA repair, DNA binding proteins, replication slow zones and topologically altered DNA structures.

5.3.1 Transcription

Replication fork and transcription complexes compete for the same template during S phase. The encounters between DNA- and RNA-polymerases result in clashes between those two machineries that strongly affect genome stability. Replicative barriers that are associated with transcription are a common feature both in Prokaryotes and higher Eukaryotes. Multiple mechanisms are developed to minimize the consequences of DNA replication and transcription collisions in order to prevent chromosomal deletions and rearrangements (Vilette et al., 1995) (Gan et al., 2011).

5.3.1.1 Directionality of replication-transcription collisions

Depending on the orientation of the transcribed gene, the replication fork encounters the transcription machinery in either head-on or a codirectional manner. If genes are encoded on the lagging strand, they are transcribed in the opposite direction from leading-strand replication that causes a head-on clash between RNAP and DNAP complexes. In contrast, when genes are encoded on the leading-strand, the direction of transcription is the same as leading-strand replication. Head-on collisions between replication and transcription can be more deleterious than codirectional ones in preserving genome integrity and might generate fork pausing (Liu and Alberts, 1995; Olavarrieta et al., 2002). Transcription generates positive supercoiling ahead of the transcription bubble that creates a topological barrier to the fork movement. Fork restart occurs through the displacement of head-on-oriented RNAP from DNA template. Mfd, which is the transcription-repair coupling factor, promotes direct restart of the

fork (Pomerantz and O'Donnell, 2010). In contrast, the codirectional clashes between replication and transcription barely affect replication fork progression and the replication machinery can use mRNA primer to restart the replication (Kogoma, 1997; Pomerantz and O'Donnell, 2008; Srivatsan et al., 2010).

Prokaryotic genomes have evolved to minimize the frequency of head-on collisions (Brewer, 1988; Rocha, 2004). In *Bacillus subtilis* 75% of genes are transcribed codirectionally with replication (Kunst et al., 1997). Codirectional collisions might be detrimental, if transcription elongation involves extensive backtracking, which is a reversible backward sliding of RNAP along DNA and RNA (Nudler, 2012). Bacteria have evolved several mechanisms to either suppress backtracking or to remove the backtracked complexes. The presence of active ribosomes behind RNAP (Proshkin et al., 2010), the termination induction by Rho and Mfd (Park and Roberts, 2006) and transcript cleavage by GreA and GreB factors (Toulme et al., 2000) suppress DSBs formation as a consequence of codirectional collisions between replication fork and backtracked RNAP. However, the speed of replication fork in bacterial genomes is approximately 20-fold faster than in transcription (~800 nucleotides/s versus 20-50 nucleotides/s). Thus, regardless the transcribed gene orientation, head-on and codirectional collisions are inevitable. In contrary in eukaryotes, the speed of replication fork and transcription machinery is similar, making codirectional collisions unlikely.

5.3.1.2 Gene gating and DNA replication termination

Topological problems arise when the transcription apparatus moves along the DNA template. When it cannot rotate along the helixal axis, positive

supercoiling accumulation ahead the fork is compensated by negative supercoiling behind. Type II topoisomerase, Top2, not only resolves the precatenanes behind the fork but also localizes to *CEN*s in metaphase (Bachant et al., 2002) and to transcribed genes at the beginning of the S phase before replication fork's arrival (Bermejo et al., 2009). Thus, Top2 stabilizes transcription-subordinated chromosomal loops that are anchored to nuclear pores, coupling transcription with the mRNA export (Model 2A). Those two coupled processes are known as gene gating and presumably prevent the annealing of newly synthesized mRNA transcript into the negative supercoiling behind the transcription machinery (Bermejo et al., 2011). Top2 together with Hmo1, which belongs to high mobility group (HMG) proteins that modulate chromatin structure and transcription of certain RNAP transcribed genes (Thomas and Travers, 2001), act at the base of the DNA loops. Both proteins stabilize the chromosomal loop that modulates the chromosomal S phase architecture suppressing chromosome fragility.

When replication fork approaches the region where gated loop has been established, the chromatin architecture ahead the fork needs to be simplified in order to enable replication to be continued. The topological complexity of replication-gene gating domain activates Mec1/ATR that phosphorylates Mlp1, which is the inner basket protein of the nuclear pore. As a consequence of checkpoint activation, the chromosomal loop is dismantled and replication fork can continue its passage along DNA (Bermejo et al., 2011) (Model 2B).

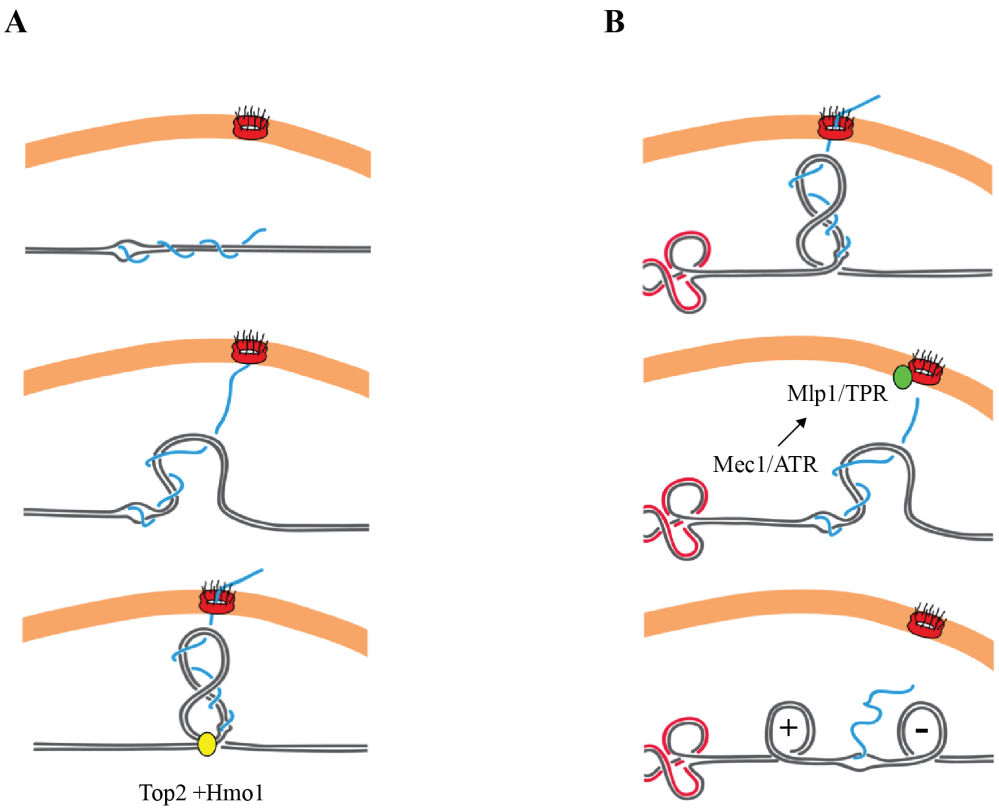

Model 2. S phase transcription coupled with gene gating.

Gene loops are formed through association of promoter and terminator regions. As RNAP initiates transcription, the nascent RNA chain rotates around the DNA template. Replication fork is depicted in red while nascent RNA in blue. Positive and negative supercoils are indicated by '+' and '-', respectively. Adapted and modified from (Bermejo et al., 2012).

(A) Gating-induced loop formation. When nascent RNA becomes longer, it intertwines with the DNA template and the chromatin is brought into contact with nuclear pore complex (NPC). Top2 and Hmo1 proteins control the integrity of the loop by binding at its base.

(B) Mec1/ATR counteracts gene gating. When a replication fork approaches the gated loop, it becomes dismantled through the local checkpoint activation. Mec1/ATR phosphorylates Mlp1 protein. Simplifying the architectural domain of transcribed region enables replication fork to restart and replicate the region.

In checkpoint defective *rad53* mutants the persistence of topological barriers at gated genes leads to positive supercoiling accumulation, which results

in fork reversal (Model 3A and B). Gene gating is abolished when components of the THO and TREX-2 complexes are mutated (Cabal et al., 2006). Alternatively, in gene gating defective mutants twin supercoiled domains persist longer and the negative supercoiling behind the transcription bubble might favor the entanglement of the nascent RNA molecules leading to the R-loops formation (Model 3C and D).

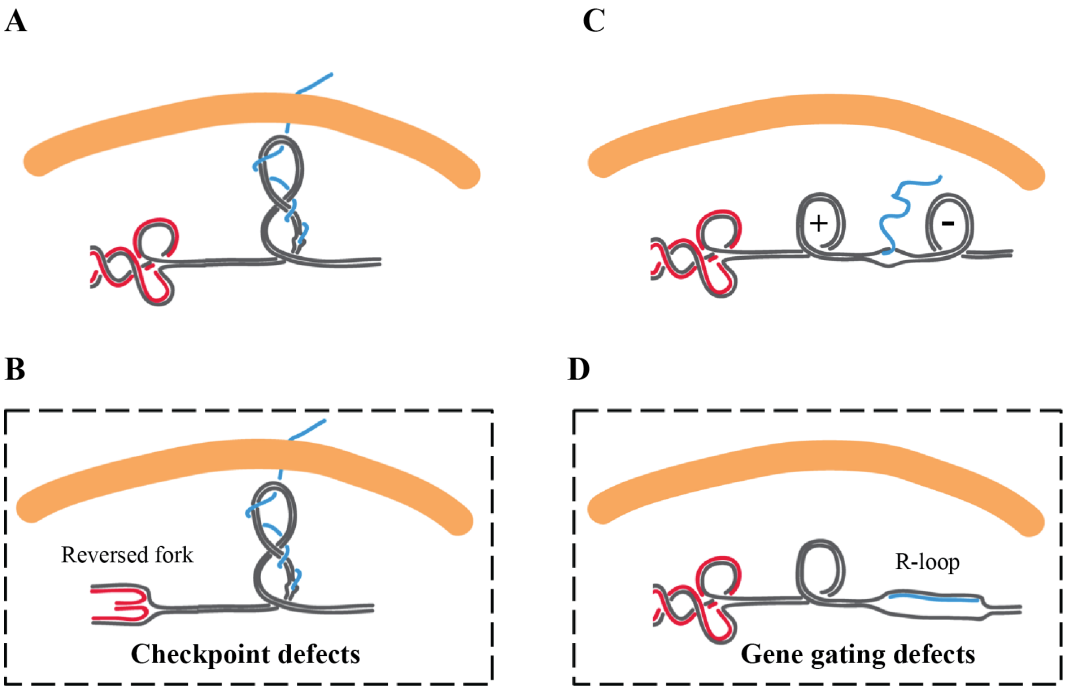

Model 3. Replication and transcription collision consequences in pathological situations. Adapted from (Bermejo et al., 2012).

(A) Gene loop formation as a natural impediment for incoming replication fork.
(B) In checkpoint-defective cells the chromatin loop is still attached to the nuclear pore and persisting topological barrier increases the positive supercoiling between approaching replication fork and gated gene that results in reversed fork formation.
(C) In physiological situations, twin supercoiled domains transiently form after checkpoint-dependent DNA loop disassembling.
(D) In gene gating-defective cells, the persistence of twin supercoiled domains and the negatively supercoiled DNA behind the transcription bubble contribute to non-transient DNA:RNA hybrids formation, which leads to R-loops accumulation.

5.3.1.3 DNA:RNA hybrids and R-loops formation

During transcription, the nascent RNA transcript can invade DNA duplex (Westover et al., 2004) and form a three-stranded nucleic acid structure containing DNA:RNA hybrid and ssDNA. DNA:RNA hybrids are the natural transcription-linked intermediates. Under unperturbed conditions, the formation of ~8 bp hybrid stretch facilitates the progression of the transcription complex (Nudler, 2012). Unlike dsDNA and dsRNA that adopt B and A conformation respectively, DNA:RNA hybrids have the intermediate conformation between these two forms (Shaw and Arya, 2008). Those structures are very stable due to their low thermal stability and favour the negative DNA supercoiling (Shaw and Arya, 2008). Thus, removing DNA:RNA hybrids requires special enzymes. The most prominent, and so far best characterized, enzyme is RNase H, which endonucleolytically cleaves the RNA moiety from the DNA:RNA hybrid. RNase H is also involved in the cleavage and RNA primer removal in the lagging strand synthesis during DNA replication.

Coordinating replication with transcription processes is essential to maintain genome integrity. Thus, DNA:RNA hybrids formation must be tightly controlled in order not to become a threat for replication fork progression. It has been recently shown that Sen1/Senataxin is a replisome component and, as a DNA/RNA helicase, travels with the leading strand of DNA polymerase promoting the progression across RNA polymerase II (RNAPII)-transcribed genes (Model 4A) (Alzu et al., 2012). In *Saccharomyces cerevisiae*, Sen1 is a component of NRD complex (Sen1, Nab3 and Nrd1) (Vasiljeva et al., 2008) and is implicated in transcription termination of many noncoding RNAs such as the

small nuclear RNAs (snRNAs) and small nucleolar RNAs (snoRNAs) (Steinmetz et al., 2001; Ursic et al., 1997).

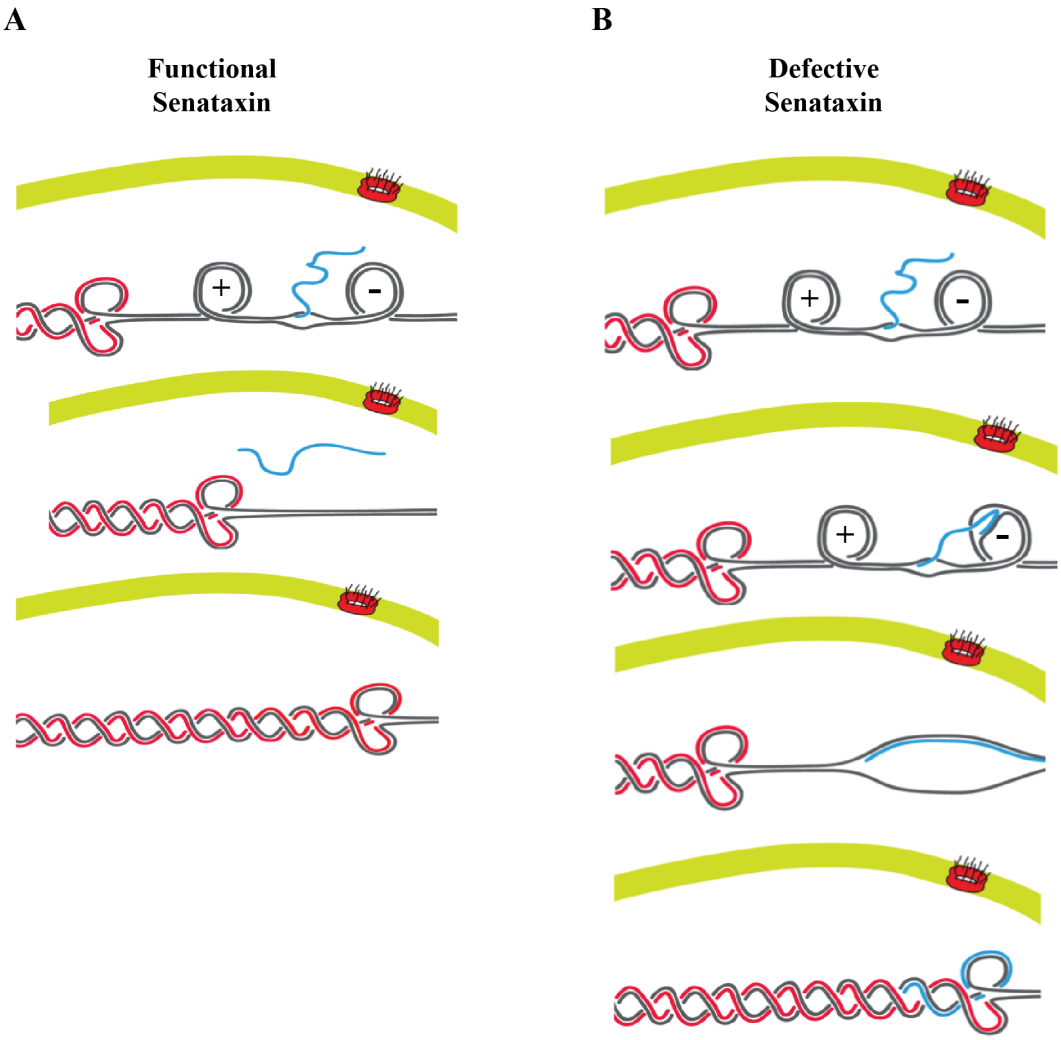

Model 4. DNA:RNA hybrids accumulation at collision sites between replication and transcription. Adapted and modified from (Alzu et al., 2012).

(A) Following gene loop dismantlement, induced by ATR checkpoint, twin supercoiled domains are transiently formed, which favours nascent transcript annealing to the negatively supercoiled DNA behind the transcription bubble. Sen1 moves with the fork and prevents DNA:RNA hybrids persistence.
(B) In the absence of Sen1, DNA:RNA hybrid accumulates and persists on the lagging strand at the site of replication-transcription collision. As a consequence, R loop is formed, which is deleterious for cell viability.

Mutated Senataxin leads to severe neurodegenerative diseases, ataxia with oculomotor apraxia type 2 (AOA2) (Moreira et al., 2004) and juvenile amyotrophic lateral sclerosis 4 (ASL4) (Chen et al., 2004). Dysfunctional Sen1 results in the persisting transcript entanglement with the negatively coiled DNA template (Roy et al., 2010) that has grave topological consequences, if not processed. Those enduring structures, formed of the DNA:RNA hybrid and ssDNA thread, are called R loops (Model 4B). Although the DNA:RNA hybrids occur naturally during replication and transcription (Aguilera and Garcia-Muse, 2012), R loops are deleterious in maintaining genome integrity. It has been proposed that the replicative, and not the transcriptional, function of Sen1 counteracts DNA:RNA hybrids accumulation. Its action is particularly essential during S phase at the regions where transcription collides with head-on oriented replication.

5.3.2 Replication Slow Zones

Particular regions in the genome are difficult to replicate and pause replication forks in unperturbed physiological conditions. Those regions have been mapped on chromosome III between early origins of replication and defined as Replication Slow Zones (RSZs) (Cha and Kleckner, 2002). Analysis of temperature sensitive mutant *mec1-4* (yeast ortholog of mammalian ATR) revealed chromosomal breakage within RSZs in late S and G2 phase. Replication fork stalling in the *mec1-4* mutant was suppressed by deleting Sml1, which is an inhibitor of the ribonucleotide reductase Rnr1. However, the depletion of dNTPs pool is not the main reason of replication fork stalling at RSZs, which do not have

a non-random base composition. Interestingly, RSZs are functionally analogous to common fragile sites (CFSs) in mammals (Sutherland et al., 1998).

5.3.3 Topologically altered DNA structures

DNA usually exists in a B form conformation. However, alternative structures can form and impair replication fork progression due to their altered topology. There is a growing body of evidence that replication can be inhibited by the presence of hairpins, triplexes (H-DNA), cruciform, Z-DNA, S-DNA and G quartets (Wells, 2007). The sequences of those structures are subjected to topological transitions depending on their base composition, DNA supercoiling, symmetry *etc*. Their non B DNA conformations are mutagenic (Samadashwily et al., 1993; Usdin and Woodford, 1995; Weaver and DePamphilis, 1982).

Interestingly, the unusual DNA structures are energetically non favourable in dsDNA. Only high degree of negative supercoiling, which facilitates DNA unwinding, stabilizes non B DNA structures. Based on the fact that oncoming replication fork accumulates positive supercoiling ahead, the unusual structures should not longer persist upon approach of the replication fork (Peter et al., 1998). Thus, the scenario of replication fork encountering a natural impediment, formed by a non B DNA structure, seems to be unlikely *in vivo*. However, lagging-strand synthesis creates transient stretches of ssDNA and provides an opportunity for unusual DNA structures formation. Those structures might be a threat for lagging-strand DNA replication elongation and can lead to the replication fork arrest. As a consequence, the non B form DNA structures contribute to the formation of gross deletions, inversions, duplications and translocations (Wells, 2007) in the genome.

5.4 The role of the checkpoint in DNA replication

Faithful transmission of the genetic material is the prerequisite of the organism survival. Given that cells are under continuous assault of endogenous and exogenous DNA damage agents, maintaining an undamaged genome is a constant challenge. The guardians of accurate DNA replication are checkpoint surveillance mechanisms that monitor genomic topological transitions throughout the cell cycle.

Intrinsic control of varied cell cycle processes, subjected to DNA damage, was first observed in the SOS DNA damage response pathway in *Escherichia coli* and in ataxia telangiectasia mutated (ATM) in mammalian cells (Chan and Hickson, 2009; George et al., 1975). In budding yeast the control mechanism was discovered few years later (Weinert and Hartwell, 1988) and named 'checkpoint control', which is the term that now applies to intrinsic control mechanisms in other organisms. All eukaryotic cells, with an exception of certain embryonic cells, possess checkpoints that control all processes involving DNA metabolism (Hartwell and Weinert, 1989).

DNA checkpoints can be classified into two groups: checkpoints that recognize and respond to DNA damage and replication checkpoints that regulate the fidelity of DNA amplification. The role of DNA damage checkpoints is to monitor the cell cycle arrest (Paulovich et al., 1997), activate DNA repair pathways (Cortez et al., 1999) and transcriptional programmes that facilitate repair (Elledge, 1996), control the telomere length (Ritchie et al., 1999), protect

stalled replication forks integrity (Katou et al., 2003; Lopes et al., 2001) and, if necessary, trigger apoptosis (Lowe et al., 1993).

The DNA damage checkpoint is active at three different phases of the cell cycle: G1/S, intra-S phase and G2/M. At the G1/S phase transition the checkpoint activation arrests the cell cycle by blocking the entrance into S phase (Siede et al., 1993; Weinert and Hartwell, 1988), at intra-S phase slows the replication fork progression (Paulovich and Hartwell, 1995) and during the G2/M transition blocks the entrance into mitosis (Weinert and Hartwell, 1988). When the damage is found, the checkpoint uses a signal mechanism and either stalls the cell cycle until the damage is repaired or targets the cell for destruction via apoptosis. The signalling pathways at each cell cycle phase use the same sensor-signal-effector mechanism.

The checkpoint control pathways are highly conserved throughout evolution. The key factors in the checkpoint response in *Saccharomyces cerevisiae* have their structural and/or functional homologues in *Schizosaccharomyces pombe* and mammalian cells.

5.4.1 DNA checkpoint activation

Triggering the checkpoint response after sensing the DNA damage becomes essential for genome integrity maintenance. Checkpoint activation requires a kinase cascade, which amplifies the signal and transmits it to the checkpoint response effectors.

A common intermediate that activates the checkpoint is ssDNA. The first evidence came from the studies in budding yeast in which the absence of Cdc13p,

ssDNA-binding protein at telomeres, activates the checkpoint (Garvik et al., 1995; Lydall and Weinert, 1996). ssDNA is also generated at the site of DSB (Lee et al., 1998; Pellicioli et al., 2001) and after HU treatment that leads to the high increase of ssDNA accumulation (~200 bp) at the replication forks (Sogo et al., 2002). ssDNA is bound by the RPA protein complex (Zou and Elledge, 2003). When RPA is mutated in its large subunit, *rfa1-t11*, it reduces Ddc2 recruitment, which is the partner of the Mec1 checkpoint kinase, to the site of damage (Lisby et al., 2004), (Lucca et al., 2004) (Nakada et al., 2004).

5.4.2 The intra-S phase checkpoint

The intra-S phase checkpoint is a signalling pathway that slows replication fork progression in the presence of DNA damage. It stabilizes the stalled replication fork, preventing the dissociation of replisome components.

In budding yeast, Mec1 (ATR ortholog) and Rad53 (Chk2 ortholog) kinases are the major components of the signal transduction pathway in S phase (Allen et al., 1994; Weinert et al., 1994). Mec1 belongs to the Phosphatidylinositol 3' kinase-like kinase (PIKK) family (Elledge, 1996) and *in vivo*, independently of DNA damage or other DNA checkpoint genes forms a complex with Ddc2 (ATRIP ortholog) (Paciotti et al., 2000). Mec1-Ddc2 complex is recruited to the site of damage caused by DSB formation and at the single strand breaks formed at telomeres in the absence of Cdc13 protein (Melo et al., 2001). The binding of Ddc2 to RPA-coated ssDNA enables the Mec1-Ddc2 complex to associate with DNA (Zou and Elledge, 2003). Deletion of Ddc2

causes DNA damage defects and replication block similar to *mec1Δ* cells (Paciotti et al., 2000; Wakayama et al., 2001).

Rad53 belongs to transducing protein kinases that contain a forkhead-associated domain (FHA), needed for protein-protein interactions, (Sun et al., 1998) and plays a central role in the checkpoint-signaling pathway. Rad53 becomes phosphorylated by Mec1 and due to its auto-phosphorylation capacity that magnifies the signal (Pellicioli et al., 1999; Sanchez et al., 1996; Sun et al., 1996). Rad53 phosphorylation in response to DNA damage also requires other checkpoint factors; Rad24, an RFC-related protein and the PCNA-like proteins: Rad17, Ddc1 and Mec3 (Model 5) (Paciotti et al., 1998). The treatment with methyl methanesulfonate (MMS), which is an alkylating agent, decreases the Rad53 activity in both mutated Rad24 and PCNA-like complex (Pellicioli et al., 1999). Analogously to PCNA-RFC complex that stabilizes DNA polymerases on the replication fork, the checkpoint sliding clamp might hold the checkpoint sensors at the site of damage.

When replication fork encounters perturbations while synthesising DNA, the DNA damage checkpoint stalls the replication machinery until the damage is repaired. Two-dimensional gel technique (2D-gel) and electron microscopy showed that *rad53Δ* mutants accumulate gapped and hemireplicated molecules at replication forks (Lopes et al., 2001; Sogo et al., 2002), which exhibit a defective replisome-fork association that turns into pathological intermediates (Lucca et al., 2004). The DNA polymerase α-primase complex (Pellicioli et al., 1999), RPA (Brush et al., 1996) and Mrc1 (Katou et al., 2003) are implicated in replisome-fork stabilization. Stalled forks do not accumulate breaks or recombinogenic

intermediates (Sogo et al., 2002) and Rad51 or Rad52 are not involved in the intra S-phase checkpoint response (Lucca et al., 2004).

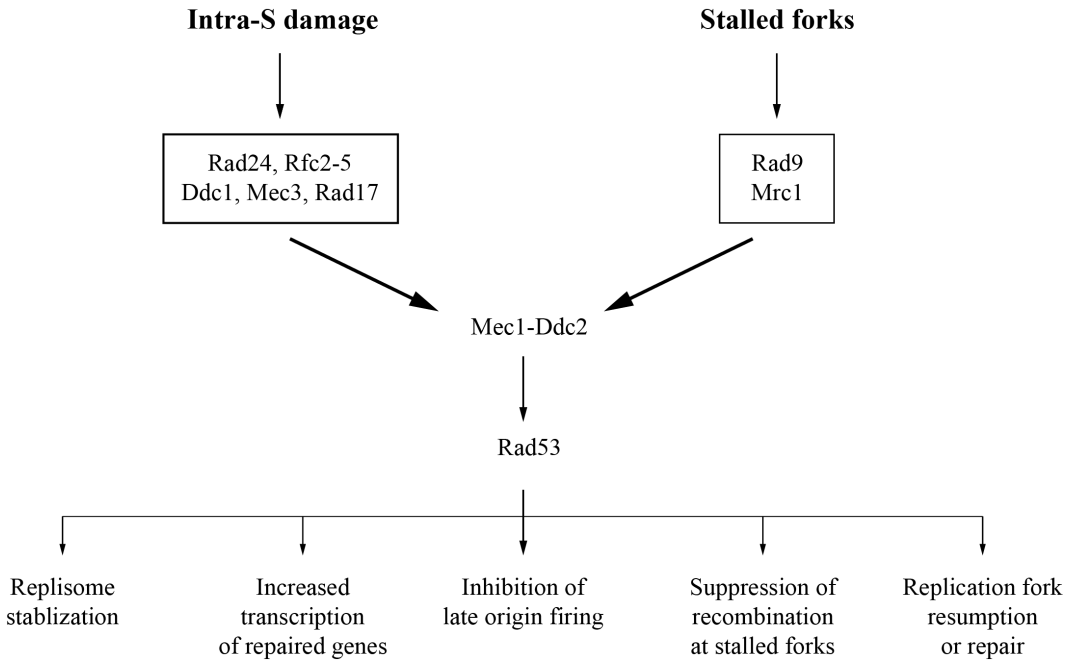

Model 5. The DNA damage checkpoint response.

Schematic representations of DNA damage sensors, signalling pathways and effector mechanism. Adapted from (Branzei and Foiani, 2006).

The checkpoint proteins also monitor the activation of replication origins. In replication stress conditions, Mec1 and Rad53 prevent the firing of late origins (Desdouets et al., 1998; Shirahige et al., 1998). Although the origin activation and replication fork progression during DNA synthesis are similar both in the presence or absence of HU, the time frame is very different. Thus, with functional DNA replication checkpoints the firing of late origins is not inhibited but delayed (Alvino et al., 2007).

In addition to the main DNA damage sensors described above, chromatin modifications play a role in checkpoint activation and/or in the checkpoint signals amplification. The common DNA damage marker is a histone H2A isoform (H2AX) phosphorylation at serine 129 (γH2AX). The histone H2AX modification occurs through Mec1 and Tel1 phosphorylation and is immediately detected after DNA damage induction at the chromatin flanking DSB (Shroff et al., 2004). γH2AX contributes to DNA repair by accumulation of essential proteins at the site of damage in the presence of DNA damaging agents (Celeste et al., 2003; Downs et al., 2000).

5.4.3 DNA replication block and replication fork arrest in G2/M

The G2/M checkpoint provides a cell more time to complete DNA synthesis and repair potential DNA damage before mitosis. The transcription activation of genes involved in DNA repair requires Dun1 kinase phosphorylated in a Rad53-dependent manner (Allen et al., 1994). In budding yeast Rad9 is an essential gene for the cell cycle arrest in G2/M. In response to DNA damage Rad9 is required for a transient cell cycle block and triggering transcription of DNA repair genes. DNA damage induces Rad9 phosphorylation in a Mec1/Tel1-dependent way and phosphorylated Rad9 associates with Rad53 through its FHA domain (Sun et al., 1998) (Vialard et al., 1998) (Schwartz et al., 2002). In unperturbed conditions *rad9Δ* cells accumulate spontaneous chromosome loss. The mutants are viable but sensitive to X- and UV irradiation and defective for cell cycle arrest in G2/M (Weinert and Hartwell, 1990).

Rad9 functions with Mrc1 (Model 5), which is involved in an intra-S phase checkpoint response (see above). Mrc1 is present at replication forks and interacts with Tof1 regulatory protein (Katou et al., 2003). In response to DNA replication stress Mrc1 is phosphorylated by Mec1 that activates Rad53 (Osborn and Elledge, 2003). *mrc1Δ* mutants are sensitive to HU and are defective in the checkpoint response due to decreased Rad53 phosphorylation rate. *MRC1* mutation combined with *RAD9* deletion deactivates Rad53 (Alcasabas et al., 2001).

5.5 Genome instability at chromosome fragile sites

Chromosome fragile sites are chromosomal regions that are particularly prone to form gaps or breaks on metaphase chromosomes after partial restraint of DNA replication. Among all chromosome fragile sites within the genome are present rare fragile sites (RFSs) and common fragile sites (CFSs).

Rare fragile sites are found in less than 5% of individuals and segregate in a Mendelian way. RFSs are classified into two subgroups based on the sequence that cause breakage: folate-senstitive, characterized by an expansion of CGG repeats, and folate non-sensitive that contains many AT-rich repeats (Kremer et al., 1991; Sutherland et al., 1998). The most important RFS is FRAXA associated with the fragile X syndrome that is a hereditary mental retardation. Late replication is a characteristic feature of rare RFSs and first was shown for the fragile X site in the *FMR1* gene (Hansen et al., 1993). The reason of delayed replication termination is the capacity of CGG and AT-repeats to form secondary

structures, such as hairpins, which blocks replication fork progression (Gacy et al., 1995; Hewett et al., 1998).

Common fragile sites belong to the biggest class of fragile sites and their presence does not depend on the nucleotide repeat expansion mutations. CFSs are found in all individuals in a population and under unperturbed conditions most of them are not inclined to form spontaneous breaks.

Until now more than 100 CFSs have been identified and listed in the genome database (GDB). CFSs are not stable under conditions of replicative stress, such as a treatment with aphidocilin (APH), an inhibitor of DNA polymerase α (Glover et al., 1984). CFSs studies can help in understanding mechanisms and consequences of genomic instability under replication stress in both normal and tumour cells.

The instability of CFSs is due to the delay in completing DNA replication at those loci (Hellman et al., 2000) (Palakodeti et al., 2004). Late replication, like in RFSs, is a common feature in CFS that contain relatively long AT-rich sequences, which can be a reason for an increased fragility and extended replication time (Boldog et al., 1997). *FRA3B* exhibits delayed replication termination and the addition of APH results in further retardation in completing DNA synthesis, leaving 16.5% of unreplicated DNA at this locus in G2/M (Le Beau et al., 1998). As a consequence, unreplicated regions become hotspots for introducing metaphase chromosome gaps, breaks and chromosome rearrangements (Glover and Stein, 1987). Deletions and translocations at CFSs can affect associated genes and might lead to genes amplification. MicroRNA genes, involved in chromosomal alterations, are frequently located at fragile sites (Calin et al., 2004). Deregulation of microRNAs can be of diagnostic significance

for cancers. Additionally, Herpes simplex and human papillomavirus (De Braekeleer et al., 1992) appear to integrate within chromosomal fragile sites.

Instability at the CFSs is caused by stalled polymerases at those loci that block replication fork progression, which is exacerbated by APH treatment. It results in uncoupling of replicative polymerases with helicase and topoisomerase complexes. The continued DNA unwinding carried on by helicases leads to ssDNA stretches accumulation, which are prone to form secondary structures. Interestingly, co-treatment with topoisomerase I inhibitor, camptothecin (CPT), reduces APH-induced breakage (Arlt and Glover, 2010).

Chromosome gaps and breaks at fragile sites activate the checkpoint, which strongly contributes in regulating CFSs stability. In mammalian cells ATR transduces the checkpoint response to stalled replication forks (Casper et al., 2002). *ATR*-defective cells exhibit a dramatic increase in CFSs expression, both with APH addition and in unperturbed conditions.

CFSs instability is also related to the formation of DSBs at those regions that are repaired through DNA recombination processes. Both Rad51-dependent homologous recombination and nonhomologous end-joing (NHEJ), which involves phosphorylated DNA-PKcs, regulate fragile sites stability (Schwartz et al., 2005).

Interestingly, replication fork collisions with RNA transcripts could contribute to CFSs formation (Mirkin and Mirkin, 2007). Under replication stress, on the one hand transcription promotes repair by recruiting particular factors. On the other hand, it increases the frequency of mutations on the nontemplate DNA and the process is known as transcription-associated mutation (TAM). It also stimulates recombination through transcription-associated recombination (TAR)

mechanism. Thus, transcription colliding with replication machinery strongly affects genome integrity that might involve CFSs stability perturbation.

CFSs are highly conserved in mammals' evolution (McAllister and Greenbaum, 1997; Ruiz-Herrera et al., 2004; Smeets and van de Klundert, 1990; Stone et al., 1991). This evolutionary conservation extends from higher to lower Eukaryotes, such as budding yeast. As described above, there are particular regions in *Saccharomyces cerevisiae* that are difficult to replicate, where replication forks proceed slower even in unperturbed conditions. RSZs are functionally analogous to CFSs due to increased DSBs formation within those regions in temperature sensitive *mec1-4* mutants in late S and G2 phase.

Budding yeast genome exhibits replication stress-sensitive loci. Restraining α DNA polymerase activity in *Saccharomyces cerevisiae* results in increased chromosome translocations and chromosome loss. The translocations affect retrotransposons (Ty elements) and the process is mediated by homologous recombination (Lemoine et al., 2005). Moreover, chromosomal regions containing multiple tRNA genes, known to stall replication forks, are frequent sites of chromosome breakage and translocations that are exacerbated under replication stress (Admire et al., 2006). Genome-wide studies in *rad53* and *mec1* mutants have revealed that replication forks stall and eventually collapse at specific sites close to the origins (Raveendranathan et al., 2006). Those regions are prone to chromosome breakage both in the presence or absence of replication stress. Thus, unstable chromosomal regions in yeast are functionally analogous to common fragile sites in the human genome.

6 Materials and Methods

6.1 Yeast strains genotypes used

Strain	Genotype	Source
SY2080	*Mat***a** *ade2-1 trp1-1 leu2-3,112 his3-11,15 ura3 can1-100 GAL PSI$^+$ RAD5$^+$*	H. Klein
CY11007	*Mat***a** *ade2-1 trp1-1 leu2-3,112 his3-11,15 ura3 can1-100 GAL PSI$^+$ RAD5$^+$ ura3::URA3/GPD-TK(7X)*	This study
CY10731	*Mat***a** *ade2-1 trp1-1 leu2-3,112 his3-11,15 ura3 can1-100 GAL PSI$^+$ RAD5$^+$ rrm3::HIS3MX6*	This study
CY11008	*Mat***a** *ade2-1 trp1-1 leu2-3,112 his3-11,15 ura3 can1-100 GAL PSI$^+$ RAD5$^+$ rrm3::HIS3MX6 ura3::URA3/GPD-TK(7X)*	This study
CY8702	*Mat***a** *ade2-1 trp1-1 leu2-3,112 his3-11,15 ura3 can1-100 GAL PSI$^+$ RAD5$^+$ sen1::GAL-URL-3HA-SEN1-KANMX6*	This study
CY10300	*Mat***a** *ade2-1 trp1-1 leu2-3,112 his3-11,15 ura3 can1-100 GAL PSI$^+$ RAD5$^+$ sen1-G1747D-HIS3*	G. Liberi
CY11009	*Mat***a** *ade2-1 trp1-1 leu2-3,112 his3-11,15 ura3 can1-100 GAL PSI$^+$ RAD5$^+$ sen1::GAL-URL-3HA-SEN1-KanMX6 ura3::URA3/GPD-TK(7X)*	This study
CY11224	*Mat***a** *ade2-1 trp1-1 leu2-3,112 his3-11,15 ura3 can1-100 GAL PSI$^+$ RAD5$^+$ rad51::HPH*	This study
CY11893	*Mat***a** *ade2-1 trp1-1 leu2-3,112 his3-11,15 ura3 can1-100 GAL PSI$^+$ RAD5$^+$ rrm3::HIS3MX6 rad51::HPH*	This study
CY11746	*Mat***a** *ade2-1 trp1-1 leu2-3,112 his3-11,15 ura3 can1-100 GAL PSI$^+$ RAD5$^+$ sen1::GAL-URL-3HA-SEN1-KANMX6 rad51::HPH*	This study
CY10715	*Mat***a** *ade2-1 trp1-1 leu2-3,112 his3-11,15 ura3 can1-100 GAL PSI$^+$ RAD5$^+$ sen1::GAL-URL-3HA-SEN1-KANMX6 rrm3::HIS3MX6*	This study
CY11010	*Mat***a** *ade2-1 trp1-1 leu2-3,112 his3-11,15 ura3 can1-100 GAL PSI$^+$ RAD5$^+$ sen1::GAL-URL-3HA-SEN1-KanMX6 rrm3::HIS3MX6 ura3::URA3/GPD-TK(7X)*	This study
CY11894	*Mat***a** *ade2-1 trp1-1 leu2-3,112 his3-11,15 ura3 can1-100 GAL PSI$^+$ RAD5$^+$ sen1::GAL-URL-3HA-SEN1-KANMX6 rrm3::HIS3MX6 rad51::NAT*	This study
CY10300	*Mat***a** *ade2-1 trp1-1 leu2-3,112 his3-11,15 ura3 can1-100 GAL PSI$^+$ RAD5$^+$sen1-G1747D-HIS3*	G. Liberi

CY12093	*Mat***a** *ade2-1 trp1-1 leu2-3,112 his3-11,15 ura3 can1-100 GAL PSI$^+$ RAD5$^+$ rad9::hph ura3::URA3/GPD-TK(7X)*	This study
CY12095	*Mat***a** *ade2-1 trp1-1 leu2-3,112 his3-11,15 ura3 can1-100 GAL PSI$^+$ RAD5$^+$ rrm3::HIS3MX6 rad9::hph ura3::URA3/GPD-TK(7X)*	This study
CY12096	*Mat***a** *ade2-1 trp1-1 leu2-3,112 his3-11,15 ura3 can1-100 GAL PSI$^+$ RAD5$^+$ sen1::GAL-URL-3HA-SEN1-KanMX6 rad9::hph ura3::URA3/GPD-TK(7X)*	This study
CY12117	*Mat***a** *ade2-1 trp1-1 leu2-3,112 his3-11,15 ura3 can1-100 GAL PSI$^+$ RAD5$^+$ sen1::GAL-URL-3HA-SEN1-KanMX6 rrm3::HIS3MX6 rad9::hph ura3::URA3/GPD-TK(7X)*	This study

Table 1. *Saccharomyces cerevisiae* strains used in this study.

6.2 Growth media and buffers composition

Media for *Saccharomyces cerevisiae*:

Yeast extract	10 g
Peptone	20 g
H_2O	up to 1000 ml
Glucose/Galactose/Raffinose	2% final concentration
pH	5.4
agar (agar plates)	2% final concentration

Minimum Media + YNB:

YNB without amino acids (Difco)	6.7 g
Amino Acid Dropout Mix	2 g of AAs
Glucose/Galactose/Raffinose	2% final concentration
H_2O	up to 1000 ml
agar (agar plates)	2% final concentration

Buffers:

Laemmli buffer 3X: Tris 0.187 M, SDS 6%, β-Mercaptoethanol 15%, Glycine 30%, BPB 0.003%

SDS-PAGE running buffer 5X: Glycine 2 M, Tris 0.25 M, SDS 0.02 M, pH 8.3

SSC 20X: NaCl 3 M, Sodium Citrate 0.3 M, pH 7.5

TBE 10X: Tris borate 0.9 M, EDTA 0.02 M

TBS 10X: NaCl 1.5 M, Tris 0.5 M, pH 8.0

TAE 50X: Tris-acetate 0.04 M, EDTA 0.001 M

TE 1X: Tris-HCl 10 mM, EDTA 1 mM, pH 7.4

6.3 Yeast transformation

The main procedure used is described by (Gietz et al., 1995). Exponentially growing cells are treated for 30 min with Lithium Acetate (LiAc) 0.1 M in TE 1X. A 50 µl aliquot, corresponding to 10^8 cells, is incubated at 30°C with 2-5 µg of PCR-amplified linear DNA cassette or 1 µg of plasmid DNA and 20 µg of ssDNA carrier for at least 30 min. 5 volumes of freshly prepared 40% PEG-4000 are added and cells are incubated for 30 min at 30°C. DMSO is added to a final concentration 10% of the final volume, what is followed by 15-20 minutes of heat-shock at 42°C. The cells are centrifuged at low speed (3000 rpm) and if they carry a *KAN* or *NAT* marker, they are re-suspended in YPD or YPG medium and subjected to 4-5 hours recovery and then plated on selective plates.

6.4 Genetic methods

Genetic analyses are performed by using standard procedures for mating, diploid selection, sporulation and tetrad dissection. For spot assays, the strains are grown at equal cellular concentrations and are diluted sequentially 1:6 before being spotted on the specific plates.

6.5 Cell cycle arrest

There are commercially available substrates that allow blocking the cell cycle at the specific phases. In this thesis I used the α-Factor pheromone, that blocks the cells in G1, and nocodazole, which depolymerizes the microtubules and arrests the cells in pro-metaphase.

α-Factor – This pheromone is produced by *Saccharomyces cerevisiae "*α" cells and by inducing mating genes expression arrests "a" cells in G1 phase. The growth of "a" cells is polarized towards the mating partner and cells undergo morphological elongation into pear-shaped "shmoos". Exponentially growing cells are treated with 4 μg/ml (3 μg/ml + 1 μg/ml added after 1 hour 30 minutes) of the synthetic peptide α-Factor (Primm). When approximately 90% of cells show the shmooing phenotype, cells are centrifuged and washed with YP in order to wash the α-Factor away and release the cells in fresh medium.

Nocodazole – It is an anti-neoplastic agent, which by depolymerizing microtubules, arrest cycling cells in G2/M phase. Nocodazole-treated cells do enter mitosis but cannot form metaphase spindles. Cells are arrested in G2/M phase by the addition of 10 μg/ml of Nocodazole (Sigma-Aldrich) dissolved in

DMSO. The arrest is maintained for 3 hours by re-adding 5 µg/ml of Nocodazole or 10 µg/ml, to maintain the arrest for a longer time.

6.6 Total protein extract

The yeast protein extraction is performed using TCA as described by (Reid and Schatz, 1982). 10^8 cells samples are collected, centrifuged at 4°C at 4000 rpm, washed with 1 ml of TCA 20% and transferred to a 2 ml tube. The pellet is re-suspended in 100 µl of TCA 20% and an equal volume of glass beads (425-600 µm, Sigma-Aldrich) is added leaving a layer of a supernatant over the beads. Cells are broken by continuous vortexing for 7-10 minutes. 200 µl of TCA 5% is added and the lysate is transferred to a new 1.5 ml tube and centrifuged for 10 minutes at 3000 rpm at RT. The pellet is re-suspended in 100 µl of Laemmli Buffer 1X. The pH is neutralized with 50 µl of Tris Base 2M (the colour needs to turn from yellow to blue). The protein extract is boiled for at least 3 minutes and centrifuged for 10 minutes at 3000 rpm at RT. The supernatant is collected and the protein extract is subjected to SDS-PAGE analysis.

6.7 Western blot procedure

Proteins are separated by their molecular weight in the denaturing conditions using gel electrophoresis in polyacrylamide gels. The concentration of acrylamide determines the resolution of the gel. The polyacrylamide gel consists of two parts: running and stacking. The lower the acrylamide concentration is in the running part of the gel, the better the resolution of big molecular weight proteins becomes. The protein migration is performed in a SDS-PAGE running buffer. The

procedure is described by (Laemmli, 1970). Proteins with a known molecular weight serve as a marker. The gel with separated proteins is transferred on a nitrocellulose filter (Whatman Protrane, Nitrocellulose Transfer Membrane, Pore size 0.45 μm) O/N at 0.2 Ampere in a transfer buffer (Glycin 1%, Tris-HCl 0.02 M, Methanol 20%). After the transfer the filter is washed with TBST 1X and coloured with Ponceau S staining solution (Ponceau S 1gr, acetic acid 50 ml, up to 1000 ml ddH_2O) that enables the visualization of the total protein extract. The filter is washed again with TBST and then is incubated for at least 30 minutes with milk 4% in TBST. The primary antibody is added and incubated for 2 h at RT. The membrane is washed 3X for 10 minutes in TBST and the filter is incubated with secondary antibody for 1 hour at RT. After the hybridization the filter is washed again 3X for 10 minutes with TBST. Finally, the membrane is incubated for 5 minutes at RT with SuperSignal West Femto Chemiluminescent Substrate (Thermo Scientific) and the signal is developed using ChemiDoc (Bio-Rad, Molecular Imager ChemiDoc XRS+). The antibodies used in this work are presented in Table 1.

Protein	Protein size	1st Antibody	2nd Antibidy	Acrylamide concentration
H2AX	14 kDa	Anti-Histone H2A (phospho S129) antibody (ab15083) Rabbit polyclonal 0.1 mg/ml, dilution used: 1:500	Anti-rabbit Goat polyclonal (Bio-rad #170-6515) IgG-HRP (H+L), 1:20000	15% Acrylamide in Running part of the gel
Rad53p	92 kDa	F9.1 Antibody 1:200	Anti-mouse, Goat polyclonal (Bio-rad	10% Acrylamide in Running part of the gel

			#170-6516) IgG-HRP (H+L), 1:20000	
HA-Sen1p	252.5 kDa	anti-HA Mouse monoclonal 12CA5 (Roche Applied Science) 5 mg/ml, dilution used: 1:1000	Anti-mouse, Goat polyclonal (Bio-rad #170-6516) IgG-HRP (H+L), 1:20000	7.5% Acrylamide in Running part of the gel
PGK1p	44.5 kDa	Mouse monoclonal 1 mg/ml, Invitrogen, dilution used: 1:10000	Anti-mouse, Goat polyclonal (Bio-rad #170-6516) IgG-HRP (H+L), 1:20000	10% Acrylamide in Running part of the gel

Table 2. Antibodies used in Western blotting in this work.

The dilutions of the primary and secondary antibodies against phosphorylated Serine 129 at histone H2A, phosphorylated Rad53p, HA-tagged Sen1p and expressed level of PGK1p (loading control) are shown in the table. Due to different protein sizes, adequate acrylamide concentration is used to separate the proteins.

6.8 FACS analysis

Approximately 10^7 cells are blocked with 70% Ethanol in Tris 250 mM pH 7.6. After 1 minute centrifugation (at the maximum speed) the cells are re-suspended in 500 µl of Tris 50 mM pH 7.6-solution containing 2 mg/ml of RNase A and are incubated at 37°C for at least 1 hour. Then, the cells are stained with Propidium

Iodide 50 μg/ml in 180 mM Tris-HCl pH 7.6, 190 mM NaCl, 70 mM $MgCl_2$. A 1:10 dilution in Tris-HCl 50 mM pH 7.6 is analysed in Becton Dickinson FACS-calibur for FL2H fluorescence.

6.9 *In vivo* psoralen-crosslinking

Psoralen efficiently intercalates into the dsDNA and upon 366 nm light ultraviolet irradiation (UV) form covalent crosslinks between pyrimidines between two DNA strands. Psoralen derivatives easily penetrate living cells membranes. TMP is the most commonly used form of psoralen for *in vivo* DNA crosslinking (Wellinger and Sogo, 1998).

Cells (blocked with 0.1% Sodium Azide) subjected to 2D-gel analysis (see Materials and Methods 5.13) before either CTAB or Qiagen Kit genomic DNA extraction (see Materials and Methods 5.10 and 5.11 respectively) are treated with TMP. Cells are transferred to a standard Petri dish in ice, mixed with 1 ml of TMP (200 μg/ml Sigma-TMP dissolved in Ethanol 100%) and incubated for 5 minutes in darkness. The Petri dish (kept in ice) is put in the Stratalinker (with pre-warmed lamps) and under UV lights 366 nm the cells are irradiated 4 x for 10 minutes. The appropriate distance between the lamp and the sample surface has to be determined for each light source employed. When the psoralen-crosslinking is done, the cells are transferred to 50 ml Falcon tubes and washed with ice-cold water.

6.10 CTAB genomic DNA extraction

Materials and Solutions:

- Sodium Azide 10% stored at 4°C
- 10 mg/ml Zymolyase, 1000 U/ml (Seikagaku BioBusiness)
- Spheroplasting buffer: 1 M Sorbitol, 100 mM EDTA pH 8.0, 0.1% β-mercaptoethanol, zymolyase 1mg/ ml final concentration
- Solution I: 2% w/v CTAB, 1.4 M NaCl, 100 mM Tris-HCl pH 7.6, 25 mM EDTA pH 8.0
- 10 mg/ml RNase A, DNase free (Sigma-Aldrich)
- 20 mg/ml Proteinase K (Roche)
- 24:1 Chloroform:Isoamyl alcohol
- Corex glass tubes
- Solution II: 1% w/v CTAB, 50 mM Tris-HCl pH 7.6, 10 mM EDTA
- Solution III: 1.4 M NaCl, 10 mM Tris-HCl pH 7.6, 1 mM EDTA
- Isopropanol
- Cold 70% Ethanol
- 10 mM Tris-HCl pH 8.0

Procedure:

1) Start from 2 X 10^9 cells (200 ml of a culture 1 X 10^7 cells/ml).
2) Collect samples in a JA-14 Beckman tubes, block the cells with 0.1% of Sodium Azide (final concentration), keep at least 5 minutes in ice, centrifugate at 6000-8000 rpm for 5 minutes and wash with 20 ml of ice-cold water.

3) Transfer cells in 50 ml Falcon tubes, re-suspend in 5 ml of spheroplasting buffer and incubate for 10-30 minutes at 30°C. Time of spheroplasting strictly depends on the sugar the cells were grown in. In galactose cells are smaller, cell walls are thinner and spheroplasting lasts only 10 minutes whereas in glucose it lasts around 20 minutes.
4) Collect spheroplasts by centrifugation at 4000 rpm (in Falcon tubes) for 10 minutes at 4°C.
5) Re-suspend spheroplasts in 2 ml of cold water, add 2.5 ml of Solution I and 200 µl of RNase A. Vortex the suspension and incubate at 50°C for at least 30 minutes.
6) Add 200 µl of Proteinase K and incubate for 1.5 hour at 50°C. Re-add 100 µl of Proteinase K and incubate O/N at 30°C to increase the yield of extracted DNA.
7) Centrifugate the solution at 4000 rpm at RT for 10 minutes to separate the pellet from the supernatant. Both fractions are processed as indicated below.

Supernatant

1) Transfer the supernatant into a 15 ml Falcon tube and add 2.5 ml of Chloroform:Isoamyl alcohol 24:1.
2) Mix vigorously and separate the two phases by centrifugation at 4000 rpm for 10 minutes at RT.
3) Carefully transfer the clear upper phase into a Corex glass tube with a pipette and add two volumes (10 ml) of Solution II. The prolonged incubation (1-2 hours) with Solution II helps DNA precipitation in the next step.

4) Centrifugate the solution at 8500 rpm for 10 minutes at RT in a Beckman JS 13.1 swinging bucket rotor, discard the supernatant and re-suspend the pellet in 2.5 ml of Solution III.

Pellet

1) Re-suspend the pellet in 2 ml of Solution III and incubate at least 1 hour at 50°C.
2) Transfer the solution into a new 15 ml Falcon tube already containing 1 ml of Chloroform:Isoamyl alcohol 24:1.
3) Mix vigorously and separate the two phases by centrifugation at 4000 rpm for 10 minutes at RT.
4) Carefully transfer the clear upper phase into the Corex glass tube containing Solution III obtained from the treatment of the supernatant (see *Supernatant* step 4).
5) Precipitate DNA with 1 volume (4.5 ml) of isopropanol and centrifugate at 8500 rpm for 10 minutes in a Beckman JS 13.1 swinging bucket rotor at RT.
6) Wash the pellet with 1 ml of ice-cold Ethanol 70%.

After centrifugation carefully remove the Ethanol with a pipette, dry the pellet and dissolve it in 250 ml of 10 mM Tris-HCl pH 8. Extracted genomic DNA is stored at 4°C.

6.11 Genomic DNA extraction with the Qiagen genomic Kit

Materials and Solutions:

Solutions Y1, G2, QBT, QC and QF are supplied with the Qiagen Kit:

- Buffer Y1 (Yeast Lysis Buffer) 1 M Sorbitol, 100 mM EDTA, 14 mM β-mercaptoethanol (supplemented with 500 µl/sample of zymolyase solution)
- 10 mg/ml Zymolyase, 1000 U/ml (Seikagaku Biobusiness)
- Buffer G2 (Digestion Buffer) 800 mM guanidine HCl, 30 mM Tris-HCl pH 8.0, 30 mM EDTA pH 8.0, 5% Tween 20, 0.5% Triton X-100
- Buffer QBT (Equilibration Buffer) 750 mM NaCl, 50 mM MOPS pH 7.0, 15% Isopropanol, 0.15% Triton X-100
- Buffer QC (Wash Buffer) 1 M NaCl, 50 mM MOPS pH 7.0, 15% Isopropanol
- Buffer QF (Elution Buffer) 1.25 M NaCl, 50 mM Tris-HCl pH 8.5, 15% Isopropanol
- 10 mg/ml RNase A, DNase free (Sigma-Aldrich)
- 20 mg/ml Proteinase K (Roche)
- Isopropanol
- Cold 70% Ethanol
- 10 mM Tris-HCl pH 8.0
- Corex glass tubes

Procedure

1) Start from 2 X 10^9 cells (200 ml of a culture 1 X 10^7 cells/ml).
2) Collect samples in a JA-14 Beckman tubes, block the cells with 0.1% of Sodium Azide (final concentration), keep at least 5 minutes in ice,

centrifuge at 6000-8000 rpm for 5 minutes and washed with 20 ml of ice-cold water.

3) Transfer the cells in a 50 ml Falcon tube, re-suspend in 5 ml of Y1 buffer and incubate for 10-30 minutes at 30°C (spheroplasting).
4) Collect the spheroplasts by centrifugation at 4000 rpm for 10 minutes at 4°C.
5) Discard supernatant and re-suspend the spheroplasts in 4 ml of G2 buffer (cell breaking).
6) Add 100 µl of RNase A and incubate at least 20 minutes at 37°C.
7) Add 200 µl of Proteinase K and incubate for 2 hours at 50°C (the lysate should become clear upon proteinase K treatment). To increase the yield of extracted DNA, re-add 100 µl of Proteinase K and incubate O/N at 30°C.
8) Centrifugate the lysate for 10 minutes at 4000 rpm at 4°C.
9) Dilute the supernatant in an equal volume (4 ml) of QBT buffer.
10) Load the diluted supernatant on the Qiagen tip 100G-anion exchange column, pre-equilibrated with 4 ml of QBT buffer.
11) Wash twice with 7.5 ml of QC buffer.
12) Elute with 5 ml QF buffer in a corex glass tube.
13) Precipitate with 3.5 ml of isopropanol and centrifugate at 8500 rpm for 10 minutes in a Beckman JS 13.1 swinging bucket rotor.
14) Wash the pellet with 1 ml of ice-cold Ethanol 70%.
15) Re-suspend the pellet in 250 µl of 10 mM Tris-HCl pH 8.0 and store at 4°C.

6.12 Quantification of genomic preps

Concentration of DNA and DNA:RNA genomic preps are measured by NanoDrop. At the wavelength of 260 nm, 1.5 µl of genomic sample is subjected to the concentration quantification. If DNA and DNA:RNA concentration is higher than 200 ng/µl and 2000 ng/µl respectively, the samples are diluted and re-quantified.

6.13 Replication intermediates analysis with two-dimensional agarose gel electrophoresis

When origin of replication fires, replication forks move bidirectionally. The moving fork amplifies the DNA fragment until it encounters the replication fork arriving from the adjacent active origin. The amplified DNA fragment assumes distinct structures in their mass and shape. If the analysed replicated fragment contains a firing origin of replication, bubble-shaped structures with increasing mass are formed as the fork proceeds. In contrary, when a fragment is replicated passively, meaning that the replication fork enters the fragment either from its left or right extremity, a population of Y-shaped molecules with varied mass and shape is formed.

The Neutral-neutral two-dimensional agarose gel electrophoresis (2D-gel) technique has been widely used to analyse nascent replication intermediates at specific chromosomal locations by separation of branched DNA molecules according to their mass and shape complexity (Bell and Byers, 1983). The technique was further developed (Brewer and Fangman, 1987) and adapted to

map origins of DNA replication in the yeast genome. 2D-gels enabled to study replication- and recombination-related DNA structures in many organisms.

The principle of the method states that DNA fragments with the same mass differ in their shape complexity when replicated affecting their electrophoretic mobility. Following genomic DNA extraction that preserves branched molecules (see CTAB genomic DNA extraction), the DNA is digested with a restriction enzyme and the restriction fragments are separated by a first dimension gel. The conditions used during the first gel electrophoresis (low agarose concentration, low voltage, no ethidium bromide) minimize the contribution of shape of the molecules to the mobility. Subsequently, each sample lane is cut out and separated by the second dimension gel, where DNA runs orthogonally with respect to the first dimension gel. The second dimension gel is run in conditions to maximize the effect of the molecules' shape complexity (high agarose concentration, high voltage, the presence of ethidium bromide both in the gel and running buffer). At the end a Southern blot followed by hybridization with a specific radiolabeled probed is done, detecting the fragment of interest.

Based on the pattern of two-dimensional electrophoretic migration of branched molecules, the features of replication intermediates from analysed fragment can be deduced. Some of them have been confirmed by electron microscopy (Kuzminov et al., 1997). The migration patterns of branched DNA structures arising during replication origin firing, replication fork progression, pausing, recombination and replication termination are depicted in Model 6.

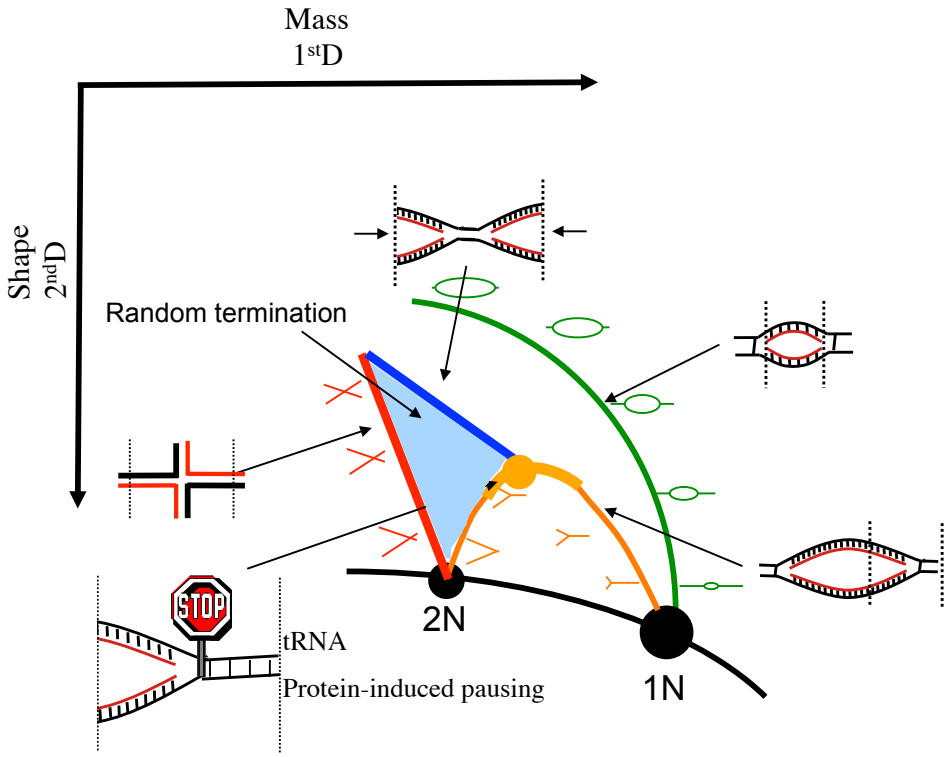

Model 6. Schematic representation of branched DNA migration patterns in 2D-gels.

The direction of first- and second-dimension gel electrophoresis is indicated. Nonreplicating molecules are seen as a shallow arc of linears (black arc). The replicating molecules run above the arc. 1*n* spot reveals nonreplicating molecules at the size of analysed fragment. The replicating molecules join the arc of linears when the fragment is almost fully replicated (2*n*). Replication intermediates of the restriction fragment are indicated with different colours: green – bubble-shaped molecules arising from the replication origin firing, yellow – Y-shaped intermediates coming from 1*n* spot and state for the newly replicated arms of a proceeding replication fork, blue – double-Y intermediates that show the position of converging forks, red - 2*n* spike resulting from crossed strands in recombination events and/or replication termination intermediates indicating fork fusion. Yellow dot is a sign of prolonged replication fork pausing when it encounters a natural impediment ahead as transcribed tRNA and/or non-histone proteins.

6.14 2D-gel procedure

After DNA extraction and DNA quantification (see Materials and Methods 6.10 and 6.12 respectively) an aliquot of sample is digested with a restriction enzyme and subjected to 2D-gel electrophoresis. When firing of the origin of replication is studied, 8-10 μg of DNA is digested. If replication termination structures arising during fork fusion are investigated, 20 μg of DNA needs to be digested due to a very fast turnover of termination intermediates.

First dimension gel (20 cm wide and 25 cm long), without Ethidium Bromide 0.35% agarose (LOW EEO, US Biological) dissolved in TBE 1X buffer, is poured at 4°C. Samples and a molecular weight DNA marker (1 kb DNA ladder, New England Biolabs) are loaded, leaving one empty well between samples, and the gel is run at the constant low voltage at RT (50 V, ca. 1 V/cm) for around 24 hours. The electrophoresis conditions vary depending on the size of the restriction fragment analysed. After the migration the gel is stained with 0.3 μg/ml Ethidium Bromide for at least 30 minutes. Slides of appropriate dimension, containing the linear and the replicated molecules from the fragment of interest, are cut out from each sample lane migrated in the first dimension gel. Subsequently, the slides are rotated 90°C anticlockwise with the respect to the first dimension direction and placed in the tray for the second dimension gel (0.3 μg /ml Ethidium Bromide 0.9% agarose, LOW EEO, US Biological). The second dimension gel is run for 8-10 hours at the constant high voltage at 4°C (180-250 V, ca. 3-5 V/cm) in TBE 1X buffer containing 0.3 μg /ml Ethidium Bromide. After second dimension gel electrophoresis, the crosslinking which was done before DNA extraction (psoralen treatment) needs to be reverted for 10 minutes under UV lamps 265 nm.

6.15 Southern blot procedure

Prior to blotting, second dimension gels need to be subjected to the following treatment:

- Depurination, 8-10 minutes in 0.25 N HCl
- Denaturation, 20 minutes in 0.5 M NaOH, 1.5 M NaCl
- Neutralization, 20 minutes in 1 M $AcNH_4$, 0.02 M NaOH

The gel is transferred in standard Southern Blot conditions using Gene Screen transfer membrane (Perkin Elmer) in SSX 10X over night. Transferred DNA is fixed to the membrane under UV lamps 265 nm.

The membrane is subjected to hybridization with a specific radiolabeled probe. The 50-80 ng of DNA is labelled with 50 μCi of ^{32}P dCTPs using a Prime-a-Gene® Labeling System in which a mixture of random hexadeoxyribonucleotides (without dCTPs) is used to prime DNA synthesis in vitro from any linear double-stranded DNA template. The reaction should last at least 1 hour at RT. For rapid purification of labeled DNA from unincorporated labeled nucleotides spin-column chromatography is used (illustra MicroSpin G-50 Columns, GE Healthcare Life Sciences). Columns are prepacked with Sephadex G-50 Grade pre-equilibrated in TE buffer with 0.05% Kathon CG/ICP Biocide.

During the radiolabelled probe preparation, the membranes with transferred and crosslinked DNA are incubated for at least 30 minutes in a pre-hybridization solution 1X (Sigma-Aldrich) at 65°C in a rotating tube. The purified probe is boiled for 10 minutes at 100°C and immediately after added together with boiled ssDNA (from salmon sperm) to a pre-hybridization mix. The hybridization reaction should persist for at least 5 hours at 65°C. Subsequently, the filters are washed two times (10 minutes + 15 minutes) with 500 ml 2X SSC, 1% SDS at

65°C, followed by two washes (15 minutes + 15 minutes) with 500 ml 0.1X SSC, 0.1% SDS at 42°C. The washed membranes are air-dried and placed in an exposure cassette with a phosphor screen. The signal is developed (after at least 5 hours) using Phosphoimager Molecular Storm 820.

6.16 Probes

***ARS305* probe** – a 3 kb BamHI (38606 bp) –NcoI (41670 bp) fragment containing origin of replication *ARS305* (39159 – 39706 bp).

Rest of the probes are obtained by PCR amplification using following oligos:

***TER704* probe**, chromosome VII from 496097 to 497366 bp. Amplified with oligos:

Fw TGTGCACATCTTGCCCATTA

Rv GCCTCTATCACTGCAAAGTG

***TER102* probe**, chromosome I from 153316 to 154434 bp. Amplified with oligos:

Fw TCTGCGCCAAGCAAAGATTC

Rv TTTCCTTGCGTCTGATTCGG

***TER603* probe**, chromosome VI from 183324 to 184552 bp. Amplified with oligos:

Fw GAATGCCCGAGCCCTAAAAA

Rv ATGTGAGCCATCTGGAAAGG

***TER802* probe**, chromosome VIII from 126307 to 127436 bp. Amplified with oligos:

Fw CTGAGACAAAGTCTTTCCAG

Rv CGAAAGCCTTCTTGACGACT

***TER302* probe**, chromosome III from 91974 to 93001 bp. Amplified with oligos:

Fw GAAGGTTCAACATCAATTGATTGATTCTGCCGCCATGATC

Rv GCTTCCCTAGAACCTTCTTATGTTTTACATGCGCTGGGTA

6.17 GIP with BrdU incorporation

Grow the cells O/N at 23°C in 200 ml –URA medium up to $1x10^7$ cells/ml.

1st Day

1) Synchronize the cells in 200 ml YPDA medium with α-Factor at 23° C. The synchronization is done in YPD or YPG medium.
2) As soon as the synchronization is reached, add BrdU 200 μg/ml 20 min before the release. The maximum solubility of BrdU in water is reached at 10mg/ml.
3) Release cells from G1 arrest into YPDA medium containing BrdU 200 μg/ml.
4) Block the cells (200 ml) with 0.1% of Sodium Azide (final concentration) and keep on ice for at least 5 minutes.
5) Centrifuge the culture using the Beckman centrifuge and the JA-14 rotor: 5000 rpm, 5 minutes at 4°C. Discard the supernatant.
6) Re-suspend the pellet in 20 ml of cold and sterilized 1X TE.
7) Centrifuge the culture at 3220 x g, 5 minutes at 4°C, discard the supernatant and carefully remove the remaining liquid with a vacuum pump. At this point the dried pellet can be stored at -20° C.

8) Extract the DNA with QIAGEN GENOMIC DNA ISOLATION KIT (Cat. No. 19060). Re-suspend the DNA in 250 µl of 1X TE pH 8.

Protein A Magnetic Beads preparation:

FOR EACH 200 ml OF CULTURE:

1) Take 20 µl of dynabeads (Invitrogen) for each IP and put in a Costar prelubricated tube.
2) Wash the beads two times with 1ml of 1X PBS, 5 mg/ml BSA, 0.1% Tween20.
3) Re-suspend the beads in 20 µl of 1X PBS, 5mg/ml BSA, 0.1% Tween20; add 4 µg of anti-BrdU antibody (MBL M1-11-3).
4) Incubate the beads O/N at 4°C rotating.

2nd Day

1) Shear the BrdU containing DNA by sonication to a length of 200-1000 bp using the Bandelin UW2070 sonicator. You can use the following parameters:
    - Power 20%
    - 20 seconds/pulse
    - 6 pulses

    After each sonication cycle, pellet the chromatin by centrifuging it at 2300 x g for 1 minute at 4°.

2) Quantify the DNA. The average amount of genomic DNA should range from 50 to 200 ng/µl.

3) Centrifuge for 5 minutes at 3000 rpm at 4°C.
4) Wash the antibody-beads complex two times with 1 ml of 1X PBS, 5mg/mL BSA, 0.1% Tween20.
5) Re-suspend the antibody-beads complex in 20 µl of 1X PBS, 5mg/ml BSA, 0.1% Tween20.
6) Divide the antibody-beads complex into two Costar prelubricated tubes, 10 µl per tube.
7) Denaturate the DNA at 100°C for 10 minutes and immediately after put on ice.
8) Add rapidly to each tube: 100 µl of ice-cold 2X PBS and 200 µl of ice-cold 1X PBS, 2% BSA, 0.2% Tween20.
9) Add the DNA solution from each tube to the 10 µl of antibody-beads complex and incubate O/N at 4°C rotating.

3rd Day

1) Place beads-containing tubes in a magnetic grid. Wait until the beads attach to the magnet leaving a clear supernatant.

2) Collect 2.5 µl + 2.5 µl of supernatant from each precipitation tube and put into a new eppendorf tube with 45 µl of ELUTION BUFFER 1X: 50 mM Tris-HCl pH 8.0, 10 mM EDTA, 1% SDS (SUP fraction); keep at RT.

3) Wash the beads as follows:

   - 2X with 1ml of ice-cold ChIP Lysis buffer: 50 mM Hepes-KOH pH 7.5, 140 mM NaCl, 1 mM EDTA, 1% Triton X-100, 0.1% Sodium deoxycholate

- 2X with 1 ml of ice-cold ChIP Lysis buffer +500 mM NaCl
- 2X with 1 ml of ice-cold ChIP Washing buffer: 10 mM Tris-HCl pH 8.0, 250 mM LiCl, 0.5% NP-40, 0.5% Sodium deoxycholate, 1mM EDTA
- 1X with 1ml of ice-cold 1X TE pH 8.0

4) Place the tubes with beads on the magnetic grid. Remove the 1X TE with a micropipette to avoid beads aspiration. Centrifuge 3 minutes at 800 x g at 4°C. Place the tubes back in the magnetic grid and thoroughly remove the remaining liquid with a vacuum pump.
5) Re-suspend the beads in 50 µl of ChIP Elution buffer (50 mM Tris-HCl pH 8.0, 10 mM EDTA, 1% SDS); incubate at 65°C for 10 minutes mixing 3 times during the incubation.
6) Centrifuge 1 minute at 16000 x g at RT.
7) Place the tubes back in the magnetic grid and transfer the eluted material into the new tubes.
8) Add to the IP and to the SUP: 49 µl of 1X TE, 1 µl of Proteinase K (Stock 50 mg/mL).
   The final concentration of Proteinase K is 0.5 mg/ml.
9) Mix, without vortexing, and incubate at 37°C for 1hour.
10) Purify DNA by Qiagen PCR purification Kit. Elute with 50 µl of EB buffer.
11) Pool two identical IP samples together and precipitate the DNA by adding 5 µl of 3 M Sodium Acetate, 1µl glycogen to the IP samples and 2.5 µl of 3 M Sodium Acetate, 0.5 µl glycogen to the SUP samples.

12) Add 2.5 volumes of cold 100% ethanol: 265 µl to the IP samples and 132.5 µl to the SUP samples.
13) Incubate at -20 °C for at least 20 minutes or O/N.
14) Centrifuge at ≥ 13400 x g for 10 minutes at 4 °C.
15) Discard the supernatant using a Gilson pipette and wash with 0.5 ml of ice-cold 70% Ethanol.
16) Centrifuge at ≥ 13400 x g for 10 minutes at 4° C.
17) Discard the supernatant using a Gilson pipette and spin again; discard the remaining Ethanol with a gel-loading tip.
18) Leave for 5 minutes at 37° C. Re-suspend the pellet in 10 µl of ddH_20 .
19) Vortex and pulse-spin for three times to recover the precipitate.
20) Proceed with WGA (Whole Genome Amplification).

Whole Genome amplification

Use WGA2 GenomePlex Complete Genome Amplification (WGA) Kit. Follow manufacturer's instructions from the *Library Preparation* step on:

- Add 2 µl of 1X Library preparation Buffer to each sample.
- Add 1 µl of Library stabilization solution.
- Vortex thoroughly, consolidate by centrifugation and place in thermal cycler at 95° C for 2 minutes.
- Cool the sample on ice. Consolidate the sample by centrifugation and return to ice.
- Add 1 µl Library Preparation Enzyme, vortex thoroughly and centrifuge briefly.

- Place the sample in a thermal cycler and incubate as follows:

  16° C for 20 minutes

  24° C for 20 minutes

  37° C for 20 minutes

  75° C for 5 minutes

  4° C hold

- Remove the samples from the thermal cycler and centrifuge briefly. Samples may be amplified immediately or stored at -20° C for 3 days.

Amplification step:

A master mix may be prepared by adding the following reagents:

- Nuclease-free water: 48.5 µl
- 10X Amplification Master Mix: 7.5 µl
- Reaction from *Library Preparation* step: 14.0 µl
- WGA DNA Polymerase: 5.0 µl

Vortex thoroughly, centrifuge briefly, and begin thermocycling:

Initial Denaturation: 95° C for 3 minutes

Perform 14 cycles as follows:

Denature: 94° C for 15 seconds

Anneal/Extend: 65° C for 5 minutes

When the cycling is complete, maintain the reactions at 4° C or store at -20° C.

After WGA:

1) Pulse-spin the samples.

2) Check the amplified DNA by loading a 1.9 µl aliquot of the reaction in a 1.2% agarose gel. A smear ranging from 100-1000 bp should be observed.
3) Purify the IP/SUP DNA using a PCR purification kit (Qiagen) following the manufacturer's instructions. Elute the DNA with 50 µl of EB buffer.
4) Precipitate the DNA by adding 2.5 µl of 3 M Sodium Acetate, 1 µl of glycogen (20 mg/ml) and 133.75 µl of ice-cold 100% Ethanol.
5) Vortex and incubate at -20 °C for at least 20 minutes or O/N. The duration of precipitation steps at -20°C can be extended without a decrease in the DNA yield.
6) Centrifuge at ≥ 13400 x g for 10 minutes at 4 °C.
7) Discard the supernatant using a Gilson pipette and wash with 1 ml of ice-cold 75% Ethanol.
8) Centrifuge at ≥ 13400 x g for 10 minutes at 4 °C.
9) Discard the supernatant using a Gilson pipette and spin again; discard the remaining ethanol with a gel-loading tip.
10) Let the pellet dry, re-suspend in 42 µl of H_2O (1.5 µl should be used for NanoDrop measure)
11) Measure DNA concentration by spectrometry at 260 nm. (NanoDrop). The DNA concentration after WGA amplification should be in between of 50 ng/µl and 100 ng/µl (linear phase of amplification). If the concentration of the sample is lower, the purified sample can be further amplified by performing 2 additional cycles of the amplification reaction. Performing more than 2 cycles may lead to non-specific material amplification.

DNAse digestion

Short DNAse incubation is performed to reduce the size of amplified DNA and increase its suitability for the hybridization on the array.

1) Prepare DNAse reaction mix (for 13 samples):
   - ddH_2O 14.8 µl
   - 10X One-Phor-All-Buffer plus 2 µl
   - 25mM $CoCl_2$ 1.2 µl
   - DNAse I (1U/ml) 2 µl
2) Prepare the following reaction mix:
   - 10X One-Phor-All-Buffer plus 4.85 µl
     (100 mM Tris-Acetate pH 7.5, 100 mM $Mg(C_2H_3O_2)_2$, 500 mM $KC_2H_3O_2$)
   - 25mM $CoCl_2$ 2.9 µl
   - DNAse I reaction mix 1.5 µl
   - DNA + ddH_2O (IP/SUP) samples 40.75 µl
3) Vortex and pulse-spin to pack the sample.
4) Incubate at 37° C for 30'' and then transfer to 95°C for 15' (Thermocycler).

DNA labeling

1) Spin to pack the sample
2) Transfer DNA into a new 1.5 ml-microcentrifuge tube.
3) Add:

   5 µl of TdT reaction buffer

1 µl Biotin-N11-ddATP (1 nM/ml)

1 µl of TdT (400 U/ml)

4) Vortex and Pulse-spin to recover the sample.

5) Incubate at 37° C for 1 hour.

Hybridization, washing, staining and scanning of chips

Hybridization, washing, chip staining and scanning, as well as discrimination analysis, are performed as described by the manufacture's instructions (Affymetrix http://www.affymetrix.com/).

6.18 GIP with DNA:RNA hybrids precipitation

Before GIP procedure:

Protein A or Protein G Magnetic beads preparation:

- Transfer 20 µl of magnetic beads in a 1.7-ml prelubricated tube.
- Place the tube in a magnetic grid and aspirate the supernatant with a vacuum pump.
- Wash the beads twice as follows: re-suspend the magnetic beads in 0.5 ml of ice cold PBS/BSA by removing the tube from the magnetic grid and gently shaking.
- Place the tube back in the magnetic grid, wait until the beads attach to the magnet leaving a clear solution and aspirate the supernatant with a vacuum pump.
- Add 7.5 µg of S9.6 antibody. Incubate with rotation overnight at 4˚C.

Immediately before use, remove the antibody containing solution; wash twice with ice-cold PBS/BSA and proceed with GIP.

GIP with DNA:RNA hybrids precipitation procedure:

1) Extract the DNA with QIAGEN GENOMIC DNA ISOLATION KIT (Cat. No. 19060) without RNase A treatment. Re-suspend each sample in 300 µl of 1X TE pH 8.
2) Shear the BrdU containing DNA by sonication to a length of 200-1000 bp using the Bandelin UW2070 sonicator. You can use the following parameters:
    - Power 20%
    - 20 seconds/pulse
    - 6 pulses
3) Precipitate 300 µg of the genomic material in a prelubricated eppendorf tube wit Na Acetate, glycogen and ice-cold Ethanol 100% (see 5.17). Precipitate at -20°C O/N.
4) Wash the precipitate with Ethanol 70% and re-suspend in 50 µl of ddH_2O. To re-suspend: vortex and centrifuge at 11600 x g for 1 minute, 3 times.
5) Add 400 µl of FA-1 buffer (0.1% SDS, 1% Triton X100, 10 mM HEPES pH 7.5, 0.1% Na Deoxycholate, 275 mM NaCl; filter), mix.
6) Add 20 µl of washed beads with S9.6 antibody bound. Leave the reaction for 90 minutes at 4°C.
7) Collect 200 µl of IP SUPERNATANT (SUP) in an Eppendorf tube. Leave on ice.
8) Wash the beads as follows (see 5-17):

- 2X with 1ml of ice-cold ChIP Lysis buffer
- 2X with 1 ml of ice-cold ChIP Lysis buffer +500 mM NaCl
- 2X with 1 ml of ice-cold ChIP Washing buffer
- 1X with 1ml of ice-cold 1X TE pH 8.0

9) Remove the TE with a micropipette in order to avoid beads aspiration. Centrifuge the beads at 800 x g for 3 minutes at 4°C. Place the tubes on the magnet and thoroughly remove the remaining liquid with the vacuum pump.
10) Elute the beads with 50 µl of ChIP Elution buffer (see 5.17). Re-suspend the beads by pipetting up and down. Incubate for 10 minutes at 65°C mixing.
11) Centrifuge the tubes for 1 minute at 16000 x g at RT. Move the eluate in a new Eppendorf tube.
12) In a new Eppendorf tube, add 5 µl of IP SUPERNATANT from #7 to 45 µl of ChIP Elution buffer.
13) Add to both the IP and SUP tubes 49 µl of TE 1X pH 8.0 and 1 µl of Proteinase K (Proteinase K stock: 50 mg/ml in 50% glycerol). Mix without vortexing.
14) Leave for 2 hours at 37°C without mixing.
15) Purify the IP/SUP DNA using a PCR purification kit (Qiagen) following the manufacturer's instructions. Elute the DNA with 50 µl of EB buffer.
16) To both the IP and SUP tubes add 50 µl of EB buffer (up to 100 µl). Precipitate with Na Acetate, glycogen and ice-cold Ethanol 100%. Precipitate at -20°C O/N.

17) Wash the precipitate with ice-cold Ethanol 70% and re-suspend in 29 µl of TE 1X + 1 µl of RNase A (stock: 10 mg/ml). Leave the samples for 1 hour at 37°C. To re-suspend: vortex and centrifuge at 11600 x g for 1 minute, 3 times.
18) Add to both the IP and SUP tubes 70 µl of TE 1X. Purify using Qiagen columns using standard protocol. Elute with 50 µl of EB buffer and add 50 µl of EB buffer up to 100 µl. Precipitate with Na Acetate, glycogen and ice-cold Ethanol 100%. Precipitate at -20°C O/N.
19) Wash the precipitate with ice-cold Ethanol 70% and re-suspend in 10 µl of ddH_2O. To re-suspend: vortex and centrifuge at 11600 x g for 1 minute, 3 times.
20) Continue with WGA protocol (see 6.16).

6.19 GIP analyses and statistical methods

Data from all GIP experiments were analyzed using a modified version of the Tiling Array Suite software (TAS) from Affymetrix. Clusters from TAS data were identified as ranges within the chromosome respecting the following conditions: i) estimated signal (IP/SUP binding ratio) positive in the whole range; ii) change P-value of the Wilcoxon signed rank test < 0.2 in the whole range, except for segments within the range shorter than 600 bp; iii) size of the region at least 600bp. The peak of each cluster has been defined as the genomic position within the cluster with the highest estimated signal.

Evaluation of the significance of the presence of BrdU and S9.6 antibody binding peaks were performed by confrontation against a null hypothesis model

generated with a Montecarlo-like simulation. For each data set (binding clusters of a specific protein or set of pausing elements), 1000 randomizations of the positions of the features were produced, maintaining unchanged the number and size of the genomic areas covered within each chromosome; the number of peaks and features with random positions within the *TER*s was then counted and taken as score for each iteration. The distribution of these random scores was validated to be approximately normal (jSkewj < 0.25 and jKurtosis excessj < 0.25), and then the average and standard deviation for this distribution were taken as null hypothesis.

The increase or decrease ratios for the scores of the actual positions with respect to the expected value for the null hypothesis (defined as the average score of random attempts) was then calculated, and the p values for the drift were estimated as Standard Normal CDF of actual_meanj deviation .

6.20 PFGE procedure

Pulse Field Gel Electrophoresis (PFGE) is a technique that enables the resolution of DNA molecules up to several million base pairs in length (Birren et al., 1989; Lai et al., 1989).

Solutions:

- 1% Pulse Field Certified Agarose (PFCA), BIO-RAD #162-0137
- SCE Solution: 1 M Sorbitol, 0.1 M Sodium Citrate, 0.06 M EDTA pH 8.0
- Solution I: SCE, 0.2% β-mercaptoethanol, 1 mg/ml Zymolyase (100 U/ml)
- Solution II: 0.5 M EDTA pH 8.0, 0.1% Sarkosyl, 1 mg/ml Proteinase K

Preparation of the DNA plugs:

1. Melt 1% PFCA and store in a both at 50°C.
2. Re-suspend the cells in Solution I (50 µl for each plug).
3. Add an equal volume of 50°C molten PFCA and mix with a pipette.
4. Fill plug-cast (BIOR-RAD) with cell/agarose mix (approximately 90 µl per plug).
5. Leave the cast for 20 minutes at RT and 10 minutes at 4°C.
6. Eject the plugs in a 50 ml Falcon tube and cover them with Solution I (~ 0.5 ml for plug.
7. Leave at 37°C for 1 hour.
8. Gently remove Solution I and wash the plugs with an abundant volume of 0.5 M EDTA pH 8.0.
9. Re-suspend the plugs with Solution II (0.5 ml/plug) and incubate O/N at 37°C.
10. Discard the Solution II and wash 3 times with an abundant volume of 1X TE pH 8.0.
11. Transfer the plugs in a new 50 ml falcon tube and wash for 2 hours with 1X TE pH 8.0 on a rotating wheel.
12. Transfer the plugs that you do not analyse in a 50 ml falcon tube and cover them with 1X TE pH 8.0. The plugs can be stored indefinitely at 4°C.
13. Transfer the plugs that you wish to analyse in an Eppendorf tube and equilibrate them for 1 hour in the running buffer of the gel (0.5 X TBE) on a rotating wheel.

Electrophoresis is performed on a 1% pulse field agarose gel for 16 hours at 200 V with 60 sec pulses followed by 90 sec pulses in 0.5 X TBE at 14°C (Gene Navigator System, Amersham).

The gel is then coloured with 0.3 μg /ml Ethidium Bromide for 30 min and then subjected to Southern blot. The membrane is then hybridized with a radiolabeled probe against specific region on the chromosome.

6.21 DAPI staining

Procedure:

1) Mix cells (~1 ml of 1 X 10^7 cells) by vigorous vortexing.
2) Spin cells down in micro-centrifuge.
3) Wash in 1X PBS.
4) Fix with Ethanol 70% for 20 minutes at RT.
5) Wash in 1X PBS.
6) Add DAPI (1mg/ml) 1:1000 dilution and leave 12 minutes at RT.
7) Wash in 1X PBS.

7 Results

7.1 *sen1 rrm3* synthetic lethality

The Rrm3 helicase facilitates replication fork progression across tRNA but not over ORFs of highly transcribed RNAPII genes (Azvolinsky et al., 2009). Moreover, Rrm3 promotes fork movement across termination sites (*TER*s). The vast majority of *TER*s contain transcribed mRNA, but also tRNA, *CEN*, Ty and LTRs as pausing elements (Fachinetti et al., 2010). *RRM3* ablated cells, in combination with certain mutations affecting a variety of DNA metabolic processes (homologous recombination, telomere maintenance, DNA damage response, DNA repair, G-quadruplexes unwinding), are not viable (Figure 1). We presumed that in certain double mutant combinations replication fork progression across *TER*s is perturbed and fork fusion does not occur at the very last step of termination.

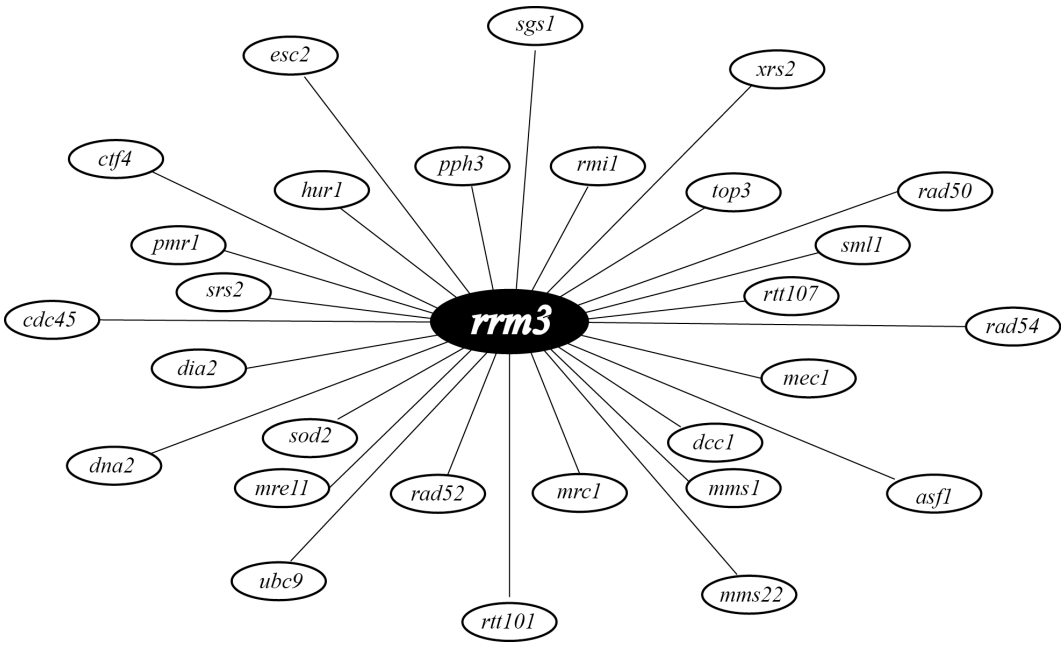

Figure 1. *rrm3* synthetic lethality with certain altered in metabolic processes factors.

The synthetic lethal interactions between *rrm3* and other ablated genes. The data comes from http://thebiogrid.org.

Replication fork progression across RNAPII-transcribed genes is promoted by the Sen1/Senataxin DNA:RNA helicase and Sen1 replication related function is independent from its role in RNA processing (Alzu et al., 2012). Alike Rrm3, Sen1 is associated and travels with replication forks. Since Sen1 exhibits synthetic lethal interactions with several mutant genes, which are also synthetic lethal with *rrm3*, we tested the interaction between *sen1-1* and *rrm3* (Figure 2A). Temperature sensitive *sen1-1* strain, which is not viable at 37°C, bears an aminoacidic substitution in the essential helicase domain (DeMarini et al., 1992). Two parental haploid strains, carrying the *sen1-1* and *rrm3* mutations, were crossed and then a heterozygous diploid was subjected to sporulation and tetrad dissection. Spores were grown at semi-permissive temperature, 30°C, at which *sen1-1* single mutant spores are still viable. Conversely, we found that the double mutants are unviable. (Figure 2B). This observation drove us to investigate both Rrm3 and Sen1 helicases in terms of DNA replication termination.

A

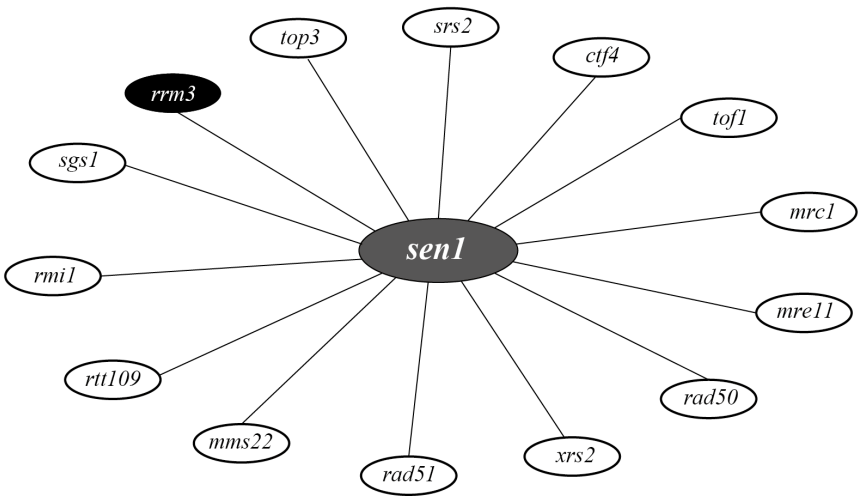

B

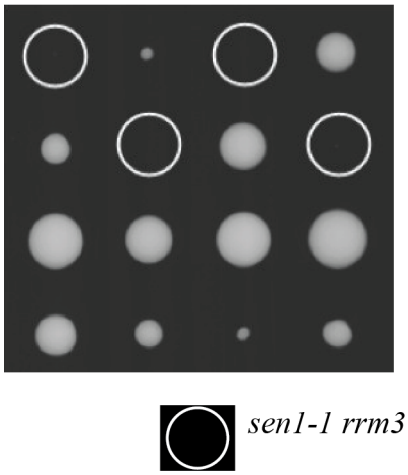

sen1-1 rrm3

Figure 2. *sen1-1* synthetic lethality.

(A) *sen1-1* synthetic lethality with specific mutations (Alzu et al., 2012).
(B) *sen1-1 rrm3* synthetic lethality. Tetrads obtained from the sporulation of the heterozygous diploid, *sen1-1 rrm3*, were grown at 30°C. White circles indicate double mutant spores.

7.1.1 Construction of a *GAL-URL-3HA-SEN1* conditional system

We did not use temperature sensitive *sen1-1* strain because turnover of termination replication intermediates at 37°C is very fast. Thus, all the experiments were performed with *GAL-URL-3HA-SEN1* conditional system with deleted *RRM3* gene. Because *SEN1* deletion causes lethality, the Sen1 depletion was achieved by fusing the ORF of *SEN1* to a ubiquitin-arginine-lacZ fusion (*URL-SEN1*) (Bachmair et al., 1986; Visintin et al., 2008) under the control of *GAL1-10* promoter. The kanmx4 marker gene confers resistance of the strain to G418 drug and *3HA* tag allows following Sen1p expression. In this *GAL-URL-3HA-SEN1* conditional system (Figure 3) Sen1 can be rapidly depleted in glucose medium.

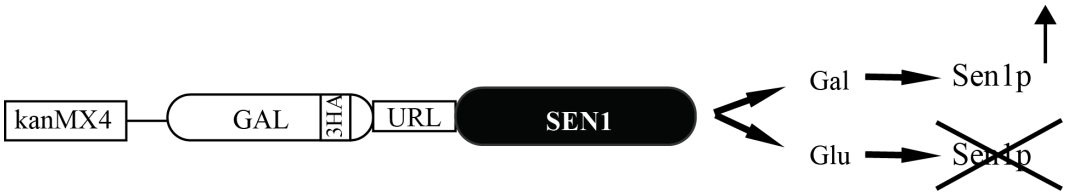

Figure 3. The scheme of the *GAL-URL-3HA-SEN1* conditional system.

Cells grown in medium supplemented with 2 % Gal are viable due to Sen1p expression. Switching the medium to 2% Glu depletes Sen1 through its protein's N-terminal amino acid modification.

The efficiency of depleting Sen1 was analysed by Western-blot (Figure 4A). *3HA*-tagged Sen1 is depleted already at 30-minute after changing the medium to YPD. Serial dilutions on YPD plates of both *GAL-URL-3HA-SEN1* and *GAL-URL-3HA-SEN1 rrm3* show that both the single and the double mutants were not viable (Figure 4B).

A

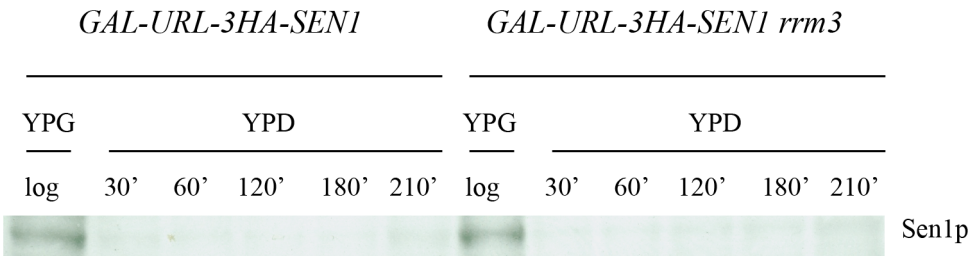

B

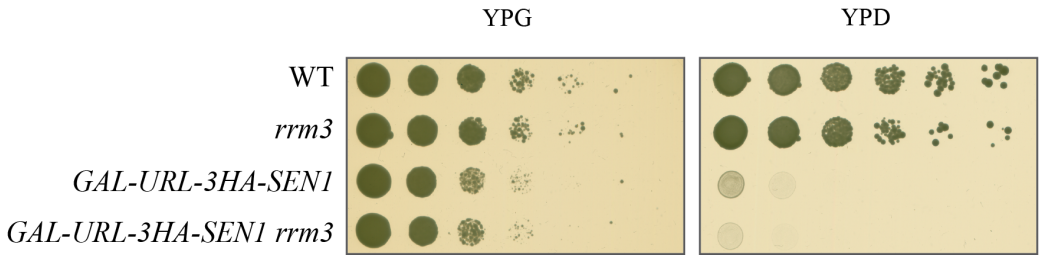

Figure 4. Efficiency of Sen1 depletion.

(A) *GAL-URL-3HA-SEN1* and *GAL-URL-3HA-SEN1 rrm3* cells were grown exponentially at 25°C (log) in YPG, synchronized with α-factor in G1 in YPG and released in YPD at 25°C. Indicated time points were collected to assess Sen1p levels by Western-blot.
(B) Serial dilutions of WT, *rrm3*, *GAL-URL-3HA-SEN1*, *GAL-URL-3HA-SEN1 rrm3* in YPG and YPD. The experiment was done at 25°C.

7.2 Cell cycle progression in Sen1- and Rrm3- depleted cells is blocked in G2/M

Sen1 depletion in *rrm3* mutants arrested the vast majority of cells in the first cell cycle. Cells depleted of Sen1 and Rrm3 completed S phase and approximately 80 % of double mutant cells were arrested in G2/M, while 20 % re-entered the next cell cycle (Figure 5). The subpopulation of Sen1- and Rrm3-depleted cells that exit mitosis was arrested in the next G2/M phase (data not shown). In contrary, WT, *rrm3* and Sen1- depleted cells kept cycling.

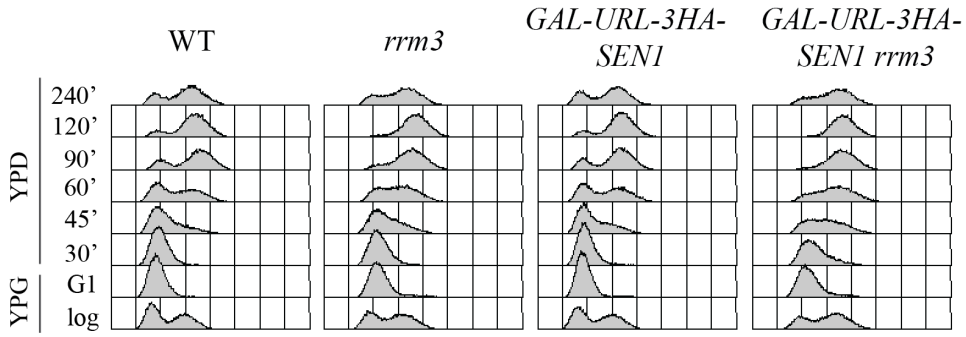

Figure 5. Cell cycle progression analyses in WT, *rrm3*, *GAL-URL-3HA-SEN1* and *GAL-URL-3HA-SEN1 rrm3* cells.

Cells were grown in YPG medium at 25°C, arrested with α-factor and released in YPD at 25°C. Samples were collected at the indicated time points for FACS analysis.

7.3 Defects in nuclei division in Sen1- and Rrm3- depleted cells

In *Saccharomyces cerevisiae*, bud emerges when DNA starts being replicated. Along with the S phase the bud is growing. When DNA replication is completed, cells can enter the G2 phase. Before anaphase and nuclear segregation, the nucleus is localized at the neck of the emerging bud. The entrance into mitosis results in the formation of elongated and bipolar nucleus. At the end, cytokinesis generates two unbudded cells.

We aimed to investigate whether Sen1- and Rrm3- depleted cells show defects in nucleus division. For this purpose we analysed WT and *GAL-URL-3HA-SEN1 rrm3* cells, at 240-minute from the release into S phase in YPD, by DAPI staining. Sen1- and Rrm3- deficient cells were arrested in G2/M, whereas WT cells kept cycling (Figure 6A). Both brightfield and fluorescent images are presented in WT and *GAL-URL-3HA-SEN1 rrm3* cells (Figure 6B). In 80% of the double mutant cells we observed the lack of division of the nucleus, which remained at the neck of the emerging bud. The nuclear division defect indicates that in the absence of Sen1 and Rrm3 helicases the cell cycle stops before anaphase.

A

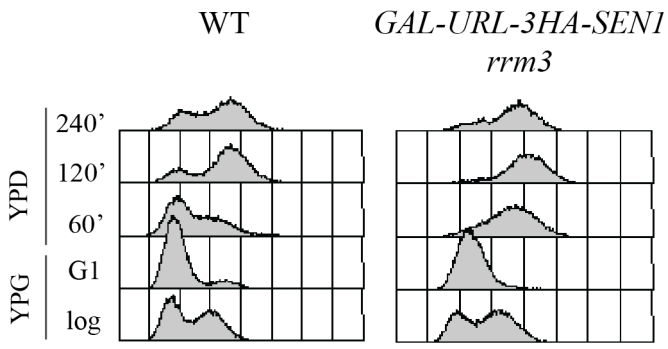

B

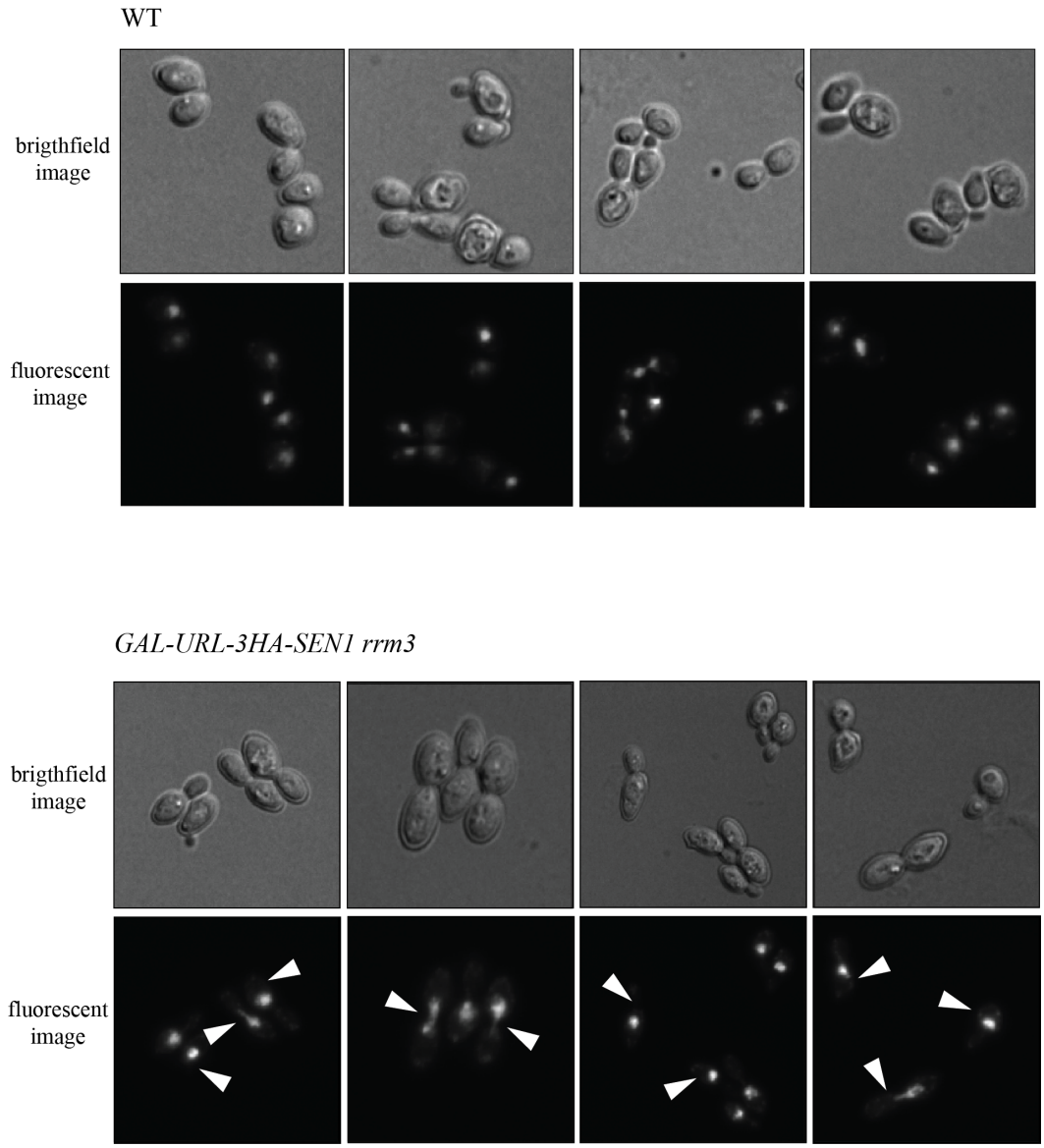

Figure 6. Nuclei division defects in *GAL-URL-3HA-SEN1 rrm3* cells.

WT and *GAL-URL-3HA-SEN1 rrm3* cells were grown exponentially at 25°C (log) in YPG, synchronized with α-factor in G1 in YPG and released in YPD at 25°C.
(A) Indicated time points were collected for FACS analysis.
(B) Cells from 240-minute time point were fixed with 70% Ethanol, stained with DAPI and visualized by taking brightfield and fluorescent images. White arrows indicate cells with nucleus at the budding neck. 500 cells were counted.

7.4 Replicated DNA in *GAL-URL-3HA-SEN1 rrm3* cells is topologically altered

The PFGE techinique enables to detect the chromosome breakage and entangling due to the topological problems. We aimed to investigate the replicating chromosomal DNA in WT, *rrm3*, *GAL-URL-3HA-SEN1* and *GAL-URL-3HA-SEN1 rrm3* cells by arresting the cultures in G1 and releasing in S phase in the presence of nocodazole to prevent the cells to enter the next cell cycle (Figure 7A). WT and both single mutants, *rrm3* and *GAL-URL-3HA-SEN1*, almost completed DNA replication within 180-minute from the release. Approximately 8% of the total DNA in all these strains remained in the well due to the topological entangling (Figure 7B and 7C). At 240-minute the replication was fully completed (~4% of DNA trapped in the well). Conversely, 46% and 25% of the *GAL-URL-3HA-SEN1 rrm3* chromosomal DNA remained entangled and still trapped within the well at 180 and 240 minute, respectively. Thus, most probably, the absence of both Sen1 and Rrm3 helicases alter the topological state of replicated DNA, generating entangled chromosomes.

A

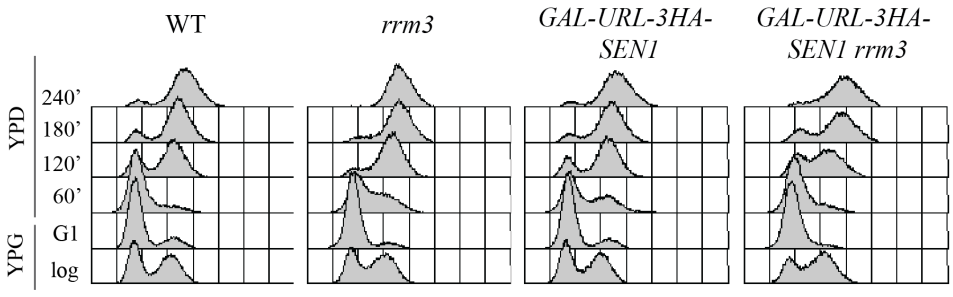

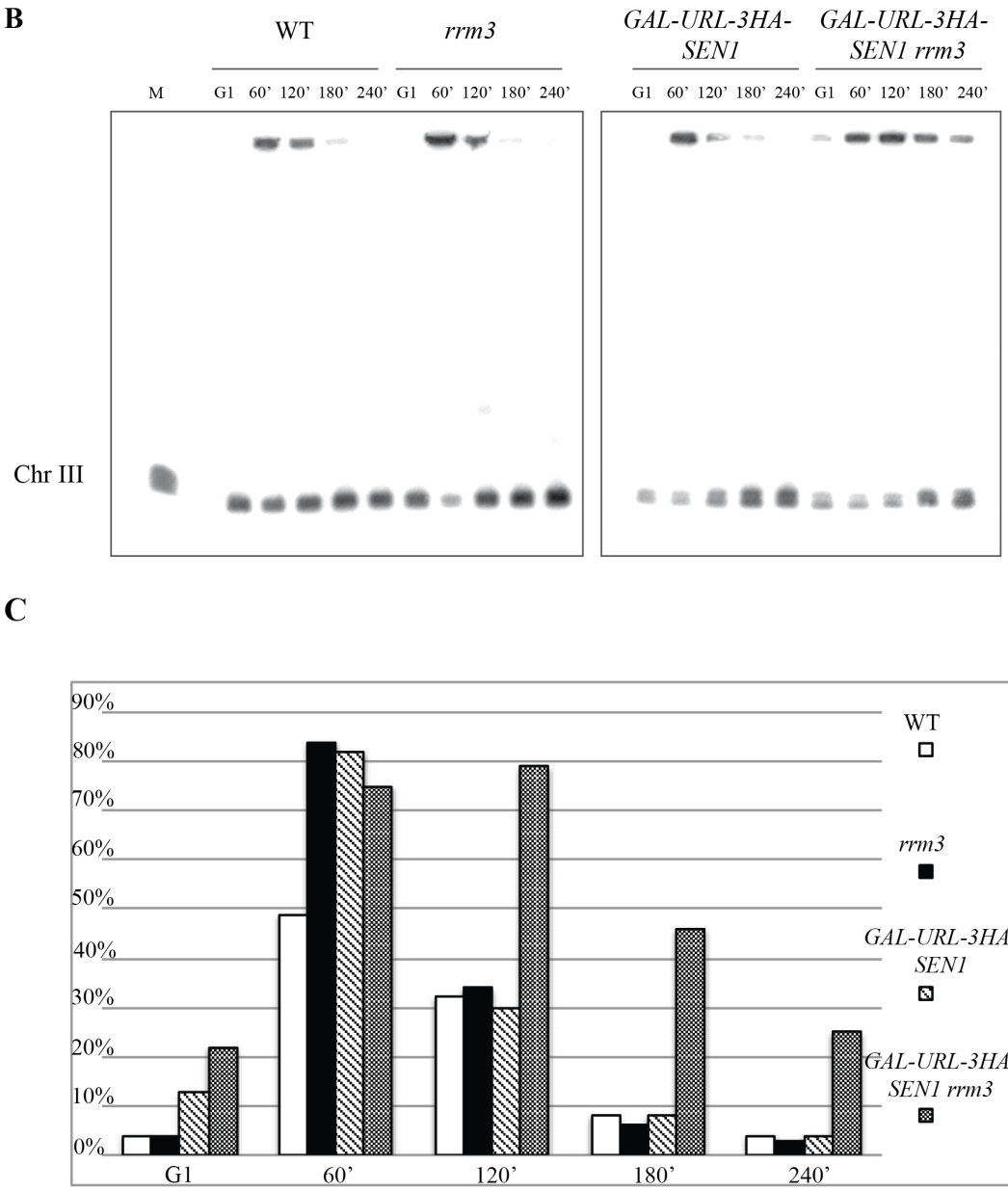

Figure 7. *GAL-URL-3HA-SEN1 rrm3* cells accumulate branched molecules in G2/M arrested cells.

WT, *rrm3*, *GAL-URL-3HA-SEN1* and *GAL-URL-3HA-SEN1 rrm3* cells were grown exponentially at 25°C (log) in YPG, synchronized with α-factor in G1 in YPG and released in YPD at 25°C in the presence of nocodazole.

(A) Indicated time points were collected for FACS analysis.

(B) Genomic DNA was extracted in agarose plugs at the indicated time points. Yeast chromosomes were separated by PFGE and analysed by Southern blot followed by radiolabelling with *ARS305* probe. M indicates the chromosome marker.

(C) Percentage of the total chromosomal DNA subjected to PFGE trapped within the well at G1, 60', 120', 180' and 240'. Quantification was done by using ImageQuant Software.

7.5 Origin firing is not affected in *GAL-URL-3HA-SEN1 rrm3* cells

Duplication of eukaryotic chromosomes proceeds bidirectionally from active origins. Both chromosomal context and chromatin structure affect origin activity. The 2D-gel technique was developed to study replication intermediates (RIs) (Brewer and Fangman, 1987) and was used to map and characterize replication origins (Brewer and Fangman, 1988). As DNA replication continues, a sample of isolated DNA from exponentially growing cells contains RIs ranging from the linear non-replicative forms (1 N) to DNA molecules almost replicated. The migration of RIs in an agarose gel is determined by the electrophoretic conditions (agarose concentration, the presence of intercalating agents, the voltage etc.) and the size and the shape of the molecule.

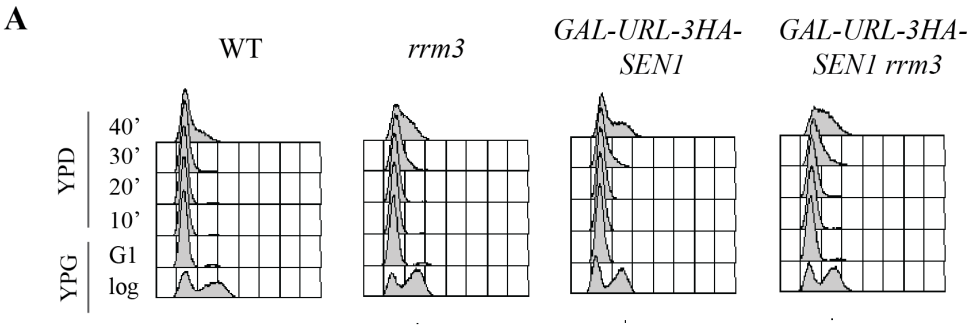

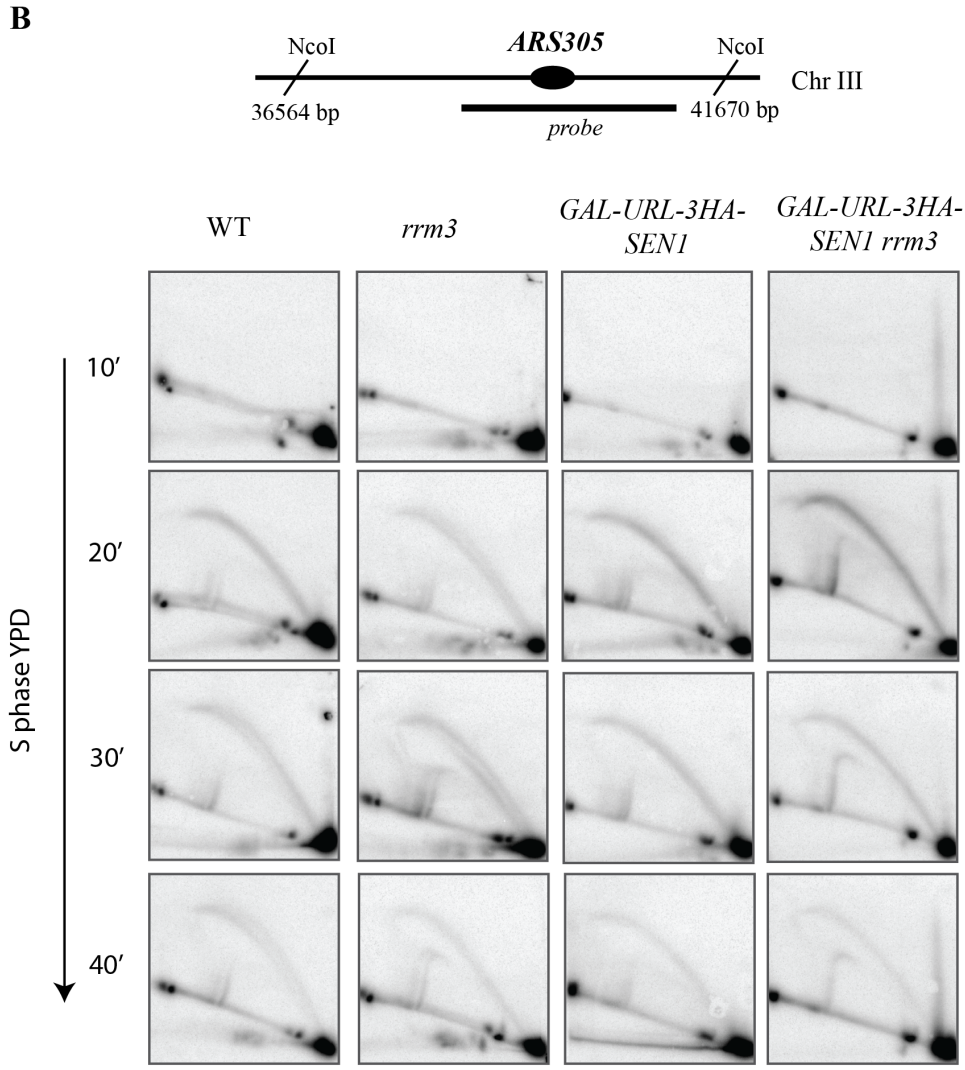

Figure 8. No delay in firing of the early replication origin in *GAL-URL-3HA-SEN1 rrm3* cells.

WT, *rrm3*, *GAL-URL-3HA-SEN1* and *GAL-URL-3HA-SEN1 rrm3* cells were grown exponentially at 25°C (log) in YPG, synchronized with α-factor in G1 in YPG and released in YPD at 25°C.

(A) Indicated time points were collected for FACS analysis.

(B) Genomic DNA was psoralen-crosslinked and extracted by CTAB technique at the indicated time points. 8 µg of DNA was digested with *Nco*I enzyme, analysed by 2D-gels, Southern-blotted and labelled with *ARS305* radioactive probe. The schematic representation of the digestion strategy and probe localization is depicted above the 2D-gels.

ARS305 is an active origin of replication that fires early in S phase in more than 90% of the population of the cells (Newlon et al., 1993). It is located 40 kbp from the left end on chromosome III. We monitored the origin firing in WT, *rrm3*, *GAL-URL-3HA-SEN1* and *GAL-URL-3HA-SEN1 rrm3* cells pre-synchronized in G1 and released into S phase (Figure 8A). As noticed by the appearance of the bubble arc, in all analysed strains replication origin fires at 20-minute and the replication forks move bidirectionally from *ARS305* locus (Figure 8B). At 40-minute time point replication bubbles are still detectable, but the signal is less strong due to moving replication forks that invade the relative flanking regions. We did not observe differences between the analysed strains at the level of origin firing or replication intermediates. Hence, Sen1 and Rrm3 depletion does not alter the timing of replication initiation.

7.6 Impaired DNA replication termination in *GAL-URL-3HA-SEN1 rrm3* cells

Using Neutral/Neutral 2D-gel technique we aimed to monitor replication termination events in Sen1- and Rrm3- depleted cells at previously characterized termination zones: *TER102*, *TER603*, *TER802*, *TER303* (data not shown) and *TER704* (data not shown) (Fachinetti et al., 2010). The visualization of replication intermediates is hampered due to the fast turnover of termination intermediates and replication fork velocity. Thus, all 2D-gel experiments were coupled with chromatin psoralen-crosslinking and DNA extraction was performed using a CTAB method, which increases the yield of extracted DNA.

TER102 and *TER802* are termination zones that contain a head-on Pol II-non-highly and highly transcribed gene, respectively, which slows a replication fork independently of Rrm3 helicase (Azvolinsky et al., 2009). While WT cells accumulate at both *TER102* and *TER802* a cone signal due to random termination, *rrm3* cells accumulate X-shaped molecules that result from the impaired fusion of merging forks. In WT cells the conversion of Xs into linear molecules is very fast, thus the spike is not observed (Fachinetti et al., 2010).

TER603 and *TER303* contain a head-on Pol III-transcribed gene (Fachinetti et al., 2010). At these termination zones, WT accumulates a pausing signal on the Y-arc and termination intermediates (above the arc). In *rrm3* cells the intensity of the spot on the Y-arc is increased and other spot in the descending arm of the arc is detectable due to Rrm3 role in facilitating fork progression even at codirectionally transcribed Pol III genes with replication fork (Fachinetti et al., 2010). In the middle of the spike an asymmetric X-spot accumulates due to termination at tRNA site.

Replication termination occurs in early S phase in all the *TER*s mentioned above, thus the experimental conditions to detect termination structures were identical. All 2D-gel experiments were done using four strains: WT, *rrm3, GAL-URL-3HA-SEN1* and *GAL-URL-3HA-SEN1 rrm3*, pre-synchronized in G1 and then released into S phase (Figure 9A).

WT and Sen1- depleted cells do not show any defects in replication fork progression across *TER*s and replication termination intermediates resolution (Figure 9B, C, D). The DNA replication termination in *GAL-URL-3HA-SEN1 rrm3* mutants is impaired due to the accumulation of X-structures at *TER102* and *TER802* and pausing signals at *TER603*. However, we failed to observe

synergistic defects in the double mutants compared to *rrm3* at *TER102*, *TER802* and *TER603* (Figure 9B, C, D). We obtained analogous results at *TER303* and at centromere-dependent termination zone *TER704* (data not shown).

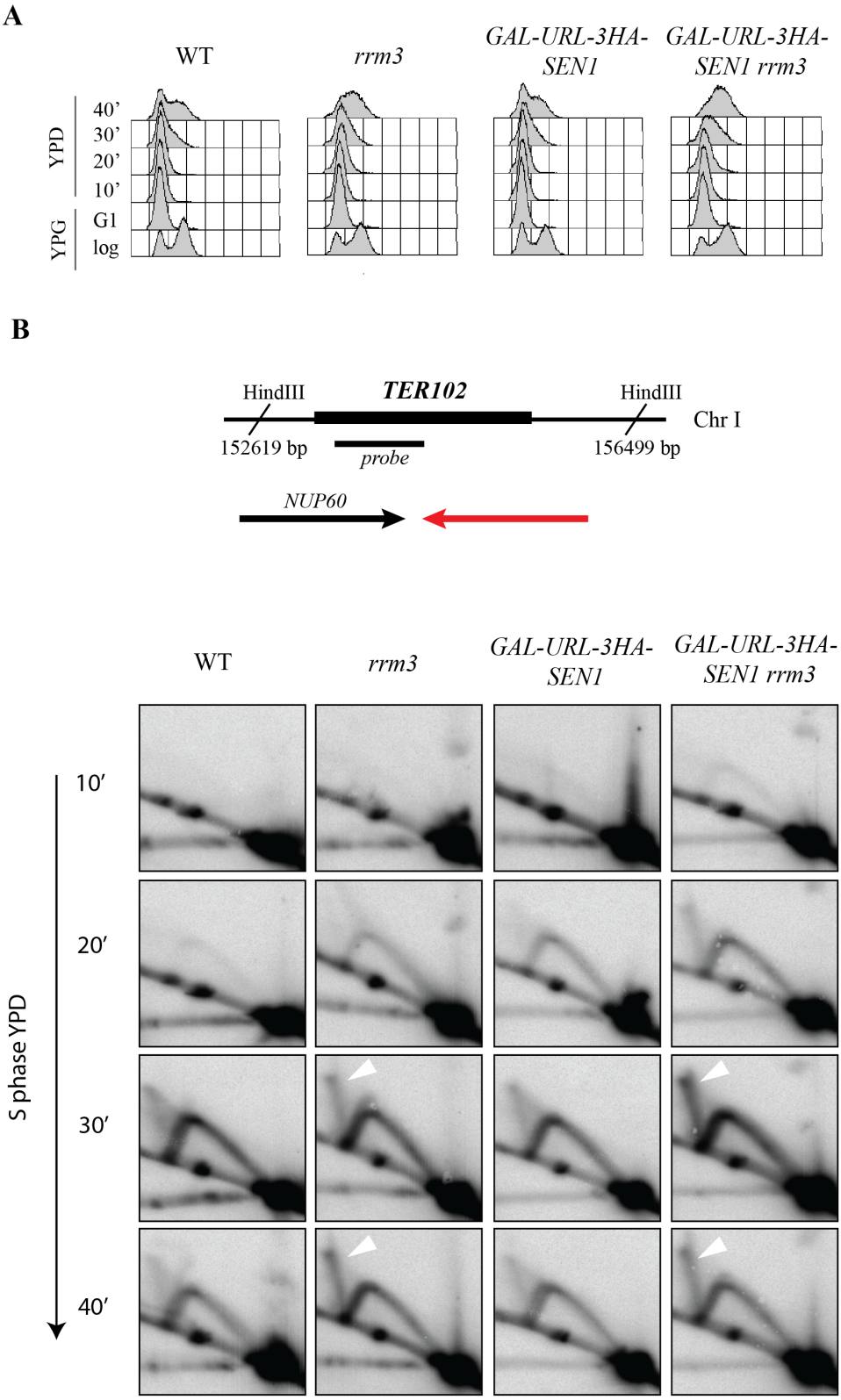

C

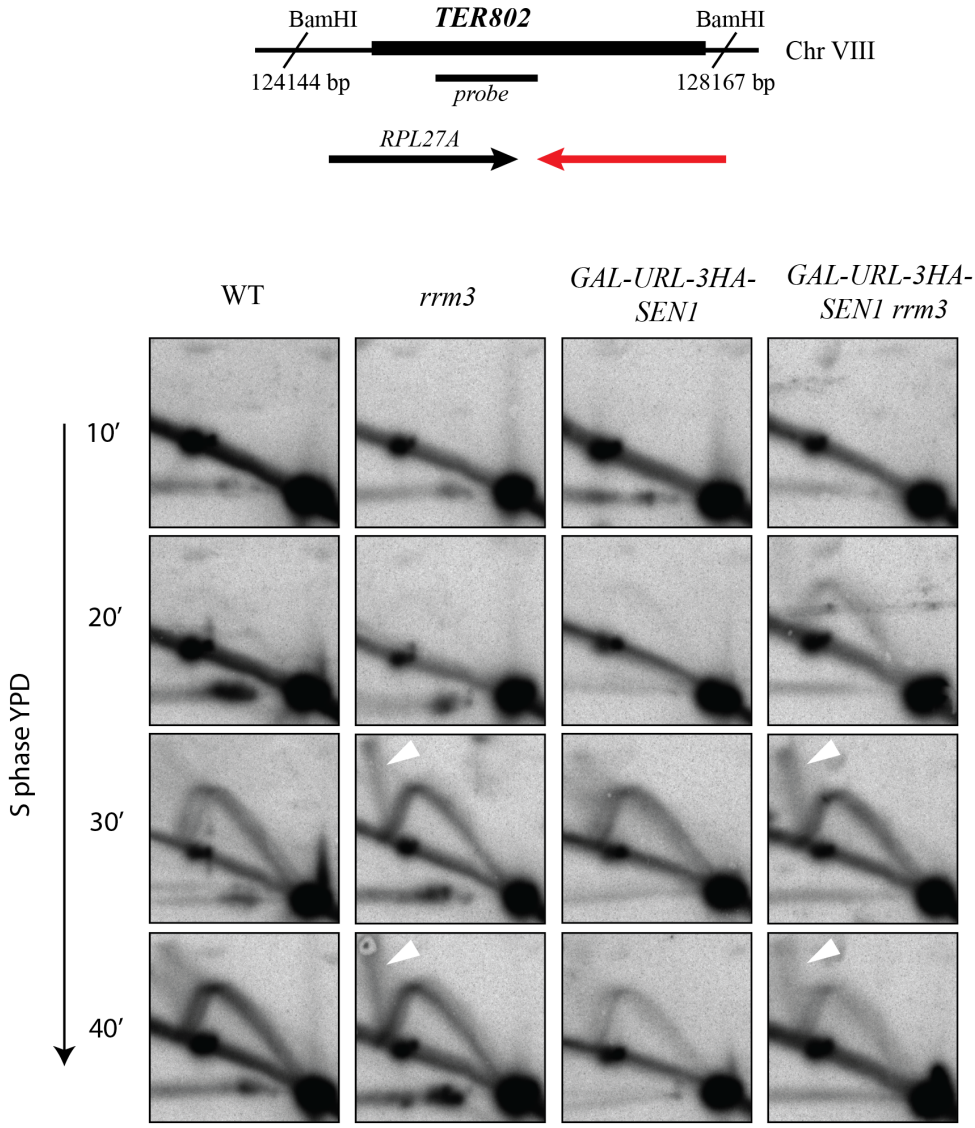
BamHI
TER802
BamHI
Chr VIII
124144 bp
probe
128167 bp
RPL27A
WT
rrm3
GAL-URL-3HA-SEN1
GAL-URL-3HA-SEN1 rrm3
S phase YPD
10′
20′
30′
40′

D

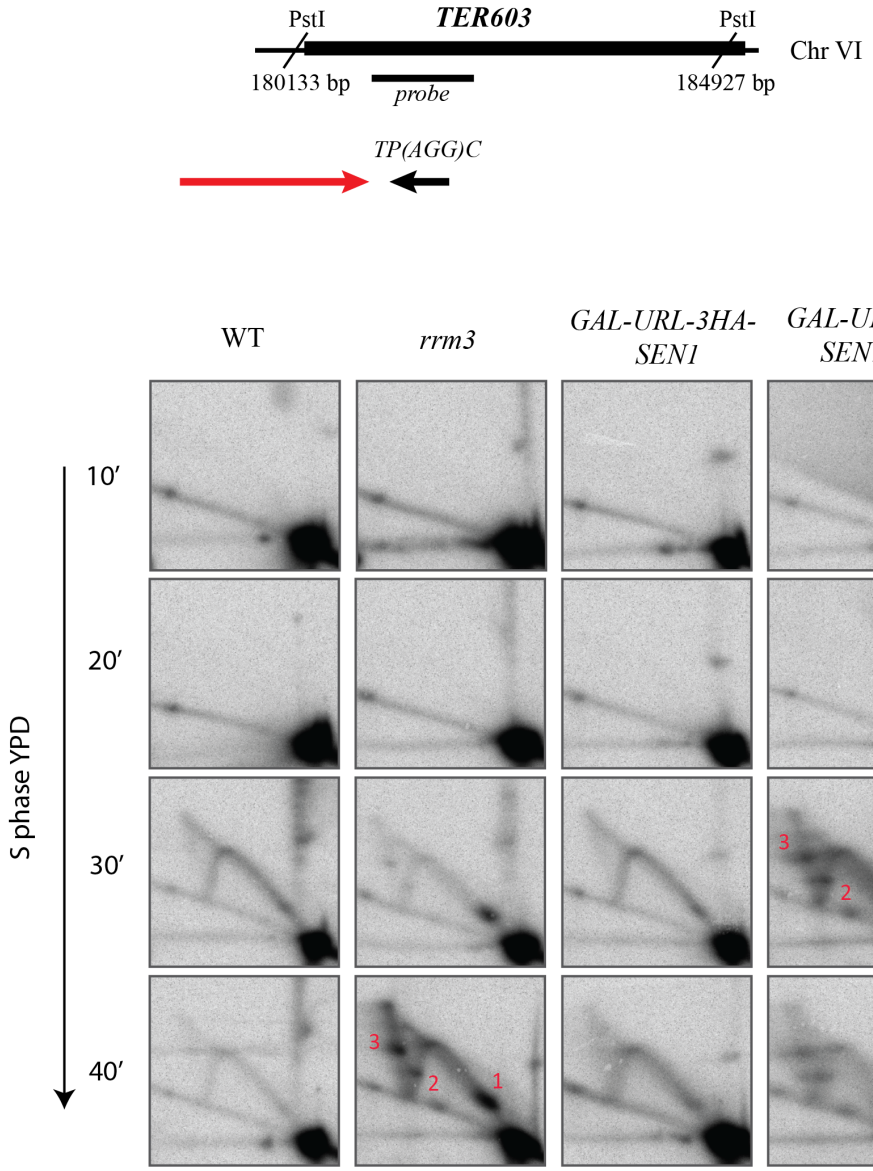

Figure 9. Both Sen1 and Rrm3 helicases are required for appropriate replication fork progression across *TER*s.

WT, *rrm3*, *GAL-URL-3HA-SEN1* and *GAL-URL-3HA-SEN1 rrm3* cells were grown exponentially at 25°C (log) in YPG, synchronized with α-factor in G1 in YPG and released in YPD at 25°C. White arrows indicate X-shaped molecules, 1 – pausing from left coming fork, 2 – pausing from right coming fork, 3 – asymmetric X-spot.

(A) Cell cycle progression followed by FACS analysis.

(B-D) Replication termination intermediates analysed by 2D-gel technique. Genomic DNA was psoralen-crosslinked and extracted by CTAB technique at the indicated time points. 20 µg of DNA was digested to increase the chance to visualize replication intermediates, subjected to 2D-gel procedure, Southern blotted and radiolabelled with a specific to each termination zone probe. The schematic representations of the digestion strategy and probe localization are depicted above each 2D-gel experiment. Red arrow indicates the direction of replication fork encountering RNA transcript depicted by black arrow. 2D-gels at *TER*s in strains described above were repeated several times with consistent results.

7.7 Recombination does not mediate termination events

Both Sen1- depleted and *rrm3* cells are lethal in combination with mutants impaired in homologous recombination (HR), such as *rad50* and *rad51*. Interestingly, in Prokaryotes recombination is engaged to deal with termination under pathological situations (Louarn et al., 1994). Therefore, we intended to address whether Rad51 mediates DNA replication termination in the absence of Rrm3 and Sen1.

Rad51 belongs to the Rad52 epistasis group, which includes Rad50, Rad52, Rad54, Rad55, Rad57, Rad59, Mre11 and Xrs2. All of these factors are involved in DNA DSBs repair. Rad51 is a recombinase that binds DNA (Shinohara et al., 1992) and catalyses the identification and exchange of homologous sequences between ssDNA and dsDNA molecule (Sung, 1994). Rad51p interacts with itself and other HR factors from *RAD52* epistasis group.

A

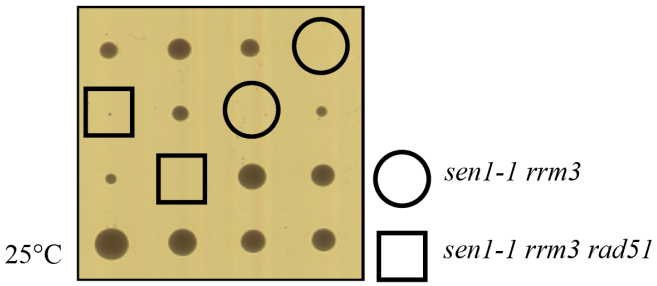

B

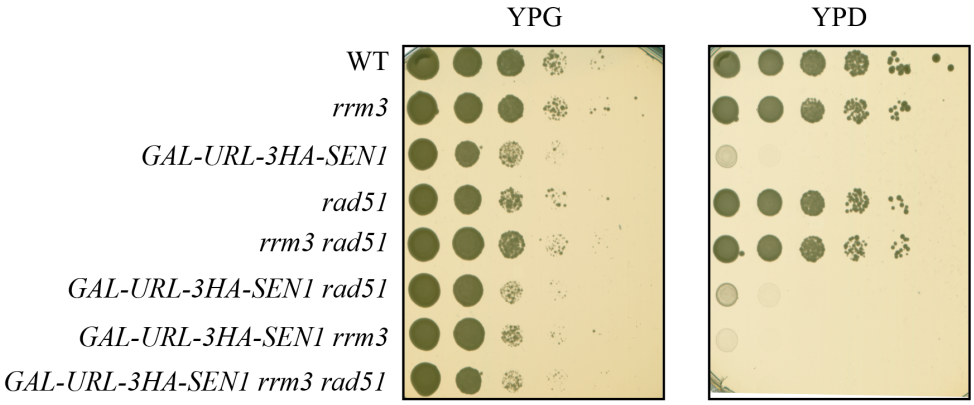

Figure 10. *RAD51* deletion does not rescue *GAL-URL-3HA-SEN1 rm3* lethality.

(A) *sen1-1 rrm3 rad51* synthetic lethality. Tetrads obtained from the sporulation of the heterozygous diploid, *sen1-1 rrm3 rad51*, were grown at 25°C. Circles indicate double mutant while squares the triple mutant spores.
(B) Serial dilutions of WT, *rrm3*, *GAL-URL-3HA-SEN1*, *rad51*, *rrm3 rad51*, *GAL-URL-3HA-SEN1 rad51*, *GAL-URL-3HA-SEN1 rrm3* and *GAL-URL-3HA-SEN1 rrm3 rad51* in YPG and YPD. The experiment was done at 25°C.

RAD51 deletion rescues the synthetic lethality of *sen1-1 sgs1* at 25°C and partially *sen1-1 srs2* at 37°C (Alzu et al., 2012). Based on these observations we tested whether *sen1-1 rrm3* lethality is also rescued by *rad51*. For this purpose *sen1-1 rrm3* was crossed with *rad51* and the tetrads from heterozygous diploid were subjected to sporulation (Figure 10A). *sen1-1 rrm3 rad51* cells are lethal and

GAL-URL-3HA-SEN1 rrm3 rad51 combination is not viable when switched to YPD medium (Figure 10B). Hence, *RAD51* deletion does not rescue the lethal phenotype of *GAL-URL-3HA-SEN1 rrm3* mutants.

We then monitored the replication termination intermediates arising from replication fork converging in *GAL-URL-3HA-SEN1 rrm3 rad51* cells, using WT, *rrm3*, *GAL-URL-3HA-SEN1*, *rad51*, *GAL-URL-3HA-SEN1 rrm3*, *GAL-URL-3HA-SEN1 rad51* and *rrm3 rad51* as control strains. At 30-minute time point in S phase (Figure 11A) we did not observe any additive effect of deleting *RAD51* in *GAL-URL-3HA-SEN1 rrm3* (Figure 11B). The Xs spike seen in the triple mutant is Rrm3-dependent and not recombination-related, because the intensity of the X spike in both *GAL-URL-3HA-SEN1 rad51* and *rad51* mutants is similar to the one of WT cells.

A

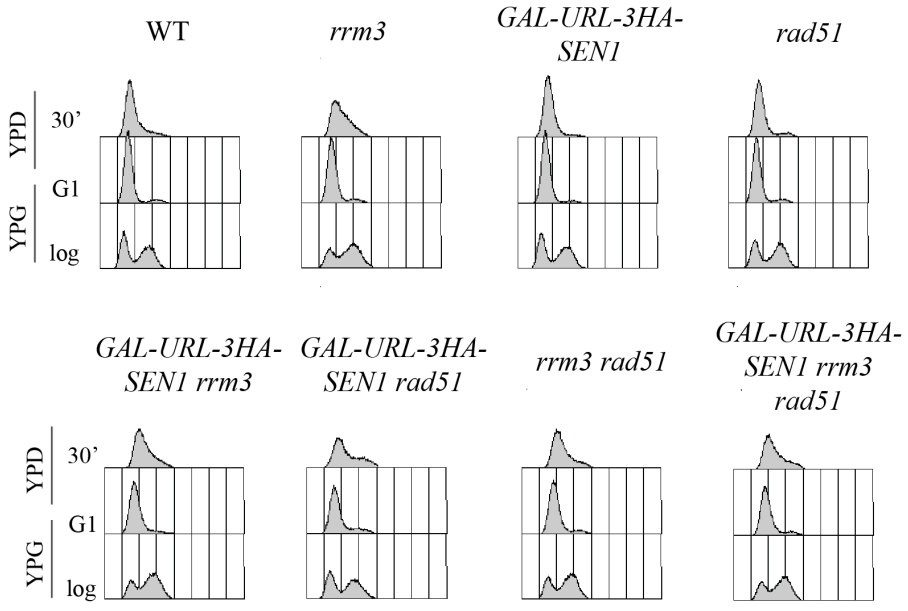

B

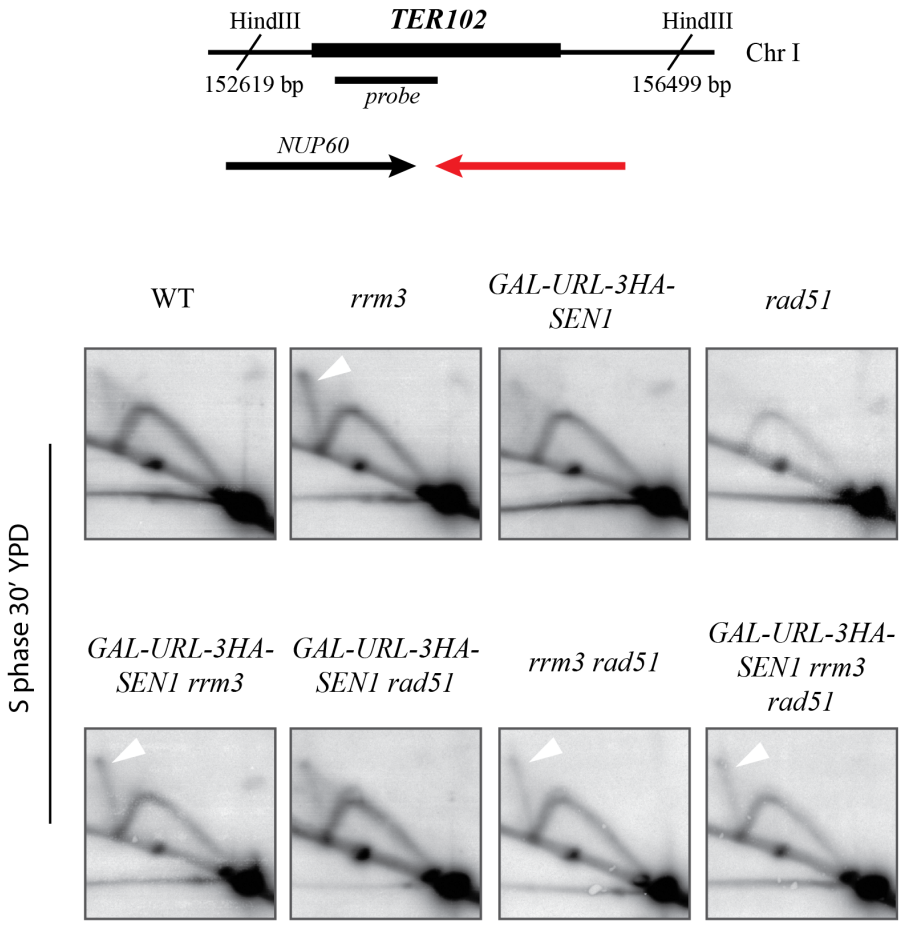

Figure 11. Rad51 does not mediate replication termination.

WT, *rrm3*, *GAL-URL-3HA-SEN1*, *rad51*, *GAL-URL-3HA-SEN1 rrm3*, *GAL-URL-3HA-SEN1 rad51*, *rrm3 rad51* and *GAL-URL-3HA-SEN1 rrm3 rad51* cells were grown exponentially at 25°C (log) in YPG, synchronized with α-factor in G1 in YPG and released in YPD at 25°C. White arrows indicate X-shaped molecules.

(A) Cell cycle progression followed by FACS analysis.

(B) 2D-gel analysis at *TER102*. Genomic DNA was psoralen-crosslinked and extracted by CTAB technique at 30-minute from the release into S phase. 20 µg of DNA was digested, subjected to 2D-gel procedure, Southern blotted and radiolabelled with *TER102* probe. The schematic representations of the digestion strategy and probe localization are depicted above the 2D-gels' panel. Red arrow indicates the direction of replication fork encountering RNA transcript depicted by black arrow.

7.8 DNA replication termination failure in the absence of Sen1 and Rrm3 helicases

Genome-wide analysis has been used to monitor the replication dynamics in the budding yeast genome (Raghuraman et al., 2001; Raveendranathan et al., 2006) (Wyrick et al., 2001). Although the activation of replication origins is well characterized in *Saccharomyces cerevisiae*, our knowledge about the control mechanisms at termination zones is very little.

In order to shed light on replication termination processes we used genome-wide immunoprecipitation (GIP) with Bromodeoxyuridine (BrdU) incorporation technique to monitor replication forks progression at termination zones in WT, *rrm3*, *GAL-URL-3HA-SEN1* and *GAL-URL-3HA SEN1 rrm3* cells. Bromodeoxyuridine is a synthetic nucleoside, which is an analogue of thymidine. BrdU can be incorporated into the newly synthesized DNA of replicating cells substituting for thymidine during DNA replication. Since yeast cells are not able to incorporate BrdU, seven copies of the Herpes simplex *TK* gene under control of the yeast *GPD* promoter were inserted at the *URA3* locus of chromosome V in a haploid *Saccharomyces cerevisiae* strain (Lengronne et al., 2001). In this way BrdU is incorporated into the newly synthesized DNA strand.

The cells were grown O/N in a medium selective for *TK* copies (-URA). In the morning the minimal medium was changed for YPG and cells were pre-synchronized in G1 with α-factor. 200 μg/ml of BrdU was added 30 minutes before the release into S phase in a fresh YPD medium containing 200 μg/ml of BrdU and 10 μg/ml of nocodazole. To keep a G2/M arrest up to 3 hours, 10 μg/ml of nocodazole was re-added after 1 hour (Figure 12A). Due to BrdU incorporation time limitations (Lengronne et al., 2001), working at 25°C and changing the

medium from YPG to YPD, which slows down replication fork progression, we were able to monitor replication fork fusion across *TER*s localized in between early firing origins with inter-origin distance up to 25 kb. 71 *TER*s has been mapped in the recent studies in replication termination (Fachinetti et al., 2010). 1/3 (23 *TER*s) of those *TER*s have inter-origin distance between 10 and 25 kb. Only in *TER503*, *TER601*, *TER704*, *TER902*, *TER1202*, *TER1604* we did observe fork fusion both in WT and *GAL-URL-3HA-SEN1 rrm3* cells. *TER704*, *TER1202* and *TER1604* are CEN-dependent while *TER503*, *TER601* and *TER902* are non-highly transcribed Pol II termination zones. In the rest of analysed *TER*s, either we observed a complete fusion in WT and a replication gap around 1 kb in *GAL-URL-3HA-SEN1 rrm3* cells (Figure 12B), or there was a 1 - 4 kb gap in WT, and a bigger gap, 0.5 - 7 kb, in the double mutant (data not shown). This difference suggests that the *GAL-URL-3HA-SEN1 rrm3* mutants are defective in the last steps of replication termination.

A

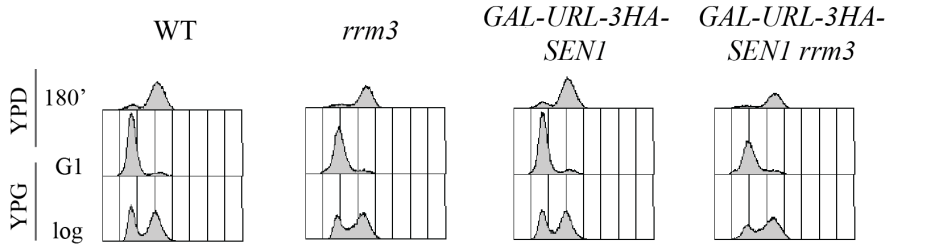

B

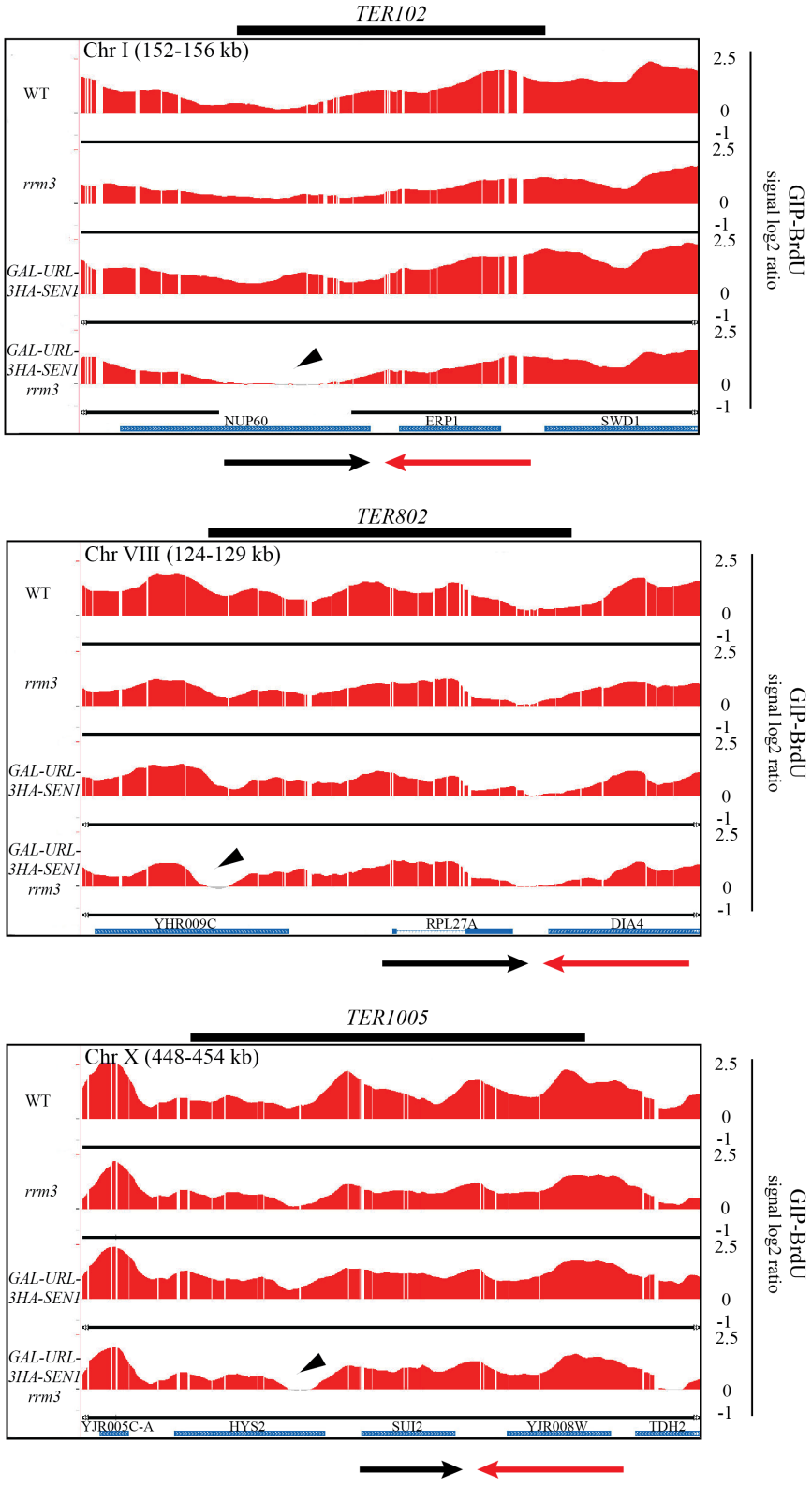
TER102
Chr I (152-156 kb)
WT
rrm3
GAL-URL-3HA-SEN1
GAL-URL-3HA-SEN1 rrm3
NUP60
ERP1
SWD1
2.5
0
-1
GIP-BrdU signal log2 ratio
TER802
Chr VIII (124-129 kb)
YHR009C
RPL27A
DIA4
TER1005
Chr X (448-454 kb)
YJR005C-A
HYS2
SUI2
YJR008W
TDH2

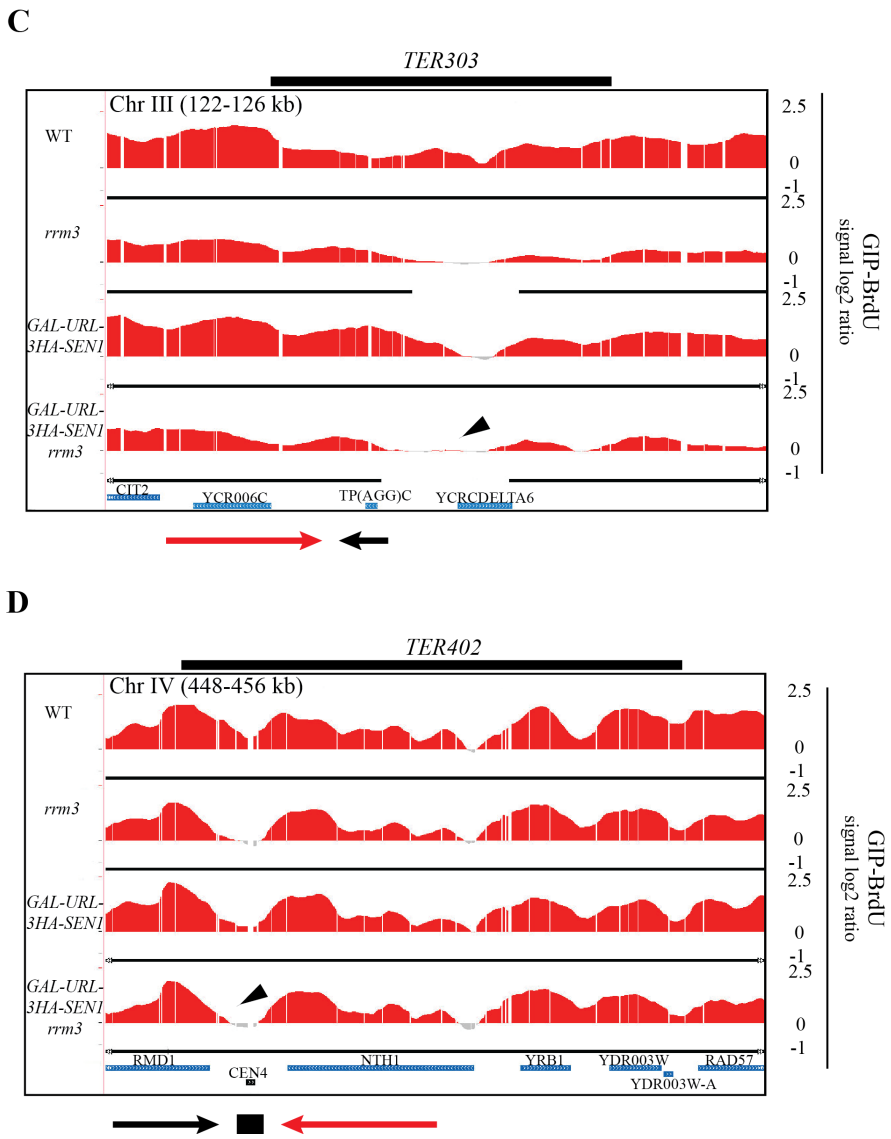

Figure 12. Sen1 and Rrm3 are indispensable in replication termination completion.

WT, *rrm3*, *GAL-URL-3HA-SEN1* and *GAL-URL-3HA-SEN1 rrm3* cells were grown in 25°C YPG, arrested with α-factor and released 25°C in YPD with nocodazole and BrdU. The arrest was kept for 3 hours.

(A) FACS analysis of studied strains.

(B-D) GIP with BrdU incorporation across three types of termination zones: Pol II (B), tRNA (C) and CEN-dependent (D). Direction of the replication forks, mRNA transcripts and the position of tRNA and *CEN* are indicated. Red peaks correspond to BrdU-IP while the grey peaks display the SUP fraction. Thin black bars below the peaks refer to statistically significant clusters of incorporated BrdU.

Thick black bars above each *TER* profile indicate the length of the zone where termination occurs. Black arrows indicate a gap between converging replication forks.

7.9 DNA:RNA hybrids accumulation at *TER*s in *GAL-URL-3HA-SEN1 rrm3* cells is transient and S phase-restricted

In budding yeast 57 out of 71 recently characterized *TER*s (Fachinetti et al., 2010) contain a Pol II transcribing unit that, in a polar way, slows the replication fork facilitating replication termination. Due to multiple origins scattered along the genome, the clashes between transcription and replication are both head-on and codirectional.

It has been previously shown that Sen1, which associates with replication forks, facilitates replication fork progression through highly transcribed Pol II units by preventing DNA:RNA hybrids formation in the negatively supercoiled DNA behind the transcription bubble (Alzu et al., 2012). The absence of Sen1 leads to DNA:RNA hybrids accumulation on the lagging strand template that forms R loops, which are energetically stable structures formed by DNA:RNA duplex and ssDNA stretch. R loops accumulation correlates with aberrant DNA replication intermediates formation and strongly alter DNA topology, which has deleterious consequences for cell viability. Thus, due to the role of Sen1 in DNA:RNA hybrids removal at highly transcribed Pol II units, its association with replication fork and the fact that most of *TER*s are transcription-dependent, we investigated the potential DNA:RNA hybrids accumulation in WT, *rrm3*, *GAL-URL-3HA-SEN1* and *GAL-URL-3HA-SEN1 rrm3* cells, both in S phase and G2/M.

In order to monitor DNA:RNA hybrids accumulation we used a technique developed in our laboratory that is called GIP-DNA:RNA (Genomic Immunoprecipitation with DNA:RNA hybrids). For this purpose we used a specific serum-free monoclonal antibody from mouse IgG2A S9.6 (Dutrow et al., 2008). S9.6 antibody has a negligible sequence specifity, does not show any bias towards GC content, efficiently recognizes DNA:RNA hybrids of a minimum length of 15 bp and is highly sensitive to mismatches. One mismatched bp in a stretch of 15 bp reduces the signal 80 times, whereas a second mismatch 2000 fold.

2D-gels at selected termination zones in early S phase (see Results 7.6) have shown impaired replication fork fusion in the absence of both Sen1 and Rrm3 helicases. Based on this observation, we aimed to monitor both BrdU incorporation and DNA:RNA hybrids accumulation genome-wide at 40-minute time point from the release into S phase (Figure 13A).

A

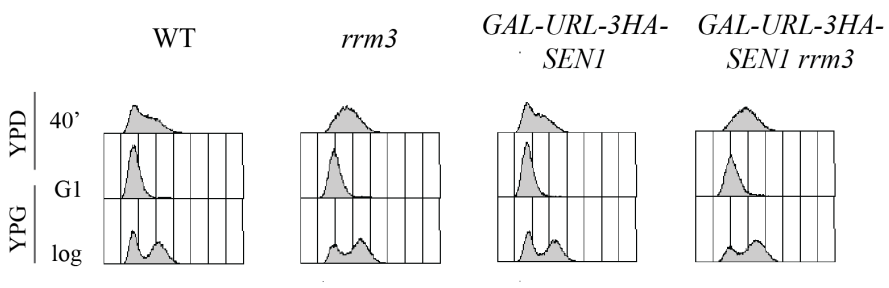

B

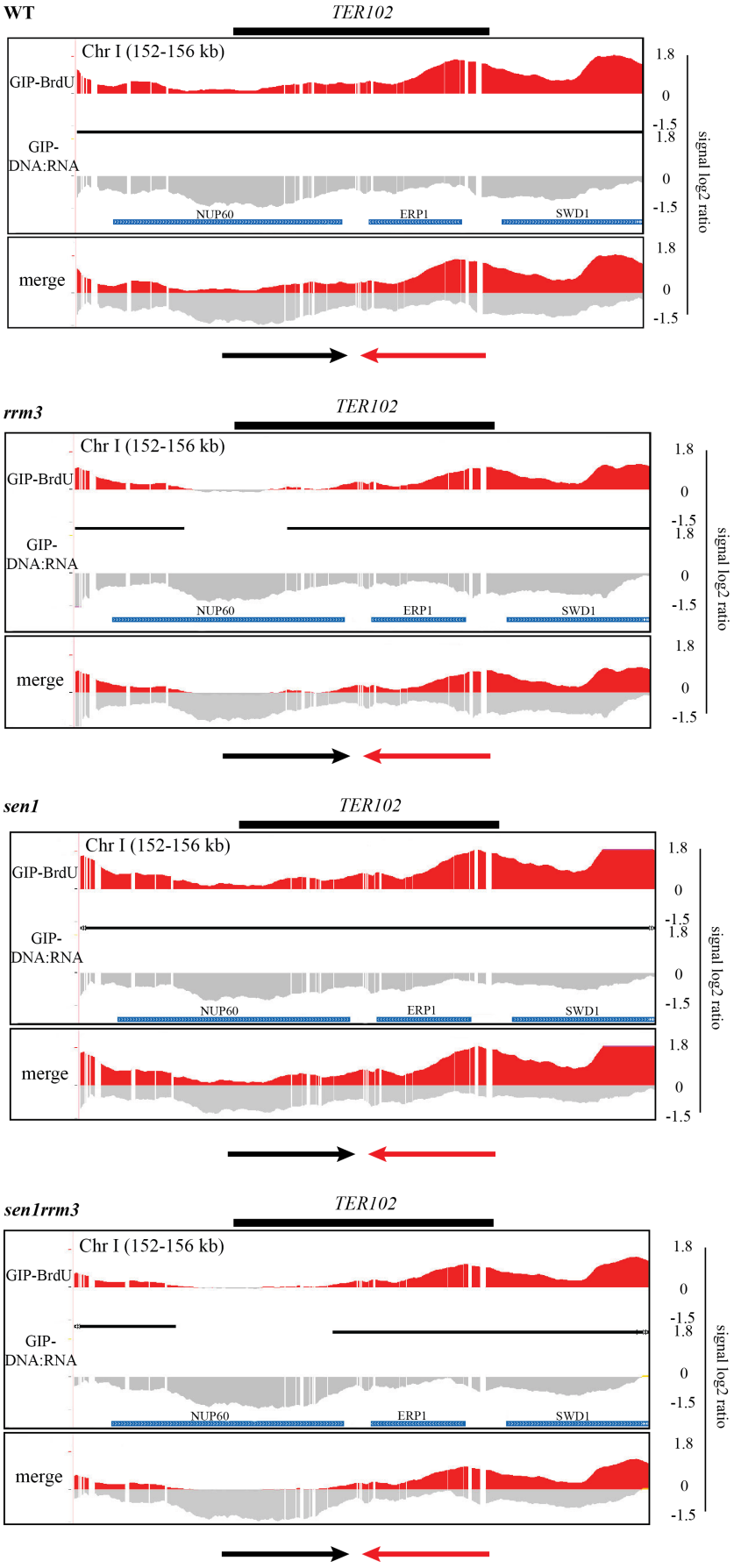
WT
TER102
Chr I (152-156 kb)
GIP-BrdU
GIP-DNA:RNA
NUP60
ERP1
SWD1
merge
1.8
0
-1.5
signal log2 ratio
rrm3
TER102
Chr I (152-156 kb)
GIP-BrdU
GIP-DNA:RNA
NUP60
ERP1
SWD1
merge
sen1
TER102
Chr I (152-156 kb)
GIP-BrdU
GIP-DNA:RNA
NUP60
ERP1
SWD1
merge
sen1rrm3
TER102
Chr I (152-156 kb)
GIP-BrdU
GIP-DNA:RNA
NUP60
ERP1
SWD1
merge

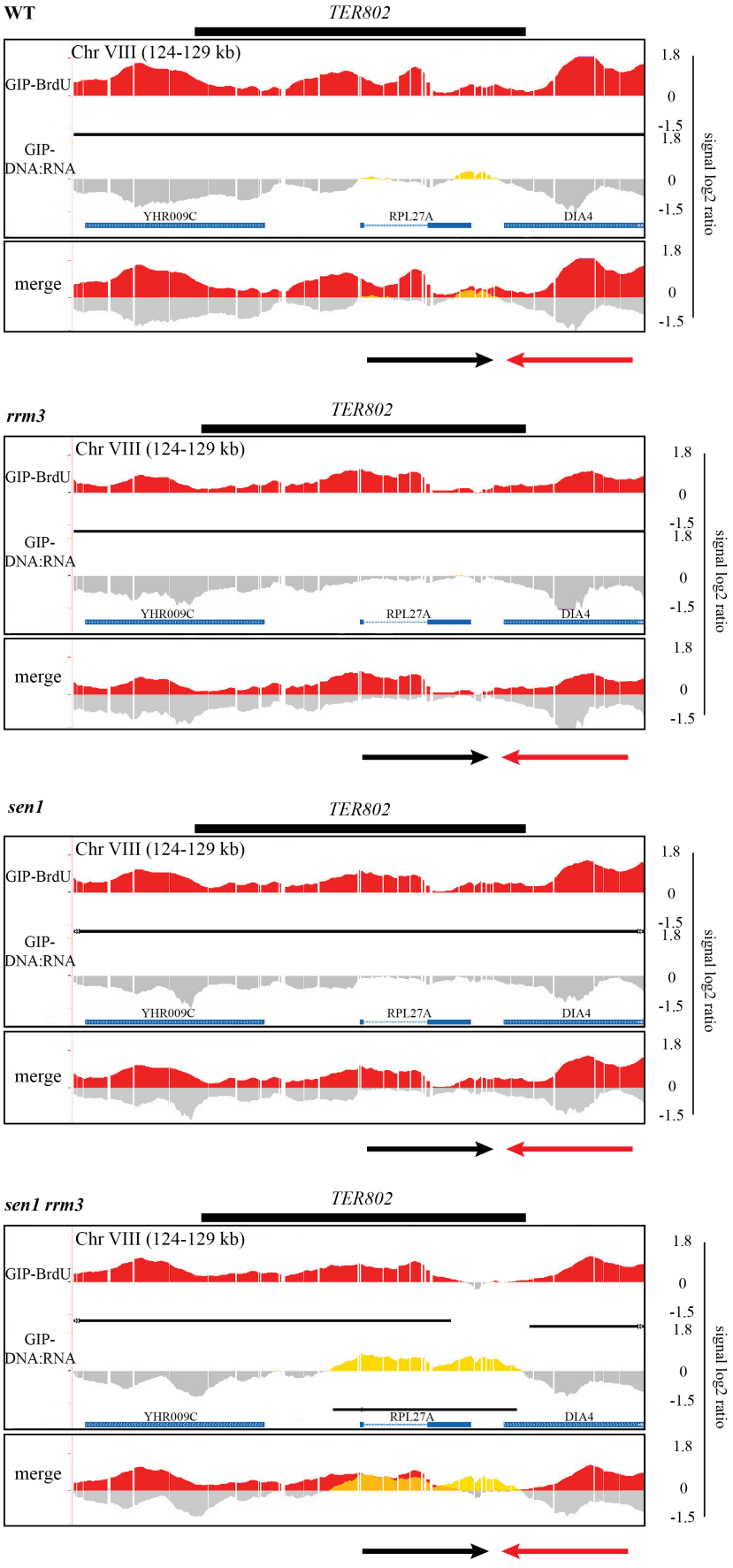
WT
TER802
Chr VIII (124-129 kb)
GIP-BrdU
GIP-
DNA:RNA
YHR009C
RPL27A
DIA4
merge
1.8
0
-1.5
signal log2 ratio
rrm3
TER802
Chr VIII (124-129 kb)
GIP-BrdU
GIP-
DNA:RNA
YHR009C
RPL27A
DIA4
merge
signal log2 ratio
sen1
TER802
Chr VIII (124-129 kb)
GIP-BrdU
GIP-
DNA:RNA
YHR009C
RPL27A
DIA4
merge
signal log2 ratio
sen1 rrm3
TER802
Chr VIII (124-129 kb)
GIP-BrdU
GIP-
DNA:RNA
YHR009C
RPL27A
DIA4
merge
signal log2 ratio

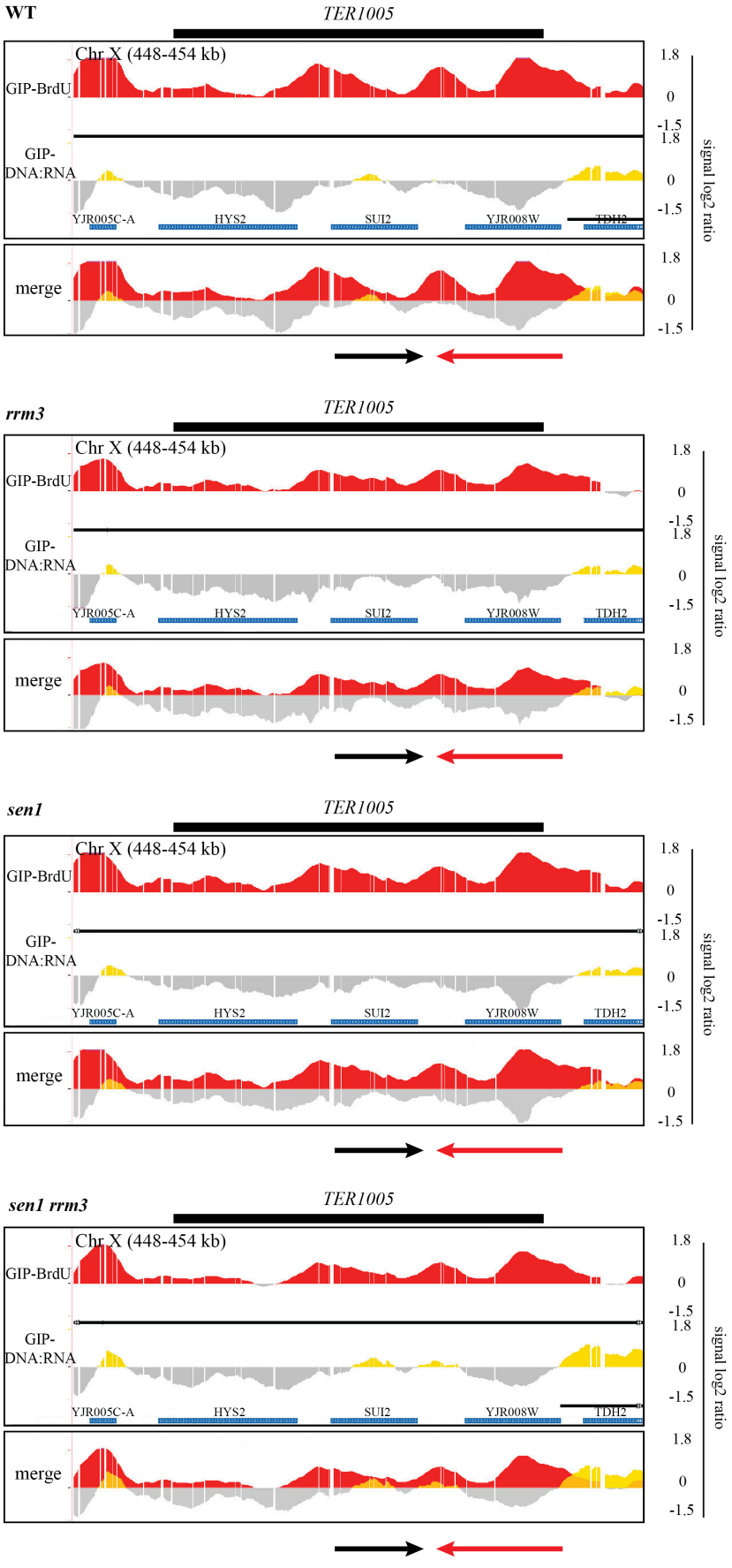
WT
TER1005
Chr X (448-454 kb)
GIP-BrdU
GIP-
DNA:RNA
YJR005C-A
HYS2
SUI2
YJR008W
TDH2
merge
1.8
0
-1.5
signal log2 ratio
rrm3
TER1005
sen1
TER1005
sen1 rrm3
TER1005

C

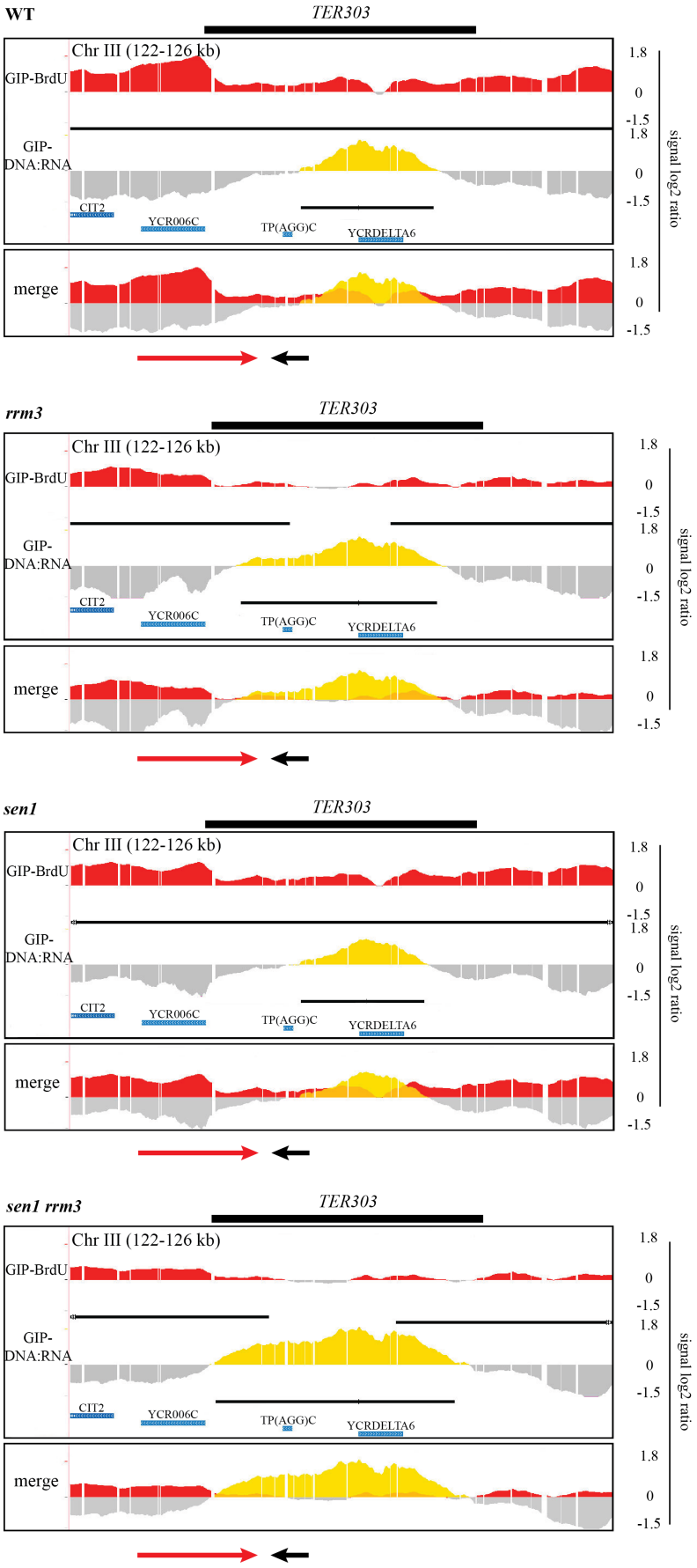
WT
TER303
Chr III (122-126 kb)
GIP-BrdU
GIP-DNA:RNA
merge
CIT2
YCR006C
TP(AGG)C
YCRDELTA6
1.8
0
-1.5
signal log2 ratio
rrm3
sen1
sen1 rrm3

D

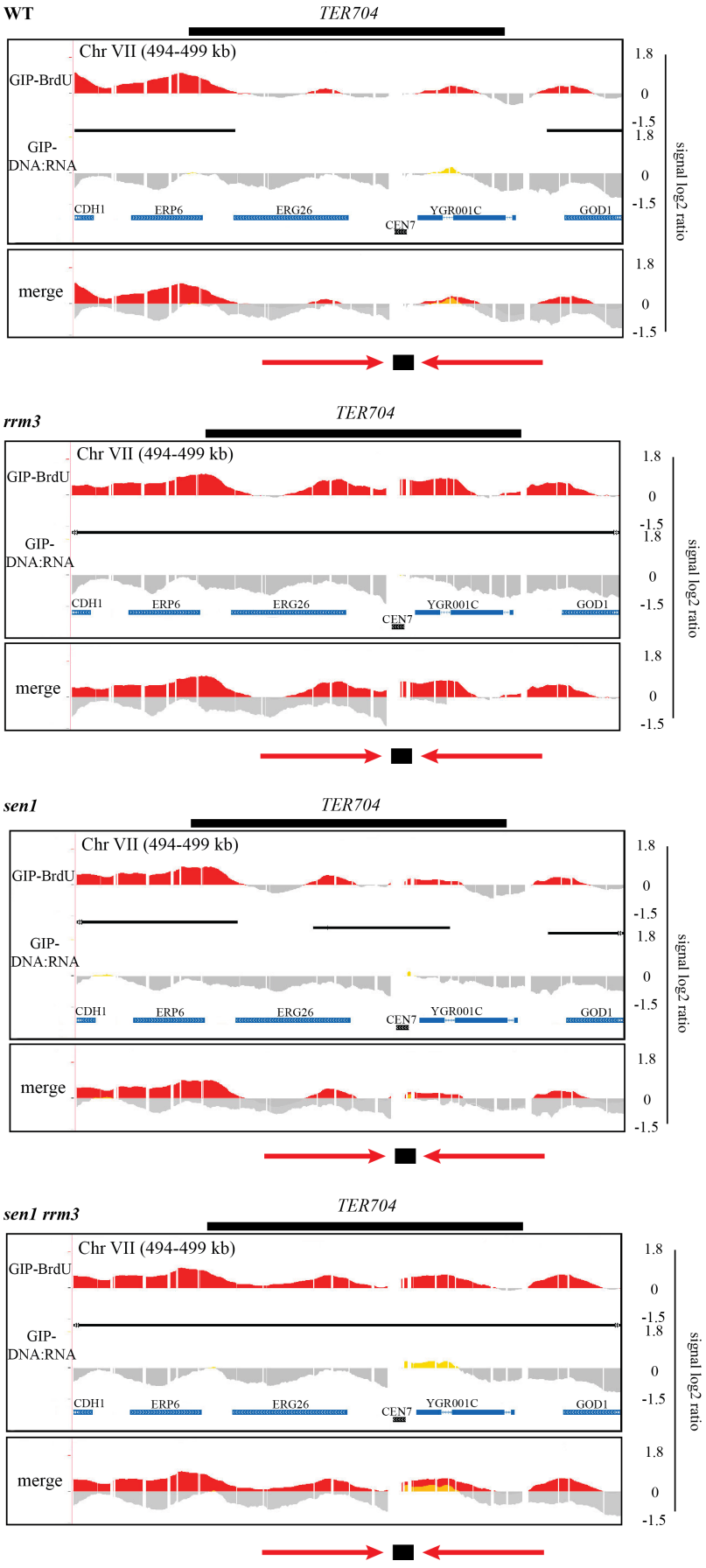
WT
TER704
Chr VII (494-499 kb)
GIP-BrdU
GIP-DNA:RNA
merge
CDH1
ERP6
ERG26
YGR001C
GOD1
CEN7
1.8
0
-1.5
signal log2 ratio
rrm3
sen1
sen1 rrm3

Figure 13. In S phase in the absence of Sen1 and Rrm3 helicases DNA:RNA hybrids form at *TER*s, and their accumulation correlates with replication termination defects.

WT, *rrm3*, *GAL-URL-3HA-SEN1* and *GAL-URL-3HA-SEN1 rrm3* cells were grown in YPG, arrested with α-factor and released in YPD with BrdU. 40-minute time point was taken separately for GIP-BrdU and GIP-DNA:RNA.
(A) Cell cycle progression of studied strains.
(B-D) GIP with BrdU incorporation, GIP with DNA:RNA hybrids accumulation and the merge between GIP-BrdU and GIP-DNA:RNA across three types of termination zones: Pol II (B), tRNA (C) and CEN-dependent (D). Direction of the replication forks, mRNA transcripts and the position of tRNA and *CEN* are indicated. Red peaks correspond to BrdU-IP, yellow peaks indicate DNA:RNA hybrids and the grey peaks display the SUP fraction. Thin black bars below the peaks refer to statistically significant clusters of either incorporated BrdU or DNA:RNA hybrids. Thick black bars above each *TER* profile indicate the length of the zone where termination occurs. The experiment has been done 3 times with consistent results.

We have monitored BrdU incorporation in S phase across *TER*s located between early origins (23/71) in *GAL-URL-3HA-SEN1 rrm3* cells (Figure 13B-D). We observed defects in termination in 17/23 analysed *TER*s except of 3 *CEN*s*: TER704*, *TER1504*, *TER1604* and 3 non-highly transcribed Pol II genes: *TER503*, *TER601*, *TER1202*. Moreover, in S phase in 46/71 *TER*s we noticed stronger DNA:RNA hybrids accumulation in the absence of Sen1 and Rrm3 compared to WT, *rrm3* and *GAL-URL-3HA-SEN1* (Figure 13B-D). The DNA:RNA hybrids were abundant at all highly transcribed Pol II units, both head-on and codirectionally-oriented, and all Pol III genes. We did not detect any DNA:RNA hybrids in 16/71 *TER*s, 3 of which were *CEN*s and 13 were non-highly transcribed Pol II genes, both head-on and codirectionally-oriented.

Interestingly, we did not observe strong DNA:RNA hybrids accumulation in S phase at *TER*s that contain highly transcribed Pol II genes in Sen1-defective cells. The single deletion of *RRM3* contributes to DNA:RNA hybrids increase at *TER*s in Pol III-dependent *TER*s, and the effect is amplified when Sen1 is not functional. Thus, in S phase both Sen1 and Rrm3 together play an important role in DNA:RNA hybrids removal at *TER*s.

The next question we have posed was whether DNA:RNA hybrids accumulation at *TER*s in the absence of Sen1 and Rrm3 persists until G2/M. For this purpose we precipitated DNA:RNA hybrids genome-wide in the presence of nocodazole in WT, *rrm3*, *GAL-URL-3HA-SEN1* and *GAL-URL-3HA-SEN1 rrm3* cells (Figure 14A). In all the strains mentioned above, GIP-DNA:RNA hybrids precipitation was compared with GIP-BrdU immunoprecipitation in G2/M arrested cells.

A

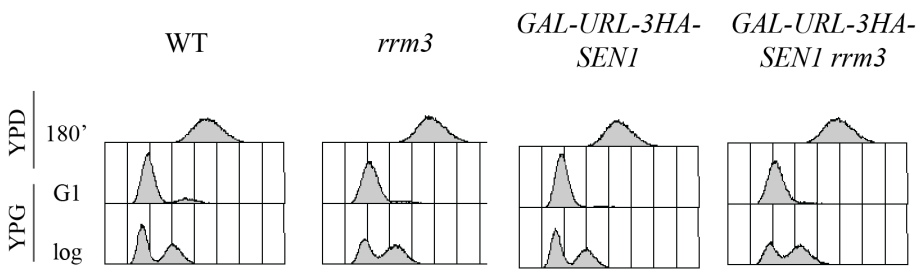

B

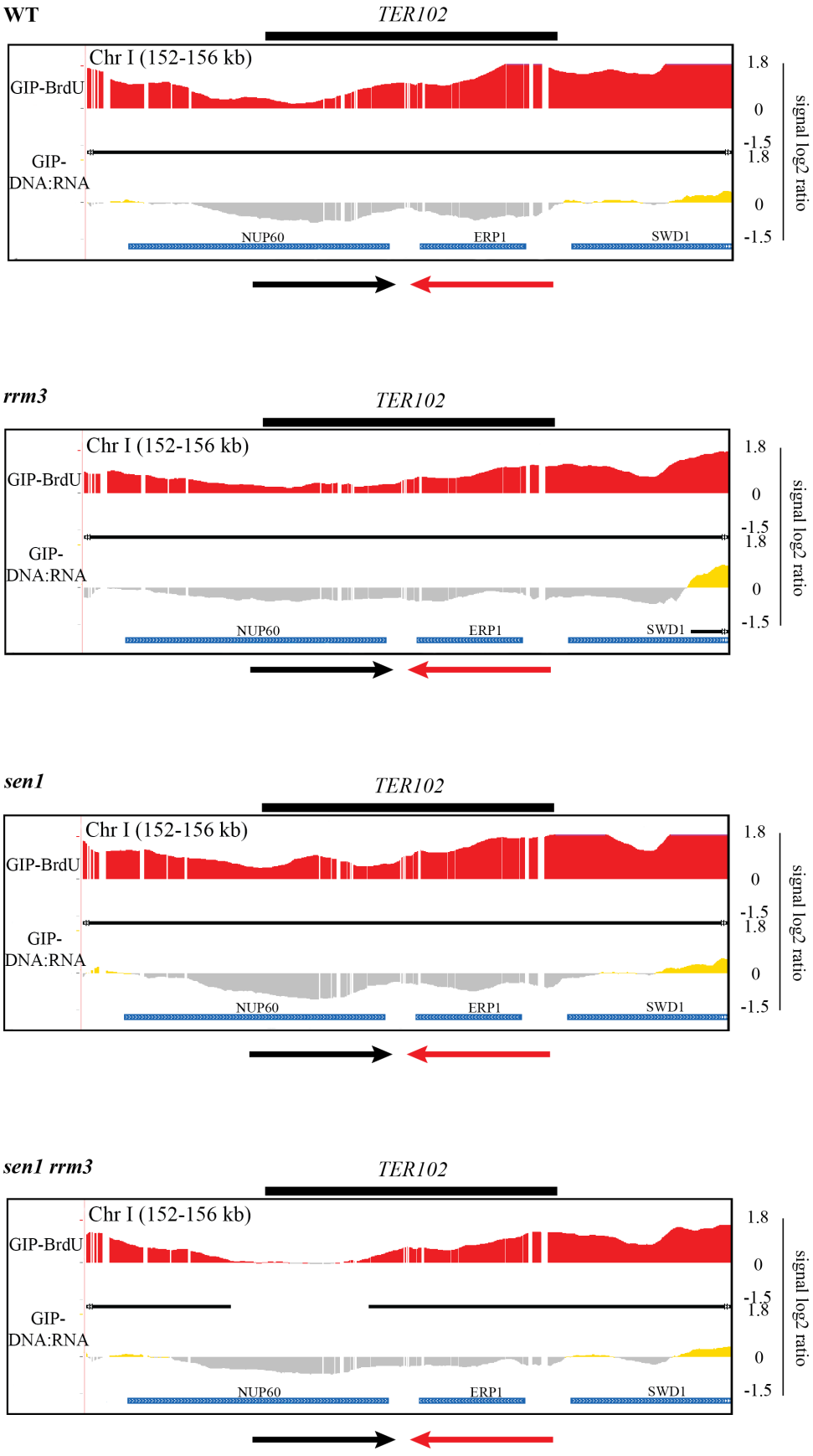
WT
TER102
Chr I (152-156 kb)
GIP-BrdU
GIP-DNA:RNA
NUP60
ERP1
SWD1
1.8
0
-1.5
signal log2 ratio
rrm3
sen1
sen1 rrm3

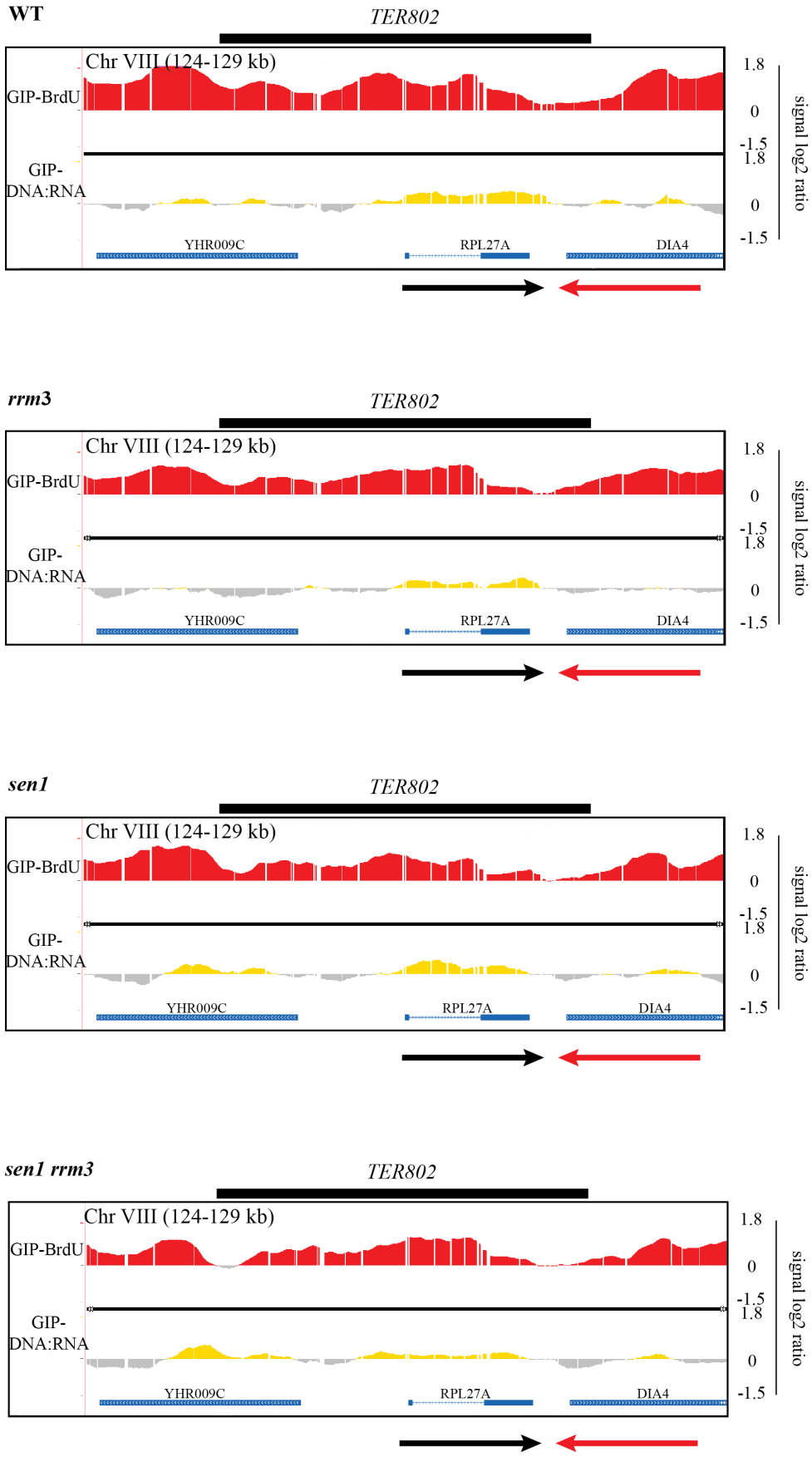
WT
TER802
Chr VIII (124-129 kb)
GIP-BrdU
GIP-
DNA:RNA
YHR009C
RPL27A
DIA4
1.8
0
-1.5
1.8
0
-1.5
signal log2 ratio
rrm3
TER802
Chr VIII (124-129 kb)
GIP-BrdU
GIP-
DNA:RNA
YHR009C
RPL27A
DIA4
1.8
0
-1.5
1.8
0
-1.5
signal log2 ratio
sen1
TER802
Chr VIII (124-129 kb)
GIP-BrdU
GIP-
DNA:RNA
YHR009C
RPL27A
DIA4
1.8
0
-1.5
1.8
0
-1.5
signal log2 ratio
sen1 rrm3
TER802
Chr VIII (124-129 kb)
GIP-BrdU
GIP-
DNA:RNA
YHR009C
RPL27A
DIA4
1.8
0
-1.5
1.8
0
-1.5
signal log2 ratio

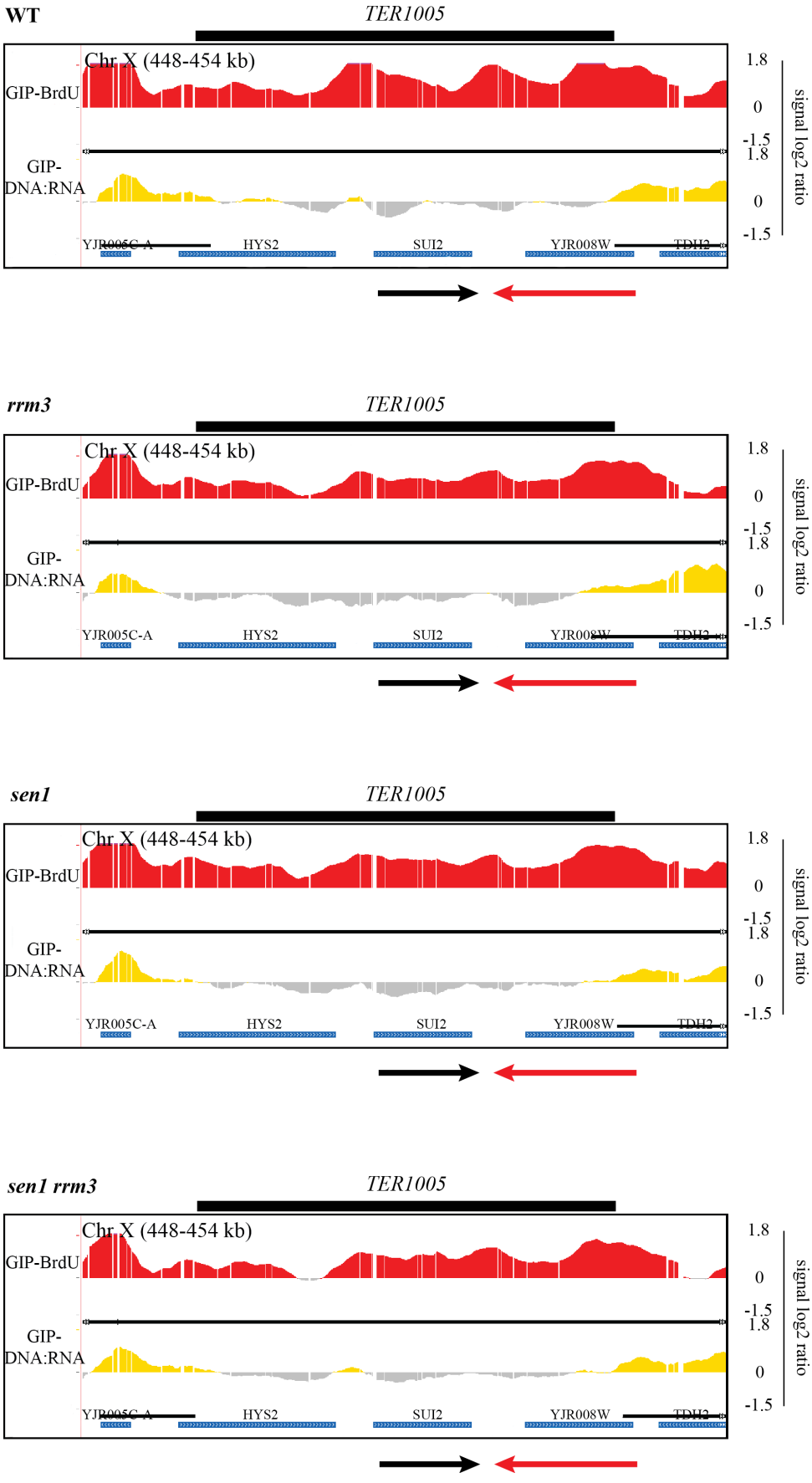
WT
TER1005
Chr X (448-454 kb)
GIP-BrdU
GIP-
DNA:RNA
1.8
0
-1.5
1.8
0
-1.5
signal log2 ratio
YJR005C-A
HYS2
SUI2
YJR008W
TDH2
rrm3
TER1005
Chr X (448-454 kb)
GIP-BrdU
GIP-
DNA:RNA
1.8
0
-1.5
1.8
0
-1.5
signal log2 ratio
YJR005C-A
HYS2
SUI2
YJR008W
TDH2
sen1
TER1005
Chr X (448-454 kb)
GIP-BrdU
GIP-
DNA:RNA
1.8
0
-1.5
1.8
0
-1.5
signal log2 ratio
YJR005C-A
HYS2
SUI2
YJR008W
TDH2
sen1 rrm3
TER1005
Chr X (448-454 kb)
GIP-BrdU
GIP-
DNA:RNA
1.8
0
-1.5
1.8
0
-1.5
signal log2 ratio
YJR005C-A
HYS2
SUI2
YJR008W
TDH2

C

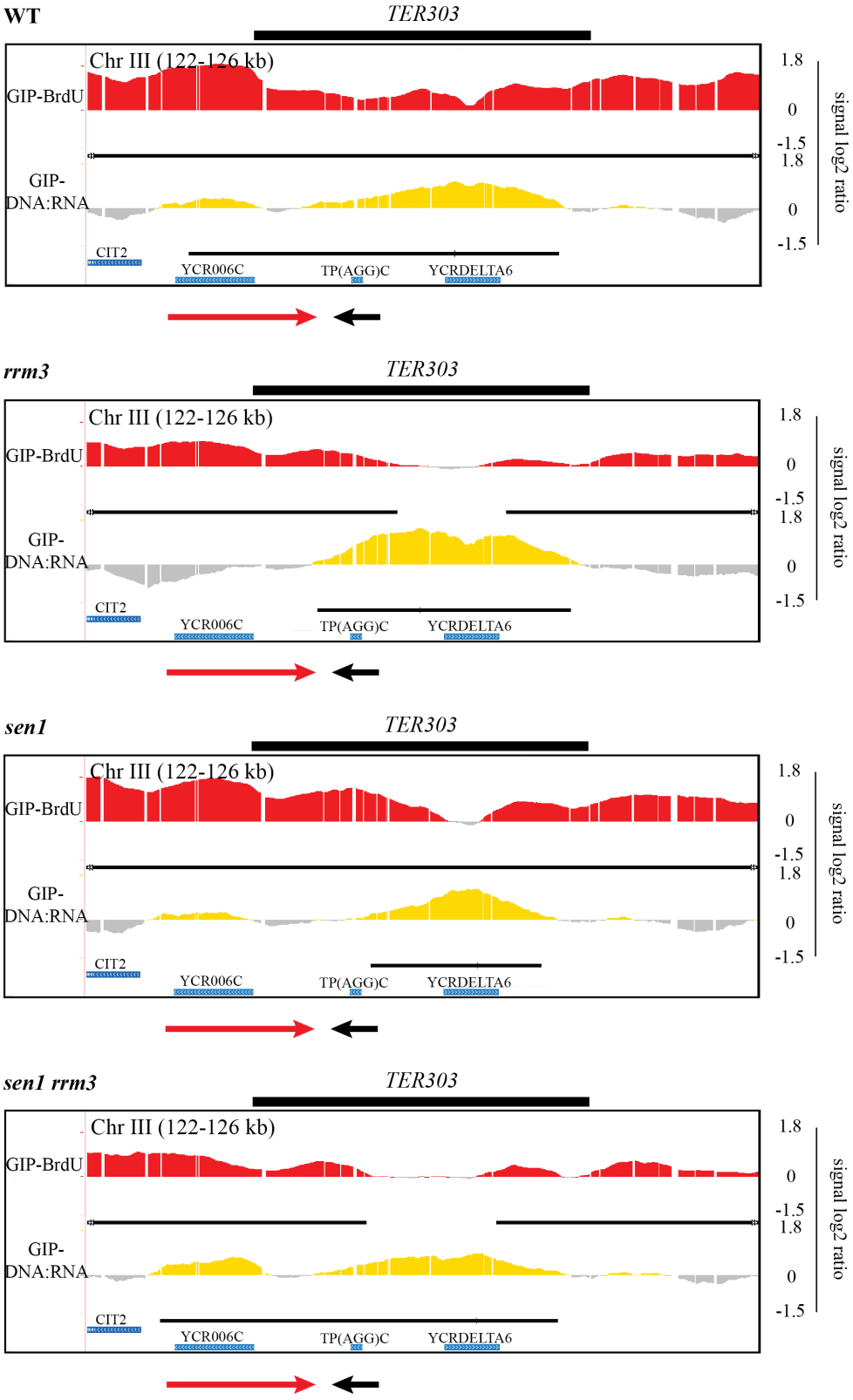
WT
TER303
Chr III (122-126 kb)
GIP-BrdU
GIP-
DNA:RNA
CIT2
YCR006C
TP(AGG)C
YCRDELTA6
1.8
0
-1.5
1.8
0
-1.5
signal log2 ratio
rrm3
TER303
Chr III (122-126 kb)
GIP-BrdU
GIP-
DNA:RNA
CIT2
YCR006C
TP(AGG)C
YCRDELTA6
1.8
0
-1.5
1.8
0
-1.5
signal log2 ratio
sen1
TER303
Chr III (122-126 kb)
GIP-BrdU
GIP-
DNA:RNA
CIT2
YCR006C
TP(AGG)C
YCRDELTA6
1.8
0
-1.5
1.8
0
-1.5
signal log2 ratio
sen1 rrm3
TER303
Chr III (122-126 kb)
GIP-BrdU
GIP-
DNA:RNA
CIT2
YCR006C
TP(AGG)C
YCRDELTA6
1.8
0
-1.5
1.8
0
-1.5
signal log2 ratio

D

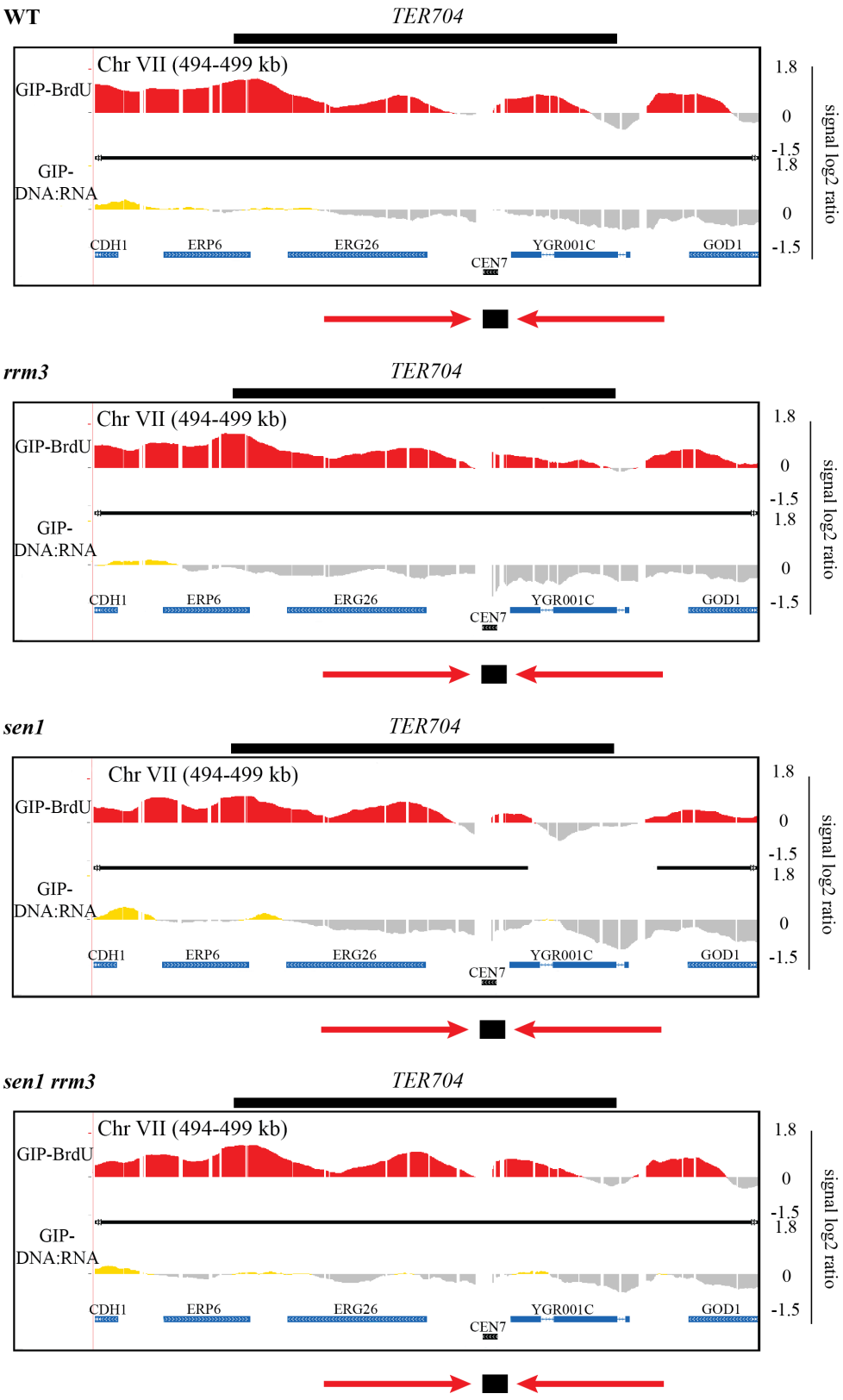
WT
TER704
Chr VII (494-499 kb)
GIP-BrdU
GIP-
DNA:RNA
1.8
0
-1.5
1.8
0
-1.5
signal log2 ratio
CDH1
ERP6
ERG26
CEN7
YGR001C
GOD1
rrm3
TER704
Chr VII (494-499 kb)
GIP-BrdU
GIP-
DNA:RNA
1.8
0
-1.5
1.8
0
-1.5
signal log2 ratio
CDH1
ERP6
ERG26
CEN7
YGR001C
GOD1
sen1
TER704
Chr VII (494-499 kb)
GIP-BrdU
GIP-
DNA:RNA
1.8
0
-1.5
1.8
0
-1.5
signal log2 ratio
CDH1
ERP6
ERG26
CEN7
YGR001C
GOD1
sen1 rrm3
TER704
Chr VII (494-499 kb)
GIP-BrdU
GIP-
DNA:RNA
1.8
0
-1.5
1.8
0
-1.5
signal log2 ratio
CDH1
ERP6
ERG26
CEN7
YGR001C
GOD1

Figure 14. Abundant DNA:RNA hybrids formed in the absence of Sen1 and Rrm3 at *TER*s in S phase do not persist until G2/M phase.

WT, *rrm3*, *GAL-URL-3HA-SEN1* and *GAL-URL-3HA-SEN1 rrm3* cells were grown in YPG, arrested with α-factor and released in YPD with BrdU and nocodazole. 180-minute time point was taken separately for GIP-BrdU and GIP-DNA:RNA.

(A) Cell cycle progression of studied strains.

(B-D) GIP with BrdU incorporation and GIP with DNA:RNA hybrids accumulation across three types of termination zones: Pol II (B), tRNA (C) and CEN-dependent (D). Direction of the replication forks, mRNA transcripts and the position of tRNA and *CEN* are indicated. Red peaks correspond to BrdU-IP, yellow peaks indicate DNA:RNA hybrids and the grey peaks display the SUP fraction. Thin black bars below the peaks refer to statistically significant clusters of either incorporated BrdU or DNA:RNA hybrids. Thick black bars above each *TER* profile indicate the length of the zone where termination occurs. The experiment has been done 2 times with consistent results.

We found that DNA:RNA hybrids accumulation at *TER*s in Sen1- and Rrm3-defective cells is transient and restricted to S phase. In *GAL-URL-3HA-SEN1 rrm3* cells the DNA:RNA-IP signal detected along the termination zones either is not considered as statistically significant or resembles WT (Figure 14B-D). Therefore, abundant DNA:RNA hybrids formed in S phase in the absence of Sen1 and Rrm3 are removed and do not persist at *TER*s in G2/M.

7.10 DNA replication termination intermediates in *GAL-URL-3HA-SEN1 rrm3* are not detectable in G2/M

Since we have detected replication termination gaps between two converging forks, we aimed to examine whether replication termination intermediates persist at *TER*s in G2/M.

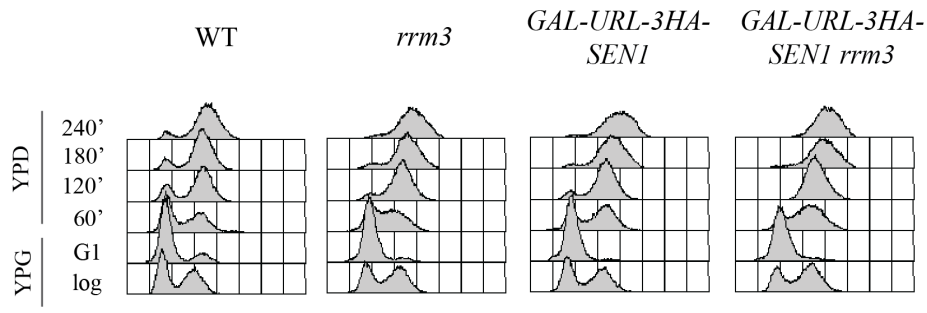

We arrested WT, *rrm3*, *GAL-URL-3HA-SEN1* and *GAL-URL-3HA-SEN1 rrm3* cells in nocodazole for 240 minutes (Figure 15A) and monitored the termination events at Pol II-dependent *TER102* (Figure 15B). We failed to detect in Sen1- and Rrm3- defective cells any replication intermediates already at 180-minute time point. Since those structures cannot be resolved, due to the persisting gap between converging replication forks, the intermediates might disappear either because of breaks formed at *TER*s or because they are backtracked. If the second hypothesis is true, the replication intermediates might be present at the flanking regions of *TER102*.

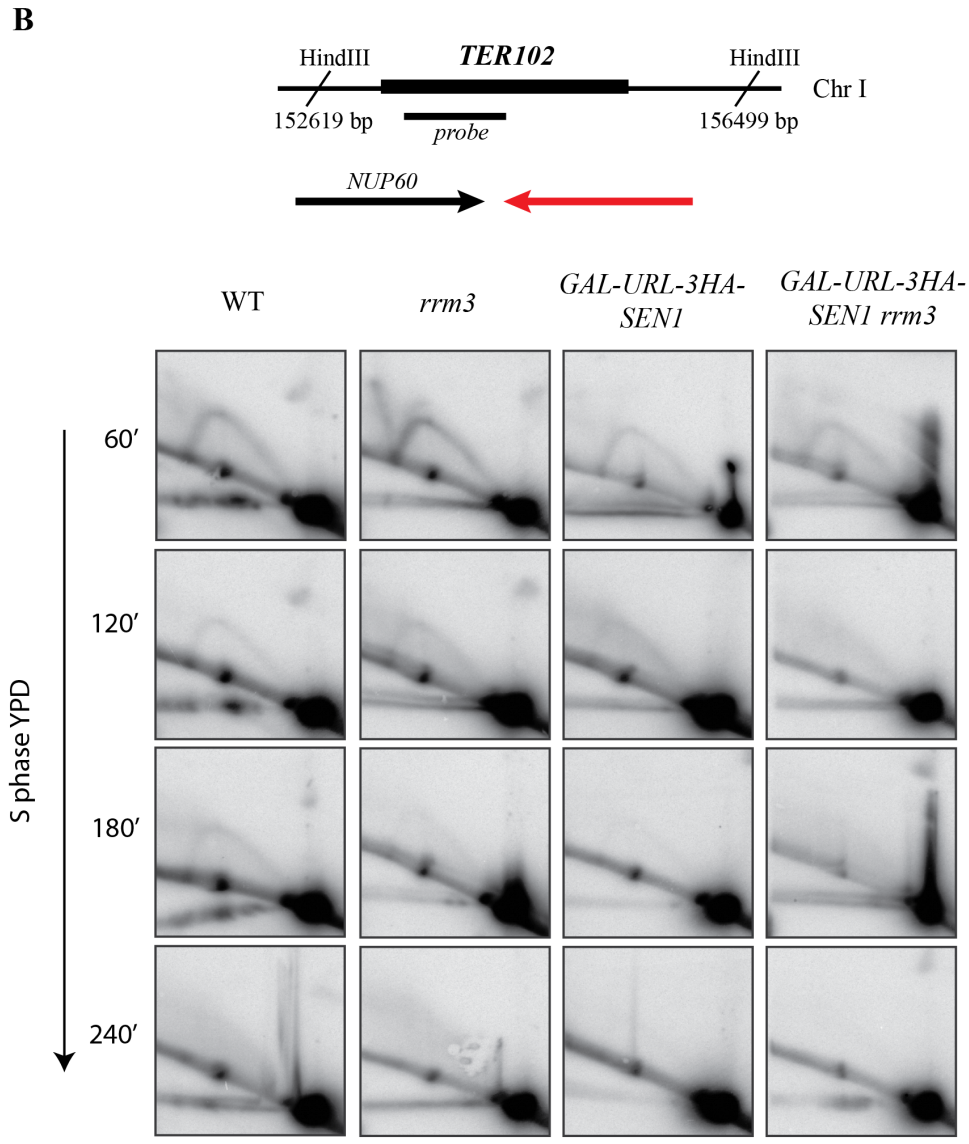

Figure 15. Absent replication termination intermediates in G2/M arrested *GAL-URL-3HA-SEN1 rrm3* cells.

WT, *rrm3*, *GAL-URL-3HA-SEN1* and *GAL-URL-3HA-SEN1 rrm3* cells were grown exponentially at 25°C (log) in YPG, synchronized with α-factor in G1 in YPG and released in YPD at 25°C in the presence of nocodazole.

(A) Cell cycle progression followed by FACS analysis.

(B) Replication termination intermediates at *TER102* analysed by 2D-gel technique. Genomic DNA was psoralen-crosslinked and extracted by CTAB technique at the indicated time points. 20 µg of DNA was digested, subjected to 2D-gel procedure, Southern blotted and radiolabelled with a *TER102* probe. The schematic representation of the digestion strategy and probe localization are

depicted 2D-gel panel. Red arrow indicates the direction of replication fork encountering RNA transcript depicted by black arrow.

7.11 Nocodazole arrested *GAL-URL-3HA-SEN1 rrm3* cells exhibit intact chromosomes

In the absence of Sen1 and Rrm3 helicases DNA replication is incomplete in G2/M (presented in Results 7.8). We failed to detect chromosome breakage in nocodazole arrested *GAL-URL-3HA-SEN1 rrm3* cells by PFGE (presented in Results 7.4, Figure 7). Nevertheless, we revealed the presence of topologically linked branched molecules in the well in G2/M arrested Sen1- and Rrm3-defective cells. In order to understand the link between the processes described above, we aimed to investigate whether in G2/M arrested cells, breaks accumulate at *TER*s.

To detect breaks at *TER* by PFGE, WT, *rrm3*, *GAL-URL-3HA-SEN1* and *GAL-URL-3HA-SEN1 rrm3* cells were arrested in nocodazole for 360 minutes (Figure 16A), DNA was extracted in agarose plugs and digested with the EagI enzyme. EagI digestion fragment of interest is ~110 kb long and contains three early and efficient origins of replication (*ARS305*, *ARS306* and *ARS307*) and two termination zones (*TER301* and *TER302*) with an inter-origin space of 35 kb (Figure 16B). We aimed to monitor *TER302*, which contains tRNA, LTR, Ty and Pol II- pausing units.

We failed to detect breaks at *TER302* in G2/M arrested *GAL-URL-3HA-SEN1 rrm3* cells. Intringuingly though, Sen1- and Rrm3- defective cells show at 360-minute an increase of branched molecules that remain trapped in the wells (Figure 16B, C). In WT, *rrm3* and *GAL-URL-3HA-SEN1* cells the percentage of

non-migrated DNA at 360-minute time point was minimal (0.8%, 1.15%, 1.8%, respectively), whereas replicated DNA in *GAL-URL-3HA-SEN1 rrm3* cells was topologically altered at *TER302* and 7-fold more trapped in the well comparing to WT cells.

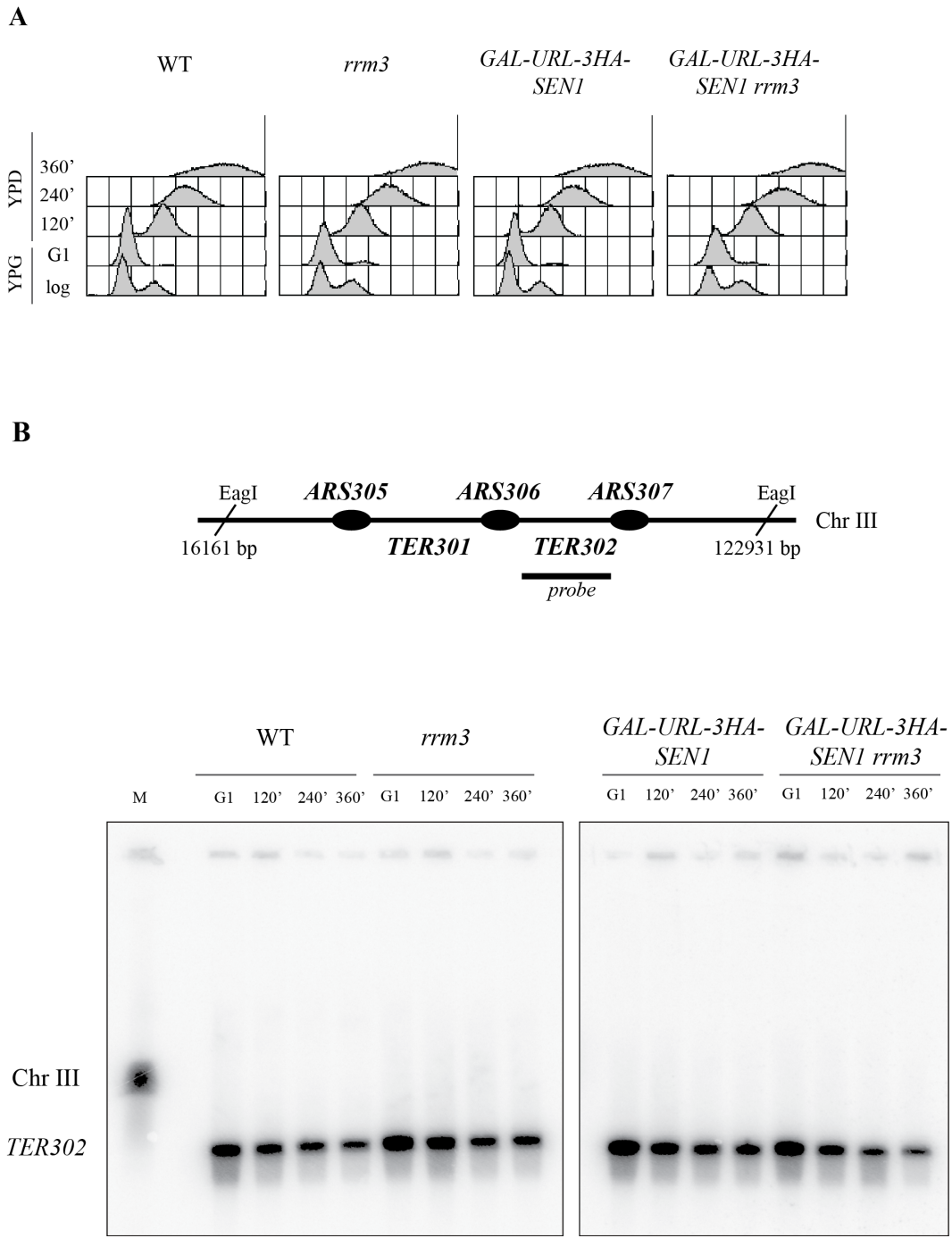

C

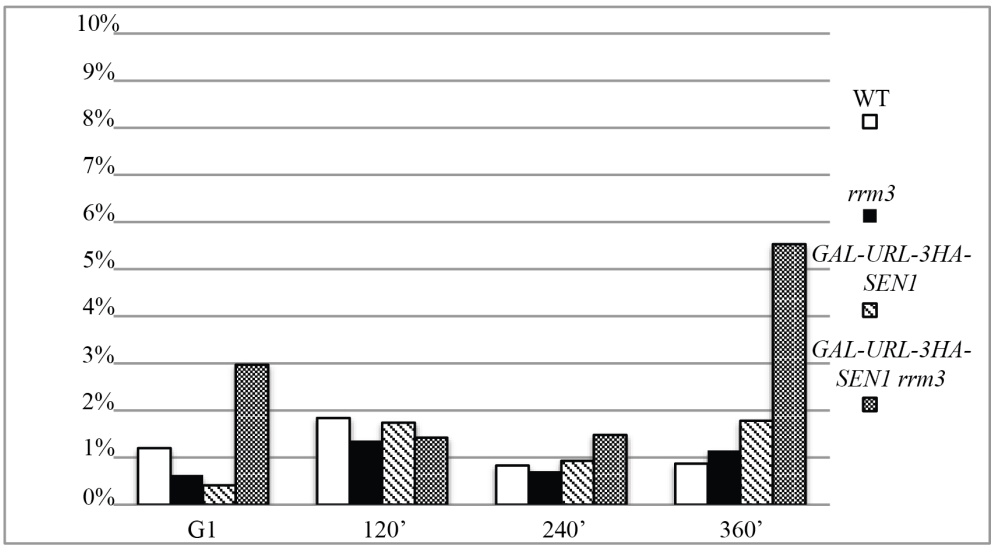

Figure 16. *GAL-URL-3HA-SEN1 rrm3* G2/M arrested cells do not accumulate breaks but branched molecules at *TER*.

WT, *rrm3*, *GAL-URL-3HA-SEN1* and *GAL-URL-3HA-SEN1 rrm3* cells were grown exponentially at 25°C (log) in YPG, synchronized with α-factor in G1 in YPG at 25°C and released in YPD at 30°C in the presence of nocodazole.

(A) Indicated time points were collected for FACS analysis.

(B) Genomic DNA was extracted in agarose plugs at the indicated time points. Agarose plugs were digested with the EagI restriction enzyme. Yeast chromosomes were separated by PFGE and analysed by Southern blot with *TER302* probe. M indicates the chromosome marker.

(C) Percentage of the total chromosomal DNA subjected to PFGE after agarose plugs digestion trapped within the well at G1, 120', 250' and 360'. Quantification was done by using ImageQuant Software.

Experiment was done 2 times.

7.12 Post-prometaphase DNA breaks formation in *GAL-URL-3HA-SEN1 rrm3* cells

In this study, all the experiments that have been done to unravel the mechanisms responsible for replication completion failure and branched molecules accumulation at *TER*s in the absence of Sen1 and Rrm3, were performed in G2/M arrested cells.

Nocodazole is an anti-neoplastic agent that does not allow metaphase spindle formation, causing the cell arrest in prometaphase. We asked whether the metaphase/anaphase transition might cause *TER*s' breakage in *GAL-URL-3HA-SEN1 rrm3* cells. We arrested in G1 WT and *GAL-URL-3HA-SEN1 rrm3* cells, released in S phase at 30°C and took 60-, 120-, 240- and 360-minute time points (Figure 17A). WT cells kept cycling whereas Sen1- and Rrm3- defective mutants showed 80% of cells arrested at 240-minute and ~100% at 360-minute. We used the same digestion strategy described in Results 7.11 to detect the integrity of *TER302*. We found that DNA breaks accumulate at 360-minute time point in *GAL-URL-3HA-SEN1 rrm3* cells. The DNA breakage indicates that *TER*s become fragile during metaphase-anaphase transition in the absence of Sen1 and Rrm3.

A

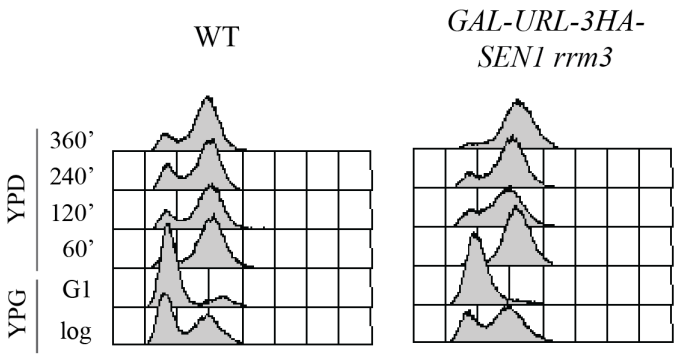

B

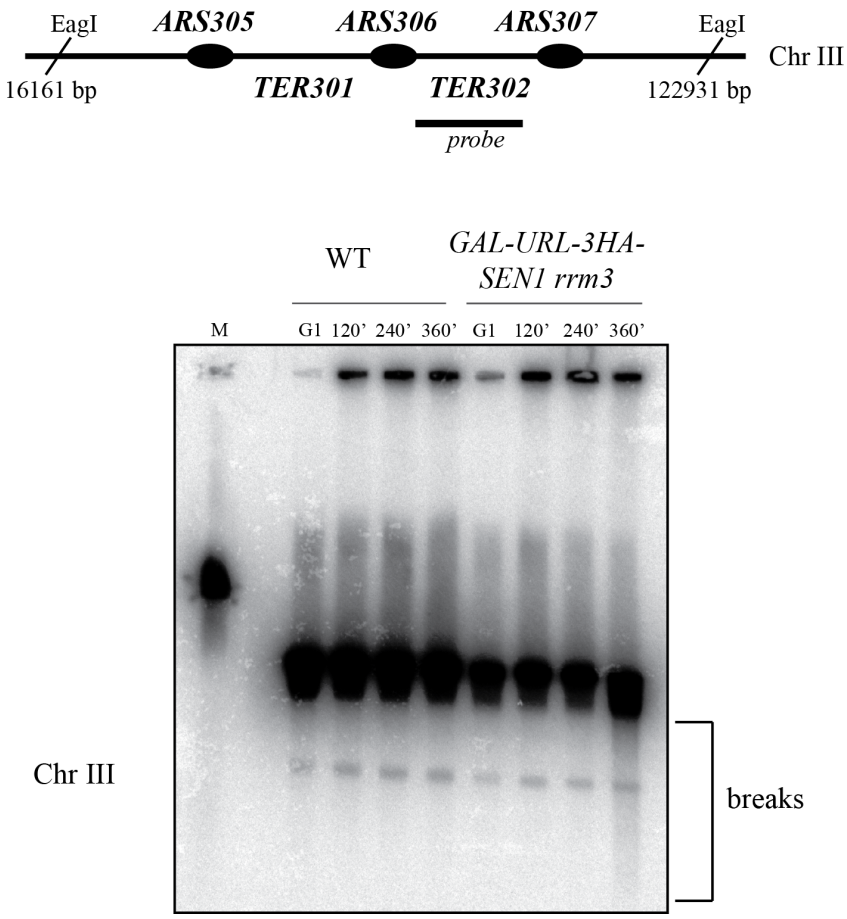

Figure 17. Post-prometaphase *TER* breakage in *GAL-URL-3HA-SEN1 rrm3* cells.

WT, *rrm3*, *GAL-URL-3HA-SEN1* and *GAL-URL-3HA-SEN1 rrm3* cells were grown exponentially at 25°C (log) in YPG, synchronized with α-factor in G1 in YPG at 25°C and released in YPD at 30°C.

(A) Indicated time points were collected for FACS analysis.

(B) Genomic DNA was extracted in agarose plugs at the indicated time points. Agarose plugs were digested with the EagI restriction enzyme. Yeast chromosomes were separated by PFGE and analysed by Southern blot with *TER302* probe. M indicates the chromosome marker.

7.13 The checkpoint contribution to termination in *GAL-URL-3HA-SEN1 rrm3* cells

GAL-URL-3HA-SEN1-rrm3 cells exhibit large budded cells and a first cell cycle arrest, indicative of a checkpoint dependent G2 block (Weinert and Hartwell, 1988). In budding yeast Rad53 is an essential protein kinase that is phosphorylated and activated in a *MEC1*- and *TEL1*-dependent manner in response to DNA damage. The signal initiated by DNA damage is conveyed to Rad53 and Chk1 through Rad9 (Sanchez et al., 1999). Activated Rad53 is involved in cell cycle arrest, deregulation of origin firing, stabilization of stalled replication forks and transcriptional induction of repair genes (Lopes et al., 2001; Santocanale and Diffley, 1998; Tercero and Diffley, 2001).

Due to the synthetic lethality of Sen1- and Rrm3-defective cells, their cell cycle block in G2/M and highly altered topological state of DNA, we monitored Rad53 and γH2AX phosphorylation in *GAL-URL-3HA-SEN1 rrm3* cells. We have also investigated whether *RAD9* deletion enables *GAL-URL-3HA-SEN1 rrm3* cells to bypass the G2/M arrest and if so, how it does affect replication termination completion.

7.13.1 The checkpoint activation and γH2AX phosphorylation in *GAL-URL-3HA-SEN1 rrm3* cells

Rad53 and γH2AX phosphorylation are the hallmarks of ssDNA stretches accumulation. By using WT as a control, we monitored DNA checkpoint activation in *GAL-URL-3HA-SEN1 rrm3* cells. The cells were arrested in G1 and

then released in non-permissive conditions for Sen1p expression. At 120-minute time point 80% of *GAL-URL-3HA-SEN1 rrm3* cells were arrested and ~100% reached the G2/M block at 360-minute (Figure 18A). We have detected both Rad53p and γH2AX phosphorylation in *GAL-URL-3HA-SEN1* cells in all analysed time points. These data suggest that *GAL-URL-3HA-SEN1 rrm3* cells accumulate checkpoint signals leading to Rad53 activation and γH2AX accumulation.

A

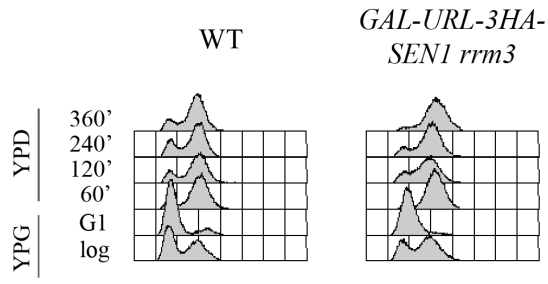

B

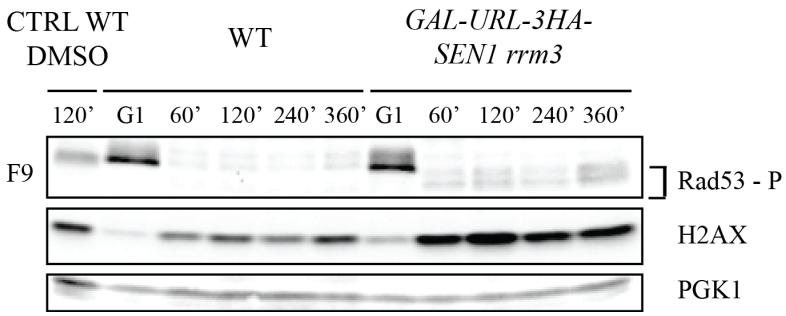

Figure 18. γ-H2AX and Rad53p are phosphorylated in the absence of Sen1 and Rrm3.

WT and *GAL-URL-3HA-SEN1 rrm3* cells were grown exponentially at 25°C (log) in YPG, synchronized with α-factor in G1 in YPG at 25°C and released in YPD at 25°C.

(A) Indicated time points were collected for FACS analysis.

(B) G1, 60', 120', 240' and 360' time points were taken and processed with TriChloroacetic Acid (TCA) extraction. WT cells treated with DMSO for 2h served as a γ-H2AX and Rad53p phosphorylation control. The antibody used to detect phosphorylated Rad53p (F9.1) gives an unspecific band in G1 arrested cells. PGK1 was used as a loading control.

7.13.2 *RAD9* deletion in *GAL-URL-3HA-SEN1 rrm3* cells bypasses the first G2/M block

Rad9 is a DNA damage checkpoint protein required throughout the cell cycle. *RAD9* null mutants are viable but exhibit strong sensitivity to X-ray and UV irradiation. *rad9* cells fail to arrest the cell cycle in response to DNA damage (Fasullo et al., 1998; Weinert and Hartwell, 1988, 1990).

A

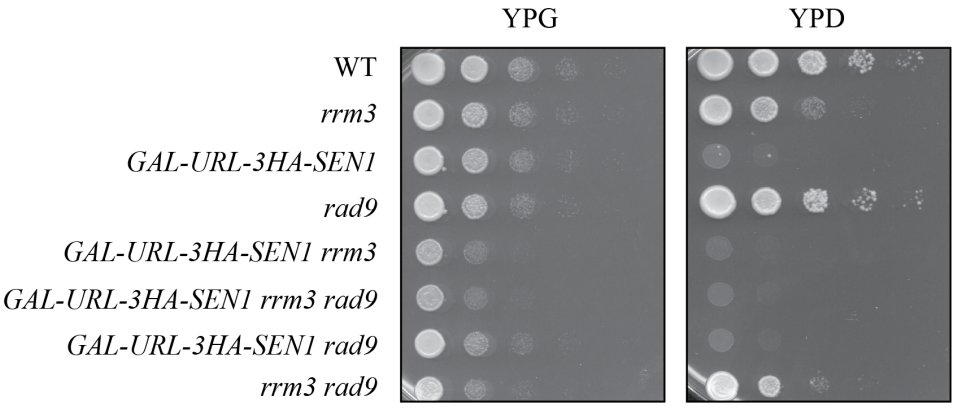

We have deleted *RAD9* in order to better understand the checkpoint role in *GAL-URL-3HA-SEN1 rrm3* cells. *RAD9* is the only DNA damage checkpoint gene, whose deletion is not lethal in permissive growth conditions (YPG) of *GAL-URL-3HA-SEN1 rrm3* cells. Mutated *MEC1*, *TEL1* and *RAD53* are already

synthetic lethal combined with used in this study *SEN1* conditional system with deleted *RRM3* grown in YPG (data not shown).

B

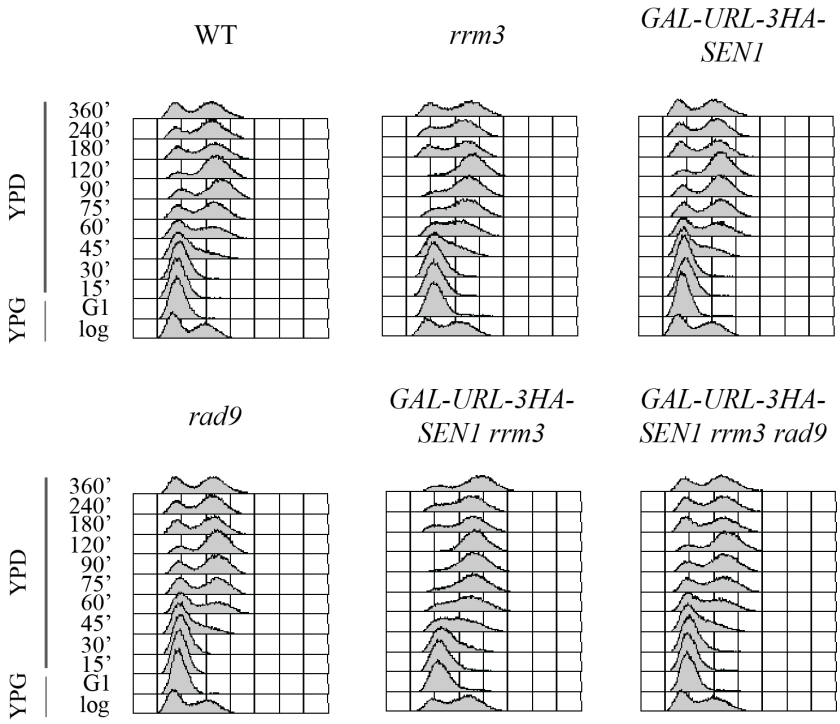

Figure 19. *GAL-URL-3HA-SEN1 rrm3 rad9* are synthetic lethal but fail to arrest at the first G2/M phase of the cell cycle.

(A) Serial dilutions of WT, *rrm3*, *GAL-URL-3HA-SEN1*, *rad9*, *GAL-URL-3HA-SEN1 rrm3*, *GAL-URL-3HA-SEN1 rrm3 rad9*, *GAL-URL-3HA-SEN1 rad9* in YPG and YPD plates. The plates were kept at 25°C.
(B) WT, *rrm3*, *GAL-URL-3HA-SEN1*, *rad9*, *GAL-URL-3HA-SEN1 rrm3*, and *GAL-URL-3HA-SEN1 rrm3 rad9* cells were grown exponentially at 25°C (log) in YPG, synchronized with α-factor in G1 in YPG at 25°C and released in YPD at 25°C. Indicated time points were taken and proceeded for FACS analysis.

Serial dilutions of *GAL-URL-3HA-SEN1 rrm3 rad9* on YPD plates showed that the triple mutants were unviable (Figure 19A). Interestingly, these

cells bypass the G2/M block of the first cell cycle as shown by FACS analysis (Figure 19B). *GAL-URL-3HA-SEN1 rrm3 rad9* cells not only fail to arrest in G2/M but also keep cycling in YPD for an extra 4 divisions when compared to *GAL-URL-3HA-SEN1 rrm3* mutants.

7.13.3 *GAL-URL-3HA-SEN1 rrm3 rad9* cells cycle with chromosomes partially replicated

Due to the observed bypass of first G2/M arrest in *GAL-URL-3HA-SEN1 rrm3 rad9* cells, we questioned the checkpoint contribution in DNA replication completion. Thus, we monitored replication forks merge at *TER*s by genome-wide BrdU incorporation. As previously described, the cells were arrested in G1 in YPG and then released in YPD (adding BrdU 20 minutes before the complete arrest) in the presence of BrdU and nocodazole. The G2/M arrest was kept for 3 hours. Together with *GAL-URL-3HA-SEN1 rrm3 rad9* we used WT and *GAL-URL-3HA-SEN1 rrm3* cells as a negative and positive control, respectively.

Due to BrdU incorporation time limitations (Lengronne et al., 2001), working at 25°C and changing the sugar source from galactose to glucose, we monitored replication fork fusion across *TER*s localized in between early firing origins with inter-origin distance up to 25 kb. The results we obtained in *GAL-URL-3HA-SEN1 rrm3 rad9* mirror replication completion failure in *GAL-URL-3HA-SEN1 rrm3* cells. In all analysed *TER*s, with the inter-origin distance between 10 and 25 kb, only in *TER503*, *TER601*, *TER704*, *TER902*, *TER1202*, *TER1604* we did observe fork fusion both in WT and *GAL-URL-3HA-SEN1 rrm3*

rad9 cells. *TER704*, *TER1202* and *TER1604* are CEN-dependent while *TER503*, *TER601* and *TER902* are non-highly transcribed Pol II termination zones.

These data suggest that the ablation of *RAD9* does not mediate replication termination in the absence of Sen1 and Rrm3 helicases.

A

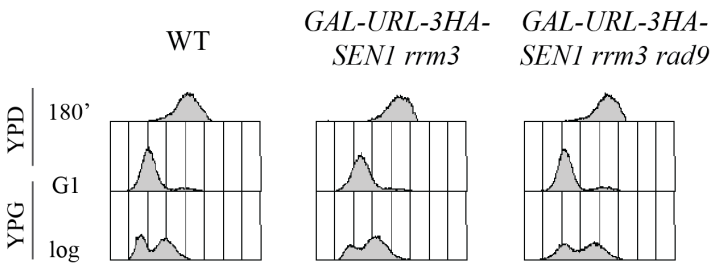

B

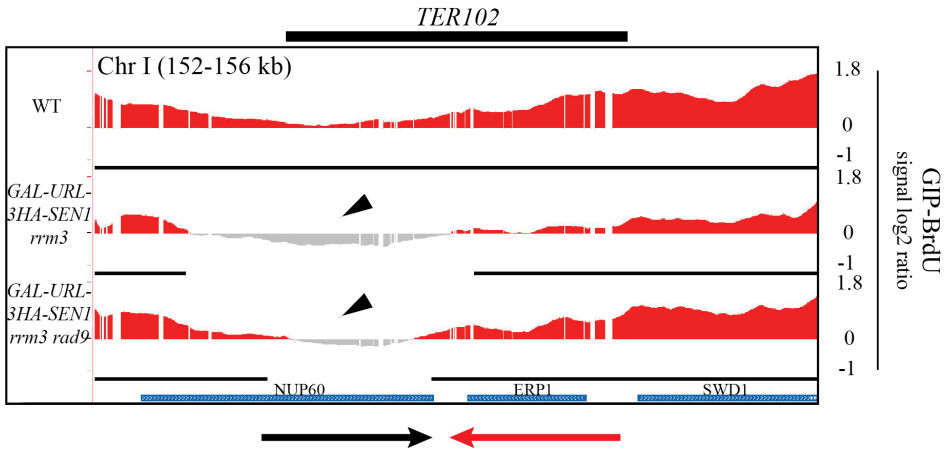

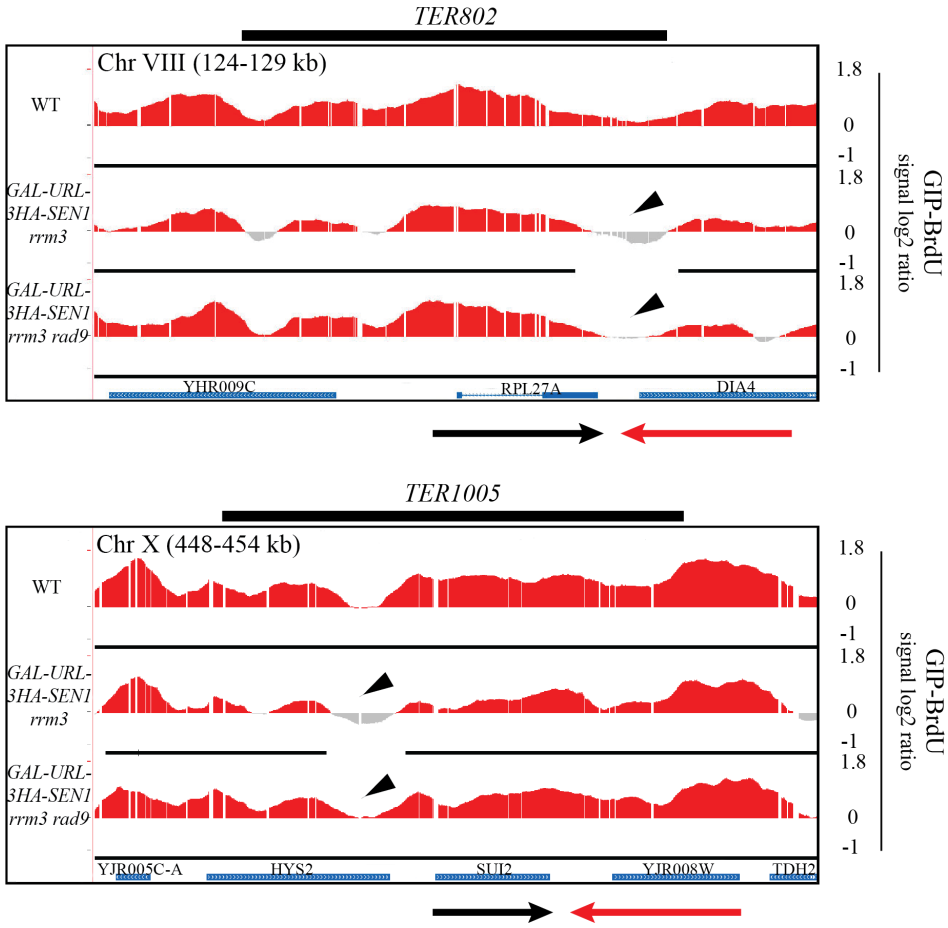
TER802
Chr VIII (124-129 kb)
WT
GAL-URL-3HA-SEN1 rrm3
GAL-URL-3HA-SEN1 rrm3 rad9
YHR009C
RPL27A
DIA4
1.8
0
-1
GIP-BrdU signal log2 ratio
TER1005
Chr X (448-454 kb)
YJR005C-A
HYS2
SUI2
YJR008W
TDH2

C

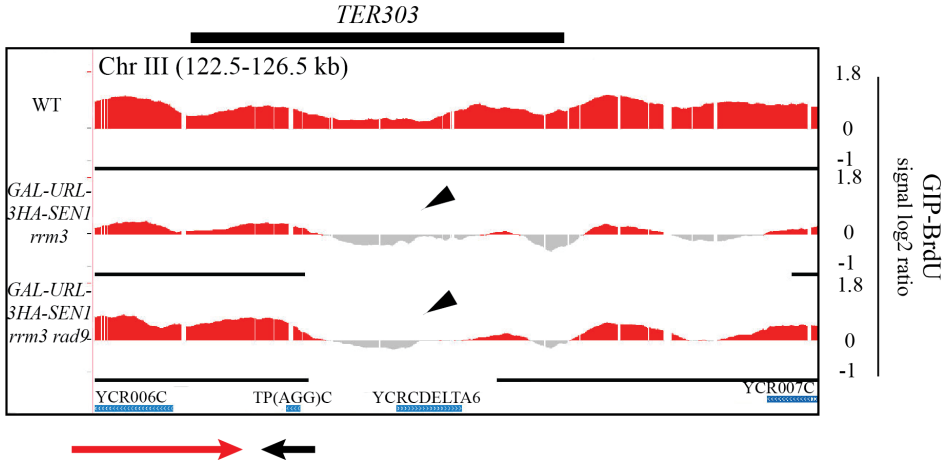
TER303
Chr III (122.5-126.5 kb)
WT
GAL-URL-3HA-SEN1 rrm3
GAL-URL-3HA-SEN1 rrm3 rad9
YCR006C
TP(AGG)C
YCRCDELTA6
YCR007C
1.8
0
-1
GIP-BrdU signal log2 ratio

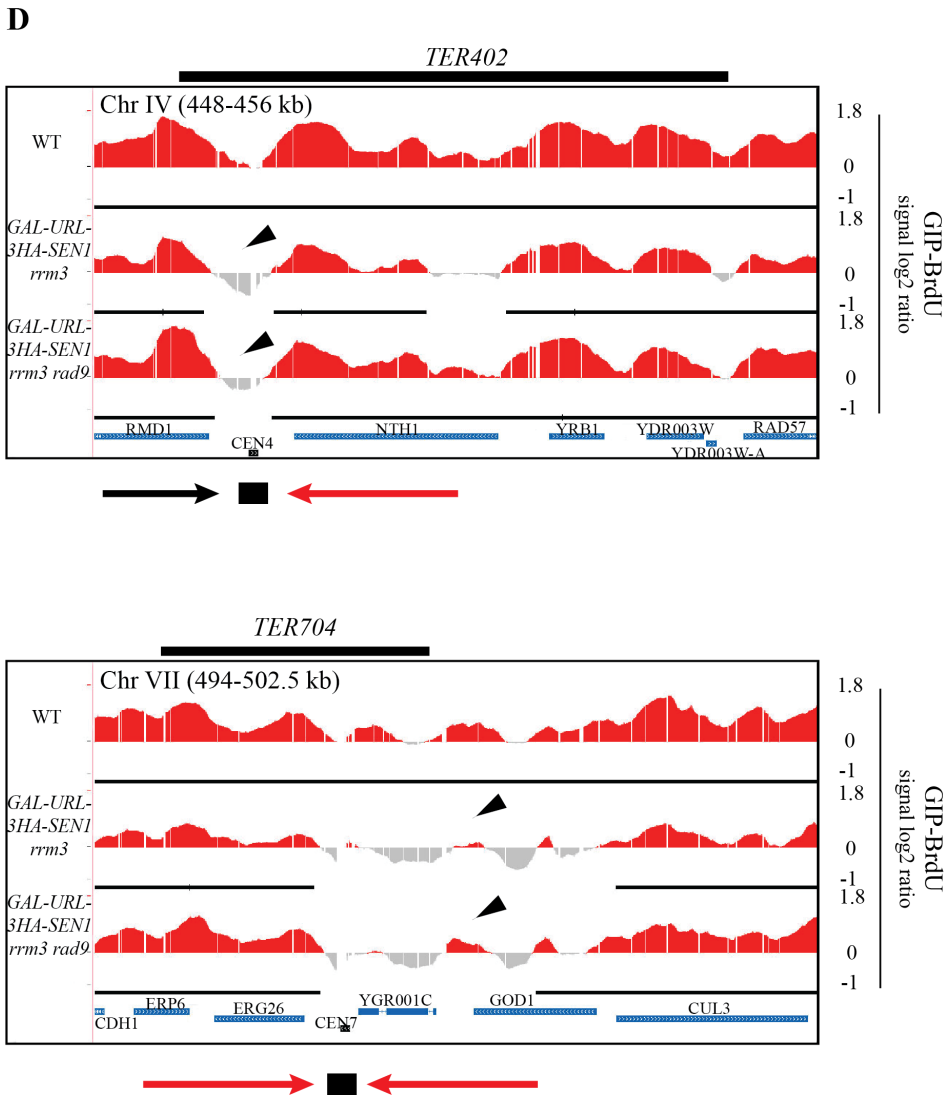

Figure 20. The checkpoint does not influence replication termination in *GAL-URL-3HA-SEN1 rrm3* cells.

WT, *GAL-URL-3HA-SEN1 rrm3* and *GAL-URL-3HA-SEN1 rrm3 rad9* cells were grown in YPG at 25°C, arrested with α-factor and released in YPD at 25°C with nocodazole and BrdU. The arrest was kept for 3 hours.

(A) FACS analysis of studied strains.

(B-D) GIP with BrdU incorporation across three types of termination zones: Pol II (B), tRNA (C) and CEN-dependent (D). Direction of the replication forks, mRNA transcripts and the position of tRNA and *CEN* are indicated. Red peaks correspond to BrdU-IP while the grey peaks display to the SUP fraction. Thin black bars below the peaks refer to statistically significant clusters of incorporated

BrdU. Thick black bars above each *TER* profile indicate the length of the zone where termination occurs. Black arrows indicate a gap between converging replication forks.

8 Discussion

8.1 Evolutionary impact of polar replication forks

Eukaryotic replication termination occurs at *TER*s that contain replication fork pausing elements. Eukaryotes and Prokaryotes share common features in terminating DNA replication within specific *TER*s, which contain polar pausing elements and are genetically unstable in certain backgrounds. In *Escherichia coli*, *Ter* regions and Tus protein, which is a trans-acting factor required for replication fork arrest, determine proper replication termination. Tus protein binds *Ter* and blocks the helicase DnaB in an orientation-specific manner. The trap mechanism of replication termination in *E. coli*, localized opposite from the single origin of replication in a circular chromosome, is similar in *Bacillus subtilis.* Even if the protein and DNA components involved in polar replication fork arrest in *B. subtilis* are different from Tus and *Ter* in *E. coli*, the replication termination protein (RTP) also has a *contrahelicase* surface that arrest approaching DNA helicase (Mirkin and Mirkin, 2007).

Sequence-specific protein binding that trigger replication fork arrest is not only restricted to prokaryotic replicons. A polar replication fork block has been also observed in Eukaryotes at ribosomal DNA loci. High density of polymerases and long transcription units challenge the integrity of rDNA by polymerase traffic. Site-specific replication fork arrest occurs in yeast (Linskens and Huberman, 1988), plants (Hernandez et al., 1993), frogs (Wiesendanger et al., 1994) and humans (Little et al., 1993). Replication fork barriers (RFBs) work in a polar manner. They assure that replicative machineries enter the pre-RNA coding

regions in the same direction as transcription, so rDNA can be replicated unidirectionally.

The recent findings in *S. cerevisiae* argue the tremendous evolutionary impact of the polar replication fork barriers in chromosome replication (Fachinetti et al., 2010). It has been noted that 58/71 *TER*s have well conserved pause sites in other yeasts. *CEN*s were excluded from these analyses because they rapidly diverge in evolution (Henikoff et al., 2001). Therefore, evolution was driven towards preserving *TER*-containing pause sites integrity.

In these studies we have shown that both Sen1 and Rrm3 assist replication fork progression across *TER*s and are indispensible in fork fusion. In the absence of Sen1 and Rrm3, we have examined BrdU incorporation at termination zones localized between early and efficient origins of replication with the inter-origin distance up to 25 kb. We observed replication termination failure in 17/23 *TER*s in *GAL-URL-3HA-SEN1 rrm3* cells. The fusion that we noted occurred within three *CEN*s (*TER704*, *TER1202*, *TER1604*) and three *TER*s containing non-highly transcribed Pol II units (*TER503*, *TER601*, *TER902*). Following BrdU incorporation profile, we noted that replication forks fuse at *TER*s in an asymmetric manner.

8.2 Transcription as a major hindrance in the replication fork progression across *TER*s

Replication forks come across many natural impediments. Stable DNA-protein complexes, DNA secondary structures, converged forks and highly transcribed genes challenge the fork progression. Transcription and transcription-

related processes cause replication stress and altered DNA topology in S phase. The S phase architecture of RNAPII genes is highly regulated (Bermejo et al., 2009) and the ATR checkpoint needs to counteract gene gating to allow replication fork progression when encounters transcription bubble (Bermejo et al., 2011). How the transcription apparatus is dismantled after releasing the gated loop from the nuclear pore still remains elusive. Conflicts arising from replication and transcription collisions are inevitable. Head-on clashes between transcription and replication machineries pose additional problem due to the high topology complexity ahead of the fork (Bermejo et al., 2012). Positive supercoiling, R-loops, non-B-DNA structures formation and promotion of DNA damage affect the genetic landscape.

Rrm3 is a Pif1-family related helicase. Pif1 is preferentially active on DNA:RNA hybrids, as seen as a faster rate on DNA:RNA hybrids unwinding compared to DNA:DNA hybrids (Boule and Zakian, 2007). Our data for the first time indicate the role of Rrm3 in unwinding hybrids at Pol III containing *TER*s, which are known to be Rrm3-dependent regions. In contrary, Sen1 is known to remove DNA:RNA hybrids at Pol II regions when transcription encounters replication fork. While we did not observe aberrant replication termination in Sen1- defective cells, the absence of *RRM3* leads to termination failures, which are deleterious for genome stability.

Here we show that replication termination needs to coordinate replication fork progression, topological dynamics and transcription processes. Our data provide evidence that in cells lacking both Sen1 and Rrm3 replication forks do not fuse at *TER*s in head-on and co-directional oriented highly transcribed Pol II and

Pol III genes. In 3/20 analysed *TER*s (excluding *CEN*s), where we detected the fork fusion, the level of transcription was very low (Azvolinsky et al., 2009). We show that both Sen1 and Rrm3 counteract DNA:RNA hybrids accumulation at *TER*s. Although the hybrids accumulate both in co-directional and head-on clashes with replication fork at *TER*s, there are more abundant in the head-on blocks with highly transcribed genes. Moreover, the more abundant DNA:RNA hybrids are, the less complete BrdU incorporation at *TER*s is observed.

8.3 Interlinked DNA molecules formation in G2/M in the absence of Sen1 and Rrm3

We showed that Sen1- and Rrm3- defective cells have abnormal morphology and arrest in G2/M in the first cell cycle. The lack of Sen1 and Rrm3 helicases does not affect origin firing but termination events. However, we failed to detect replication intermediates at *TER*s in G2/M arrested cells.

Recent studies in mammalian cells have shown that DNA replication stress generates DAPI-negative ultra-fine bridges (UFBs) of DNA connecting daughter nuclei during mitosis (Chan et al., 2009). As a consequence of UFBs formation, sister chromatids are interlinked by replication intermediates at the chromosomal fragile sites, which are loci of frequent breakage and translocations. The Fanconi anaemia proteins FANCD2 and FANC1 connect with these fragile site loci and are linked through BLM (Bloom syndrome)-associated UFBs. Both BLM and FANC A-N syndromes are associated with cancer predisposition. In budding yeast, Rad52 and RPA proteins are recognized at the structures that resemble mammalian UFBs (Michael Lisby, unpublished). The RPA detection at

UFBs indicates that these anaphase bridges contain unreplicated ssDNA stretches. Moreover, Dpb11 protein, which is a multifunctional factor acting in replication initiation and as a checkpoint sensor recruited to stalled replication forks where it activates Mec1p, also coats these structures that connect the two daughter nuclei (Michael Lisby, unpublished). Therefore, the tremendous topological force between converging forks at *TER*s might pull away the interlinked unreplicated molecules. It is also known that catenated junctions might be mobile and spread along the chromosome (Spell and Holm, 1994). In this scenario, perhaps replication intermediates cannot be visualized at the analysed restriction fragments by 2D-gels. Replisomes at stalled forks might be backtracked, allowing processing of the nascent chains through the action of exo/endonucleases. This theory needs to be verified by choosing a different digestion strategy, in which a wider fragment that includes *TER* and its adjacent regions is analysed. It is also possible that those forks that are unable to fuse due to topological constrains undergo fork reversal during processing.

Another piece of data, which confirms the formation of interlinked, not fully replicated chromosomes in G2/M arrested *GAL-URL-3HA-SEN1 rrm3* cells, comes from the PFGE analysis. Up to 25 % of the DNA exhibit topologically complex structures in the G2/M phase. We can therefore conclude that Sen1 and Rrm3 contribute in resolving the topological complexity of replicon fusion.

8.4 Are *TER*s the hot spots for DNA breakage?

The topological stress generated when replication forks approach from opposite directions, and eventually fuse at *TER*, cause the accumulation of

supercoils, precatenates and/or hemicatenates. It is known from Prokaryotes and *in vitro* studies that precatenates are mainly resolved by topoisomerase II, but can be a substrate for topoisomerase I activity. Hemicatenates resolution is instead mediated by RecQ helicases together with topoisomerase III. Due to the high-risk topological transitions at *TER*s, they may represent fragile sites prone to genome rearrangements and DNA breakage.

We have observed DNA breakage at *TER*s during metaphase-anaphase transition in *GAL-URL-3HA-SEN1 rrm3* cells (Figure 17B). We speculate that the abnormal accumulation of interlocked replication termination intermediates causes sister chromatids' entanglement. Thus, the onset of anaphase generates a mechanical stress that pulls apart the sister chromatids, which are still topologically linked. Then, internal chromosomal stress, where mechanism still needs to be unravelled, causes chromosome breakage at the linking regions at *TER*s, perhaps through activity of Topo II. Intriguingly, four of the five *TER*s on chromosome III are known as replication slow zones (*RSZ*s) (Cha and Kleckner, 2002). *RSZ*s are proposed to share the functional homology with the mammalian common fragile sites (CFSs), which stability is regulated by ATR. In budding yeast lack of *MEC1* (mammalian ATR) leads do genomewide fork collapse, which results in chromosome breakage. Breaks are not formed stochastically but occur at specific regions during G2 chromosomal transition (Cha and Kleckner, 2002). We assume that replication fork pausing elements and *RSZ*s contribute to the integrity of termination zones, which is controlled by Mec1 and Rad53. Indeed, we have detected Rad53 phosphorylation in *GAL-URL-3HA-SEN1 rrm3* cells. Moreover, deletion of a checkpoint gene, *RAD9*, results in the bypass of the

first G2/M arrest, which probably leads to high rate mutations formation and cell death.

The very recent studies of the *MEC1*-sensitive fragile sites unravelled additional events required for the break formation (Hashash et al., 2012). It has been shown that chromosome breakage at *RSZ*s is independent of the *RAD52* epistasis group genes and of *TOP3*, *SGS1*, *SRS2*, *MMS4* and *MUS81*. These data exclude the homologous recombination and recombination-related processes contribution in break formation. Considering *TER*s as break-prone regions, this is consistent with our results. We have shown that Rad51 is not involved in topological transitions during fork fusion. Moreover, *RAD51* deletion does not rescue the *sen1 rrm3* lethality as it does in *sen1 sgs1* and *sen1 srs2*. Hashash and co-workers (Hashash et al., 2012) has argued that spindle force, anaphase and cytokinesis are dispensable in break formation at *RSZ*s. The breakage at the *MEC1*-sensitive fragile sites depends on condensin subunits (*YCG1* and *YSC4*) and topoisomerase II (*TOP2*). It is proposed that internal stress during mitotic chromosome condensation is involved in break formation at *RSZ*s in *mec1* mutants. These findings are consistent with our studies regarding break formation at *TER*s. We hypothesize that Top2 and condensins are responsible for break formation at *TER*s, especially that Top2 is known to be involved in the last 1 kb catenates resolution between converging forks at *TER*s (Fachinetti et al., 2010). It will be interesting to check *GAL-URL-3HA-SEN1 rrm3 top2-1* and *GAL-URL-3HA-SEN1 rrm3 ycg1*/*ysc4* mutants by PFGE and see whether chromosome breakage in these modified genetic backgrounds is repressed.

8.5 Terminating replication at *TER*s

DNA damage caused by R loops accumulation, DNA breaks and presumably ssDNA formation due to Rad53p phosphorylation cannot be repaired and leads to cell death in *GAL-URL-3HA-SEN1 rrm3* cells. Our data place Sen1 with Rrm3 at termination zones where together they counteract deleterious DNA:RNA hybrids accumulation and break formation. Failure to regulate the collisions between replication and transcription at *TER*s affect genome stability and can have relevant implications for cancer.

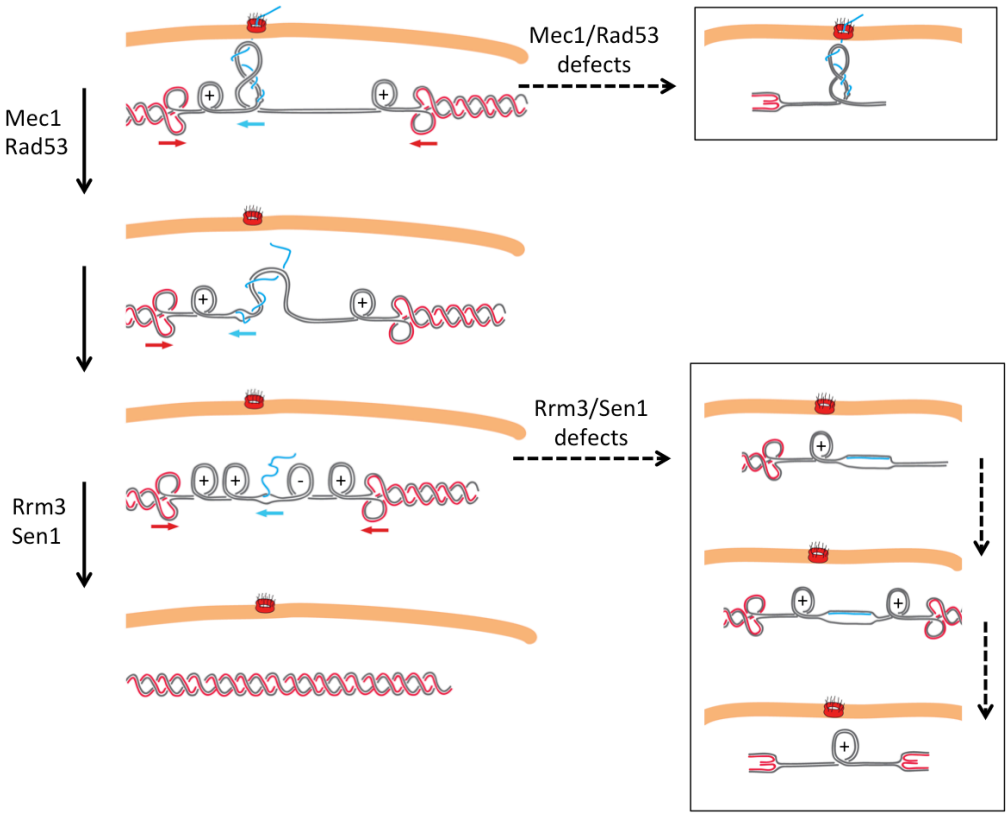

Model 7. A model of combined action of Mec1, Rad53, Sen1 and Rrm3 in replication termination at *TER*s.

The model represents replication fork fusion at *TER* with a gene gating as a threat for replication fork progression. Direction of replication forks (red) and transcribed mRNA (blue) are depicted by the arrows.
The left panel represents a physiological situation with functional checkpoint genes (Mec1 and Rad53) and replicative helicases (Sen1 and Rrm3). The right panel refers to a pathological situation in the absence of functional Mec1/Rad53 or defective Sen1 and Rrm3. The model is described in the text below.

We propose a model for terminating replication at *TER*s, in which a proper coordination of the checkpoint factors, Mec1 and Rad53, and replicative helicases, Sen1 and Rrm3, is indispensable for replication completion (Model 7).

In physiological situations (Model 7, left panel) when replication fork encounters gated loops (in the model the replication/transcription clash is head-on oriented), the local checkpoint becomes activated and leads to the gene loop's dismantlement (Model 7, top left panel). When the architectural domain of transcribed region at *TER* is simplified, the fork can continue its passage. Both types of topoisomerases, Top1 and Top2, travel with replication fork (not stressed in the Model 7). Top2 is involved in precatenanes resolution behind the fork while Top1 relaxes the positive supercoiling ahead. The polarity of the fork merge ensures that after gene loop dismantlement, the upcoming fork (co-directionally oriented with the transcript) will absorb the negative supercoils accumulated behind the transcription bubble. DNA:RNA hybrids removal at *TER* by Sen1 and Rrm3 helicases, and last 1 kb catenanes relaxation by Top2, results in a proper fork fusion and chromosome resolution.

In pathological situations (Model 7, right panel) in checkpoint-defective cells, NPC-associated gene loops are a threat for replication fork. Not dismantled gated loops redound to a tremendous torsional stress accumulation ahead of the

fork, which leads to the fork reversal and cell death (Model 7, top right panel). In a situation when both Sen1 and Rrm3 helicases are defective, DNA:RNA hybrids persist on the lagging strand. Co-directionally upcoming replication fork, with positive supercoils ahead, remove the negatively supercoiled DNA:RNA hybrids, which accumulation is transient and restricted to S phase (what we have shown). The lack of both helicases and topological tension between forks might lead to termination intermediates backtracking, and later results in break formation at *TER*s and cell death.

Our data provide a novel understanding of topological transitions and mechanisms responsible for polar replication termination at *TER*s in Eukaryotes. Those mechanisms involve replication/transcription coordination, topoisomerases activity and DNA checkpoint control. Defects in any of those processes have deleterious consequences for genome stability.

9 References

Admire, A., Shanks, L., Danzl, N., Wang, M., Weier, U., Stevens, W., Hunt, E., and Weinert, T. (2006). Cycles of chromosome instability are associated with a fragile site and are increased by defects in DNA replication and checkpoint controls in yeast. Genes Dev *20*, 159-173.

Aggarwal, B.D., and Calvi, B.R. (2004). Chromatin regulates origin activity in Drosophila follicle cells. Nature *430*, 372-376.

Aguilera, A., and Garcia-Muse, T. (2012). R loops: from transcription byproducts to threats to genome stability. Mol Cell *46*, 115-124.

Alcasabas, A.A., Osborn, A.J., Bachant, J., Hu, F., Werler, P.J., Bousset, K., Furuya, K., Diffley, J.F., Carr, A.M., and Elledge, S.J. (2001). Mrc1 transduces signals of DNA replication stress to activate Rad53. Nat Cell Biol *3*, 958-965.

Allen, J.B., Zhou, Z., Siede, W., Friedberg, E.C., and Elledge, S.J. (1994). The SAD1/RAD53 protein kinase controls multiple checkpoints and DNA damage-induced transcription in yeast. Genes Dev *8*, 2401-2415.

Alvino, G.M., Collingwood, D., Murphy, J.M., Delrow, J., Brewer, B.J., and Raghuraman, M.K. (2007). Replication in hydroxyurea: it's a matter of time. Mol Cell Biol *27*, 6396-6406.

Alzu, A., Bermejo, R., Begnis, M., Lucca, C., Piccini, D., Carotenuto, W., Saponaro, M., Brambati, A., Cocito, A., Foiani, M*., et al.* (2012). Senataxin Associates with Replication Forks to Protect Fork Integrity across RNA-Polymerase-II-Transcribed Genes. Cell *151*, 835-846.

Aparicio, O.M., Stout, A.M., and Bell, S.P. (1999). Differential assembly of Cdc45p and DNA polymerases at early and late origins of DNA replication. Proc Natl Acad Sci U S A *96*, 9130-9135.

Aparicio, O.M., Weinstein, D.M., and Bell, S.P. (1997). Components and dynamics of DNA replication complexes in S. cerevisiae: redistribution of MCM proteins and Cdc45p during S phase. Cell *91*, 59-69.

Araki, H., Leem, S.H., Phongdara, A., and Sugino, A. (1995). Dpb11, which interacts with DNA polymerase II(epsilon) in Saccharomyces cerevisiae, has a dual role in S-phase progression and at a cell cycle checkpoint. Proc Natl Acad Sci U S A *92*, 11791-11795.

Arlt, M.F., and Glover, T.W. (2010). Inhibition of topoisomerase I prevents chromosome breakage at common fragile sites. DNA Repair (Amst) *9*, 678-689.

Azvolinsky, A., Dunaway, S., Torres, J.Z., Bessler, J.B., and Zakian, V.A. (2006). The S. cerevisiae Rrm3p DNA helicase moves with the replication fork and affects replication of all yeast chromosomes. Genes Dev *20*, 3104-3116.

Azvolinsky, A., Giresi, P.G., Lieb, J.D., and Zakian, V.A. (2009). Highly transcribed RNA polymerase II genes are impediments to replication fork progression in Saccharomyces cerevisiae. Mol Cell *34*, 722-734.

Bachant, J., Alcasabas, A., Blat, Y., Kleckner, N., and Elledge, S.J. (2002). The SUMO-1 isopeptidase Smt4 is linked to centromeric cohesion through SUMO-1 modification of DNA topoisomerase II. Mol Cell *9*, 1169-1182.

Bachmair, A., Finley, D., and Varshavsky, A. (1986). In vivo half-life of a protein is a function of its amino-terminal residue. Science *234*, 179-186.

Baxter, J., and Diffley, J.F. (2008). Topoisomerase II inactivation prevents the completion of DNA replication in budding yeast. Mol Cell *30*, 790-802.

Bell, L., and Byers, B. (1983). Separation of branched from linear DNA by two-dimensional gel electrophoresis. Anal Biochem *130*, 527-535.

Bell, S.P., and Stillman, B. (1992). ATP-dependent recognition of eukaryotic origins of DNA replication by a multiprotein complex. Nature *357*, 128-134.

Bergerat, A., Gadelle, D., and Forterre, P. (1994). Purification of a DNA topoisomerase II from the hyperthermophilic archaeon Sulfolobus shibatae. A thermostable enzyme with both bacterial and eucaryal features. J Biol Chem *269*, 27663-27669.

Bermejo, R., Capra, T., Gonzalez-Huici, V., Fachinetti, D., Cocito, A., Natoli, G., Katou, Y., Mori, H., Kurokawa, K., Shirahige, K., *et al.* (2009). Genome-organizing factors Top2 and Hmo1 prevent chromosome fragility at sites of S phase transcription. Cell *138*, 870-884.

Bermejo, R., Capra, T., Jossen, R., Colosio, A., Frattini, C., Carotenuto, W., Cocito, A., Doksani, Y., Klein, H., Gomez-Gonzalez, B., *et al.* (2011). The replication checkpoint protects fork stability by releasing transcribed genes from nuclear pores. Cell *146*, 233-246.

Bermejo, R., Doksani, Y., Capra, T., Katou, Y.M., Tanaka, H., Shirahige, K., and Foiani, M. (2007). Top1- and Top2-mediated topological transitions at replication forks ensure fork progression and stability and prevent DNA damage checkpoint activation. Genes Dev *21*, 1921-1936.

Bermejo, R., Lai, M.S., and Foiani, M. (2012). Preventing replication stress to maintain genome stability: resolving conflicts between replication and transcription. Mol Cell *45*, 710-718.

Bessman, M.J., Lehman, I.R., Simms, E.S., and Kornberg, A. (1958). Enzymatic synthesis of deoxyribonucleic acid. II. General properties of the reaction. J Biol Chem *233*, 171-177.

Birren, B.W., Hood, L., and Lai, E. (1989). Pulsed field gel electrophoresis: studies of DNA migration made with the programmable, autonomously-controlled electrode electrophoresis system. Electrophoresis *10*, 302-309.

Boldog, F., Gemmill, R.M., West, J., Robinson, M., Robinson, L., Li, E., Roche, J., Todd, S., Waggoner, B., Lundstrom, R., *et al.* (1997). Chromosome 3p14 homozygous deletions and sequence analysis of FRA3B. Hum Mol Genet *6*, 193-203.

Boule, J.B., and Zakian, V.A. (2007). The yeast Pif1p DNA helicase preferentially unwinds RNA DNA substrates. Nucleic Acids Res *35*, 5809-5818.

Branzei, D., and Foiani, M. (2006). The Rad53 signal transduction pathway: Replication fork stabilization, DNA repair, and adaptation. Exp Cell Res *312*, 2654-2659.

Brewer, B.J. (1988). When polymerases collide: replication and the transcriptional organization of the E. coli chromosome. Cell *53*, 679-686.

Brewer, B.J., and Fangman, W.L. (1987). The localization of replication origins on ARS plasmids in S. cerevisiae. Cell *51*, 463-471.

Brewer, B.J., and Fangman, W.L. (1988). A replication fork barrier at the 3' end of yeast ribosomal RNA genes. Cell *55*, 637-643.

Brewer, B.J., Lockshon, D., and Fangman, W.L. (1992). The arrest of replication forks in the rDNA of yeast occurs independently of transcription. Cell *71*, 267-276.

Brush, G.S., Morrow, D.M., Hieter, P., and Kelly, T.J. (1996). The ATM homologue MEC1 is required for phosphorylation of replication protein A in yeast. Proc Natl Acad Sci U S A *93*, 15075-15080.

Burgers, P.M. (2009). Polymerase dynamics at the eukaryotic DNA replication fork. J Biol Chem *284*, 4041-4045.

Cabal, G.G., Genovesio, A., Rodriguez-Navarro, S., Zimmer, C., Gadal, O., Lesne, A., Buc, H., Feuerbach-Fournier, F., Olivo-Marin, J.C., Hurt, E.C.*, et al.* (2006). SAGA interacting factors confine sub-diffusion of transcribed genes to the nuclear envelope. Nature *441*, 770-773.

Cadoret, J.C., Meisch, F., Hassan-Zadeh, V., Luyten, I., Guillet, C., Duret, L., Quesneville, H., and Prioleau, M.N. (2008). Genome-wide studies highlight indirect links between human replication origins and gene regulation. Proc Natl Acad Sci U S A *105*, 15837-15842.

Calin, G.A., Sevignani, C., Dumitru, C.D., Hyslop, T., Noch, E., Yendamuri, S., Shimizu, M., Rattan, S., Bullrich, F., Negrini, M.*, et al.* (2004). Human microRNA genes are frequently located at fragile sites and genomic regions involved in cancers. Proc Natl Acad Sci U S A *101*, 2999-3004.

Casper, A.M., Nghiem, P., Arlt, M.F., and Glover, T.W. (2002). ATR regulates fragile site stability. Cell *111*, 779-789.

Celeste, A., Fernandez-Capetillo, O., Kruhlak, M.J., Pilch, D.R., Staudt, D.W., Lee, A., Bonner, R.F., Bonner, W.M., and Nussenzweig, A. (2003). Histone H2AX phosphorylation is dispensable for the initial recognition of DNA breaks. Nat Cell Biol *5*, 675-679.

Cha, R.S., and Kleckner, N. (2002). ATR homolog Mec1 promotes fork progression, thus averting breaks in replication slow zones. Science *297*, 602-606.

Champoux, J.J. (2001). DNA topoisomerases: structure, function, and mechanism. Annu Rev Biochem *70*, 369-413.

Chan, K.L., and Hickson, I.D. (2009). On the origins of ultra-fine anaphase bridges. Cell Cycle *8*, 3065-3066.

Chan, K.L., Palmai-Pallag, T., Ying, S., and Hickson, I.D. (2009). Replication stress induces sister-chromatid bridging at fragile site loci in mitosis. Nat Cell Biol *11*, 753-760.

Chen, Y.Z., Bennett, C.L., Huynh, H.M., Blair, I.P., Puls, I., Irobi, J., Dierick, I., Abel, A., Kennerson, M.L., Rabin, B.A.*, et al.* (2004). DNA/RNA helicase gene mutations in a form of juvenile amyotrophic lateral sclerosis (ALS4). Am J Hum Genet *74*, 1128-1135.

Codlin, S., and Dalgaard, J.Z. (2003). Complex mechanism of site-specific DNA replication termination in fission yeast. Embo J *22*, 3431-3440.

Cortez, D., Wang, Y., Qin, J., and Elledge, S.J. (1999). Requirement of ATM-dependent phosphorylation of brca1 in the DNA damage response to double-strand breaks. Science *286*, 1162-1166.

Coskun-Ari, F.F., and Hill, T.M. (1997). Sequence-specific interactions in the Tus-Ter complex and the effect of base pair substitutions on arrest of DNA replication in Escherichia coli. J Biol Chem *272*, 26448-26456.

Dalgaard, J.Z., and Klar, A.J. (1999). Orientation of DNA replication establishes mating-type switching pattern in S. pombe. Nature *400*, 181-184.

Dalgaard, J.Z., and Klar, A.J. (2000). swi1 and swi3 perform imprinting, pausing, and termination of DNA replication in S. pombe. Cell *102*, 745-751.

Dalgaard, J.Z., and Klar, A.J. (2001). A DNA replication-arrest site RTS1 regulates imprinting by determining the direction of replication at mat1 in S. pombe. Genes Dev *15*, 2060-2068.

De Braekeleer, M., Sreekantaiah, C., and Haas, O. (1992). Herpes simplex virus and human papillomavirus sites correlate with chromosomal breakpoints in human cervical carcinoma. Cancer Genet Cytogenet *59*, 135-137.

Dellino, G.I., Cittaro, D., Piccioni, R., Luzi, L., Banfi, S., Segalla, S., Cesaroni, M., Mendoza-Maldonado, R., Giacca, M., and Pelicci, P.G. (2013). Genome-wide mapping of human DNA-replication origins: levels of transcription at ORC1 sites regulate origin selection and replication timing. Genome Res *23*, 1-11.

DeMarini, D.J., Winey, M., Ursic, D., Webb, F., and Culbertson, M.R. (1992). SEN1, a positive effector of tRNA-splicing endonuclease in Saccharomyces cerevisiae. Mol Cell Biol *12*, 2154-2164.

Desdouets, C., Santocanale, C., Drury, L.S., Perkins, G., Foiani, M., Plevani, P., and Diffley, J.F. (1998). Evidence for a Cdc6p-independent mitotic resetting event involving DNA polymerase alpha. Embo J *17*, 4139-4146.

Dimitrova, D.S., and Gilbert, D.M. (1998). Regulation of mammalian replication origin usage in Xenopus egg extract. J Cell Sci *111 (Pt 19)*, 2989-2998.

Doksani, Y., Bermejo, R., Fiorani, S., Haber, J.E., and Foiani, M. (2009). Replicon dynamics, dormant origin firing, and terminal fork integrity after double-strand break formation. Cell *137*, 247-258.

Downs, J.A., Lowndes, N.F., and Jackson, S.P. (2000). A role for Saccharomyces cerevisiae histone H2A in DNA repair. Nature *408*, 1001-1004.

Dutrow, N., Nix, D.A., Holt, D., Milash, B., Dalley, B., Westbroek, E., Parnell, T.J., and Cairns, B.R. (2008). Dynamic transcriptome of Schizosaccharomyces pombe shown by RNA-DNA hybrid mapping. Nat Genet *40*, 977-986.

Edenberg, H.J., and Huberman, J.A. (1975). Eukaryotic chromosome replication. Annu Rev Genet *9*, 245-284.

Elledge, S.J. (1996). Cell cycle checkpoints: preventing an identity crisis. Science *274*, 1664-1672.

Fachinetti, D., Bermejo, R., Cocito, A., Minardi, S., Katou, Y., Kanoh, Y., Shirahige, K., Azvolinsky, A., Zakian, V.A., and Foiani, M. (2010). Replication termination at eukaryotic chromosomes is mediated by Top2 and occurs at genomic loci containing pausing elements. Mol Cell *39*, 595-605.

Fasullo, M., Bennett, T., AhChing, P., and Koudelik, J. (1998). The Saccharomyces cerevisiae RAD9 checkpoint reduces the DNA damage-associated stimulation of directed translocations. Mol Cell Biol *18*, 1190-1200.

Ferguson, B.M., and Fangman, W.L. (1992). A position effect on the time of replication origin activation in yeast. Cell *68*, 333-339.

Fisher, P.A., Wang, T.S., and Korn, D. (1979). Enzymological characterization of DNA polymerase alpha. Basic catalytic properties processivity, and gap utilization of the homogeneous enzyme from human KB cells. J Biol Chem *254*, 6128-6137.

Foiani, M., Liberi, G., Lucchini, G., and Plevani, P. (1995). Cell cycle-dependent phosphorylation and dephosphorylation of the yeast DNA polymerase alpha-primase B subunit. Mol Cell Biol *15*, 883-891.

Foiani, M., Lucchini, G., and Plevani, P. (1997). The DNA polymerase alpha-primase complex couples DNA replication, cell-cycle progression and DNA-damage response. Trends Biochem Sci *22*, 424-427.

Gacy, A.M., Goellner, G., Juranic, N., Macura, S., and McMurray, C.T. (1995). Trinucleotide repeats that expand in human disease form hairpin structures in vitro. Cell *81*, 533-540.

Gan, W., Guan, Z., Liu, J., Gui, T., Shen, K., Manley, J.L., and Li, X. (2011). R-loop-mediated genomic instability is caused by impairment of replication fork progression. Genes Dev *25*, 2041-2056.

Garg, P., Stith, C.M., Sabouri, N., Johansson, E., and Burgers, P.M. (2004). Idling by DNA polymerase delta maintains a ligatable nick during lagging-strand DNA replication. Genes Dev *18*, 2764-2773.

Garvik, B., Carson, M., and Hartwell, L. (1995). Single-stranded DNA arising at telomeres in cdc13 mutants may constitute a specific signal for the RAD9 checkpoint. Mol Cell Biol *15*, 6128-6138.

George, J., Castellazzi, M., and Buttin, G. (1975). Prophage induction and cell division in E. coli. III. Mutations sfiA and sfiB restore division in tif and lon strains and permit the expression of mutator properties of tif. Mol Gen Genet *140*, 309-332.

Gietz, R.D., Schiestl, R.H., Willems, A.R., and Woods, R.A. (1995). Studies on the transformation of intact yeast cells by the LiAc/SS-DNA/PEG procedure. Yeast *11*, 355-360.

Glover, T.W., Berger, C., Coyle, J., and Echo, B. (1984). DNA polymerase alpha inhibition by aphidicolin induces gaps and breaks at common fragile sites in human chromosomes. Hum Genet *67*, 136-142.

Glover, T.W., and Stein, C.K. (1987). Induction of sister chromatid exchanges at common fragile sites. Am J Hum Genet *41*, 882-890.

Hansen, R.S., Canfield, T.K., Lamb, M.M., Gartler, S.M., and Laird, C.D. (1993). Association of fragile X syndrome with delayed replication of the FMR1 gene. Cell *73*, 1403-1409.

Harada, Y., Ohara, O., Takatsuki, A., Itoh, H., Shimamoto, N., and Kinosita, K., Jr. (2001). Direct observation of DNA rotation during transcription by Escherichia coli RNA polymerase. Nature *409*, 113-115.

Hartwell, L.H., and Weinert, T.A. (1989). Checkpoints: controls that ensure the order of cell cycle events. Science *246*, 629-634.

Hashash, N., Johnson, A.L., and Cha, R.S. (2012). Topoisomerase II- and condensin-dependent breakage of MEC1ATR-sensitive fragile sites occurs independently of spindle tension, anaphase, or cytokinesis. PLoS Genet *8*, e1002978.

Hellman, A., Rahat, A., Scherer, S.W., Darvasi, A., Tsui, L.C., and Kerem, B. (2000). Replication delay along FRA7H, a common fragile site on human chromosome 7, leads to chromosomal instability. Mol Cell Biol *20*, 4420-4427.

Henikoff, S., Ahmad, K., and Malik, H.S. (2001). The centromere paradox: stable inheritance with rapidly evolving DNA. Science *293*, 1098-1102.

Hernandez, P., Martin-Parras, L., Martinez-Robles, M.L., and Schvartzman, J.B. (1993). Conserved features in the mode of replication of eukaryotic ribosomal RNA genes. Embo J *12*, 1475-1485.

Hewett, D.R., Handt, O., Hobson, L., Mangelsdorf, M., Eyre, H.J., Baker, E., Sutherland, G.R., Schuffenhauer, S., Mao, J.I., and Richards, R.I. (1998). FRA10B structure reveals common elements in repeat expansion and chromosomal fragile site genesis. Mol Cell *1*, 773-781.

Hill, T.M. (1992). Arrest of bacterial DNA replication. Annu Rev Microbiol *46*, 603-633.

Hill, T.M., Henson, J.M., and Kuempel, P.L. (1987). The terminus region of the Escherichia coli chromosome contains two separate loci that exhibit polar inhibition of replication. Proc Natl Acad Sci U S A *84*, 1754-1758.

Hofmann, J.F., and Beach, D. (1994). cdt1 is an essential target of the Cdc10/Sct1 transcription factor: requirement for DNA replication and inhibition of mitosis. Embo J *13*, 425-434.

Homesley, L., Lei, M., Kawasaki, Y., Sawyer, S., Christensen, T., and Tye, B.K. (2000). Mcm10 and the MCM2-7 complex interact to initiate DNA synthesis and to release replication factors from origins. Genes Dev *14*, 913-926.

Hsiao, C.L., and Carbon, J. (1979). High-frequency transformation of yeast by plasmids containing the cloned yeast ARG4 gene. Proc Natl Acad Sci U S A *76*, 3829-3833.

Ishimi, Y. (1997). A DNA helicase activity is associated with an MCM4, -6, and -7 protein complex. J Biol Chem *272*, 24508-24513.

Jackson, A.L., Pahl, P.M., Harrison, K., Rosamond, J., and Sclafani, R.A. (1993). Cell cycle regulation of the yeast Cdc7 protein kinase by association with the Dbf4 protein. Mol Cell Biol *13*, 2899-2908.

Kamimura, Y., Tak, Y.S., Sugino, A., and Araki, H. (2001). Sld3, which interacts with Cdc45 (Sld4), functions for chromosomal DNA replication in Saccharomyces cerevisiae. Embo J *20*, 2097-2107.

Katou, Y., Kanoh, Y., Bando, M., Noguchi, H., Tanaka, H., Ashikari, T., Sugimoto, K., and Shirahige, K. (2003). S-phase checkpoint proteins Tof1 and Mrc1 form a stable replication-pausing complex. Nature *424*, 1078-1083.

Keil, R.L., and McWilliams, A.D. (1993). A gene with specific and global effects on recombination of sequences from tandemly repeated genes in Saccharomyces cerevisiae. Genetics *135*, 711-718.

Khatri, G.S., MacAllister, T., Sista, P.R., and Bastia, D. (1989). The replication terminator protein of E. coli is a DNA sequence-specific contra-helicase. Cell *59*, 667-674.

Kim, R.A., and Wang, J.C. (1992). Identification of the yeast TOP3 gene product as a single strand-specific DNA topoisomerase. J Biol Chem *267*, 17178-17185.

Kobayashi, T., and Horiuchi, T. (1996). A yeast gene product, Fob1 protein, required for both replication fork blocking and recombinational hotspot activities. Genes Cells *1*, 465-474.

Kogoma, T. (1997). Stable DNA replication: interplay between DNA replication, homologous recombination, and transcription. Microbiol Mol Biol Rev *61*, 212-238.

Kremer, E.J., Pritchard, M., Lynch, M., Yu, S., Holman, K., Baker, E., Warren, S.T., Schlessinger, D., Sutherland, G.R., and Richards, R.I. (1991). Mapping of DNA instability at the fragile X to a trinucleotide repeat sequence p(CCG)n. Science *252*, 1711-1714.

Krings, G., and Bastia, D. (2004). swi1- and swi3-dependent and independent replication fork arrest at the ribosomal DNA of Schizosaccharomyces pombe. Proc Natl Acad Sci U S A *101*, 14085-14090.

Kunst, F., Ogasawara, N., Moszer, I., Albertini, A.M., Alloni, G., Azevedo, V., Bertero, M.G., Bessieres, P., Bolotin, A., Borchert, S.*, et al.* (1997). The complete genome sequence of the gram-positive bacterium Bacillus subtilis. Nature *390*, 249-256.

Kuzminov, A., Schabtach, E., and Stahl, F.W. (1997). Study of plasmid replication in Escherichia coli with a combination of 2D gel electrophoresis and electron microscopy. J Mol Biol *268*, 1-7.

Labib, K., Tercero, J.A., and Diffley, J.F. (2000). Uninterrupted MCM2-7 function required for DNA replication fork progression. Science *288*, 1643-1647.

Laemmli, U.K. (1970). Cleavage of structural proteins during the assembly of the head of bacteriophage T4. Nature *227*, 680-685.

Lai, C.J., and Nathans, D. (1975). Non-specific termination of simian virus 40 DNA replication. J Mol Biol *97*, 113-118.

Lai, E., Birren, B.W., Clark, S.M., Simon, M.I., and Hood, L. (1989). Pulsed field gel electrophoresis. Biotechniques *7*, 34-42.

Le Beau, M.M., Rassool, F.V., Neilly, M.E., Espinosa, R., 3rd, Glover, T.W., Smith, D.I., and McKeithan, T.W. (1998). Replication of a common fragile site, FRA3B, occurs late in S phase and is delayed further upon induction: implications for the mechanism of fragile site induction. Hum Mol Genet *7*, 755-761.

Lee, E.H., Kornberg, A., Hidaka, M., Kobayashi, T., and Horiuchi, T. (1989). Escherichia coli replication termination protein impedes the action of helicases. Proc Natl Acad Sci U S A *86*, 9104-9108.

Lee, S.E., Moore, J.K., Holmes, A., Umezu, K., Kolodner, R.D., and Haber, J.E. (1998). Saccharomyces Ku70, mre11/rad50 and RPA proteins regulate adaptation to G2/M arrest after DNA damage. Cell *94*, 399-409.

Lehman, I.R., Bessman, M.J., Simms, E.S., and Kornberg, A. (1958). Enzymatic synthesis of deoxyribonucleic acid. I. Preparation of substrates and partial purification of an enzyme from Escherichia coli. J Biol Chem *233*, 163-170.

Lemoine, F.J., Degtyareva, N.P., Lobachev, K., and Petes, T.D. (2005). Chromosomal translocations in yeast induced by low levels of DNA polymerase a model for chromosome fragile sites. Cell *120*, 587-598.

Lengronne, A., Pasero, P., Bensimon, A., and Schwob, E. (2001). Monitoring S phase progression globally and locally using BrdU incorporation in TK(+) yeast strains. Nucleic Acids Res *29*, 1433-1442.

Liang, C., and Stillman, B. (1997). Persistent initiation of DNA replication and chromatin-bound MCM proteins during the cell cycle in cdc6 mutants. Genes Dev *11*, 3375-3386.

Linskens, M.H., and Huberman, J.A. (1988). Organization of replication of ribosomal DNA in Saccharomyces cerevisiae. Mol Cell Biol *8*, 4927-4935.

Lisby, M., Barlow, J.H., Burgess, R.C., and Rothstein, R. (2004). Choreography of the DNA damage response: spatiotemporal relationships among checkpoint and repair proteins. Cell *118*, 699-713.

Little, R.D., Platt, T.H., and Schildkraut, C.L. (1993). Initiation and termination of DNA replication in human rRNA genes. Mol Cell Biol *13*, 6600-6613.

Liu, B., and Alberts, B.M. (1995). Head-on collision between a DNA replication apparatus and RNA polymerase transcription complex. Science *267*, 1131-1137.

Liu, L.F., and Wang, J.C. (1987). Supercoiling of the DNA template during transcription. Proc Natl Acad Sci U S A *84*, 7024-7027.

Lopes, M., Cotta-Ramusino, C., Pellicioli, A., Liberi, G., Plevani, P., Muzi-Falconi, M., Newlon, C.S., and Foiani, M. (2001). The DNA replication checkpoint response stabilizes stalled replication forks. Nature *412*, 557-561.

Louarn, J., Cornet, F., Francois, V., Patte, J., and Louarn, J.M. (1994). Hyperrecombination in the terminus region of the Escherichia coli chromosome: possible relation to nucleoid organization. J Bacteriol *176*, 7524-7531.

Lowe, S.W., Ruley, H.E., Jacks, T., and Housman, D.E. (1993). p53-dependent apoptosis modulates the cytotoxicity of anticancer agents. Cell *74*, 957-967.

Lucca, C., Vanoli, F., Cotta-Ramusino, C., Pellicioli, A., Liberi, G., Haber, J., and Foiani, M. (2004). Checkpoint-mediated control of replisome-fork association and signalling in response to replication pausing. Oncogene *23*, 1206-1213.

Lydall, D., and Weinert, T. (1996). From DNA damage to cell cycle arrest and suicide: a budding yeast perspective. Curr Opin Genet Dev *6*, 4-11.

Maine, G.T., Sinha, P., and Tye, B.K. (1984). Mutants of S. cerevisiae defective in the maintenance of minichromosomes. Genetics *106*, 365-385.

McAllister, B.F., and Greenbaum, I.F. (1997). How common are common fragile sites: variation of aphidicolin-induced chromosomal fragile sites in a population of the deer mouse (Peromyscus maniculatus). Hum Genet *100*, 182-188.

Mechali, M. (2010). Eukaryotic DNA replication origins: many choices for appropriate answers. Nat Rev Mol Cell Biol *11*, 728-738.

Melo, J.A., Cohen, J., and Toczyski, D.P. (2001). Two checkpoint complexes are independently recruited to sites of DNA damage in vivo. Genes Dev *15*, 2809-2821.

Mendez, J., and Stillman, B. (2003). Perpetuating the double helix: molecular machines at eukaryotic DNA replication origins. Bioessays *25*, 1158-1167.

Merchant, A.M., Kawasaki, Y., Chen, Y., Lei, M., and Tye, B.K. (1997). A lesion in the DNA replication initiation factor Mcm10 induces pausing of elongation forks through chromosomal replication origins in Saccharomyces cerevisiae. Mol Cell Biol *17*, 3261-3271.

Meselson, M., and Stahl, F.W. (1958). The Replication of DNA in Escherichia Coli. Proc Natl Acad Sci U S A *44*, 671-682.

Mirkin, E.V., and Mirkin, S.M. (2007). Replication fork stalling at natural impediments. Microbiol Mol Biol Rev *71*, 13-35.

Mohanty, B.K., Bairwa, N.K., and Bastia, D. (2006). The Tof1p-Csm3p protein complex counteracts the Rrm3p helicase to control replication termination of Saccharomyces cerevisiae. Proc Natl Acad Sci U S A *103*, 897-902.

Moreira, M.C., Klur, S., Watanabe, M., Nemeth, A.H., Le Ber, I., Moniz, J.C., Tranchant, C., Aubourg, P., Tazir, M., Schols, L.*, et al.* (2004). Senataxin, the ortholog of a yeast RNA helicase, is mutant in ataxia-ocular apraxia 2. Nat Genet *36*, 225-227.

Mott, M.L., and Berger, J.M. (2007). DNA replication initiation: mechanisms and regulation in bacteria. Nat Rev Microbiol *5*, 343-354.

Nakada, D., Hirano, Y., and Sugimoto, K. (2004). Requirement of the Mre11 complex and exonuclease 1 for activation of the Mec1 signaling pathway. Mol Cell Biol *24*, 10016-10025.

Nethanel, T., Zlotkin, T., and Kaufmann, G. (1992). Assembly of simian virus 40 Okazaki pieces from DNA primers is reversibly arrested by ATP depletion. J Virol *66*, 6634-6640.

Newlon, C.S., Collins, I., Dershowitz, A., Deshpande, A.M., Greenfeder, S.A., Ong, L.Y., and Theis, J.F. (1993). Analysis of replication origin function on chromosome III of Saccharomyces cerevisiae. Cold Spring Harb Symp Quant Biol *58*, 415-423.

Newlon, C.S., and Theis, J.F. (2002). DNA replication joins the revolution: whole-genome views of DNA replication in budding yeast. Bioessays *24*, 300-304.

Newport, J. (1987). Nuclear reconstitution in vitro: stages of assembly around protein-free DNA. Cell *48*, 205-217.

Neylon, C., Kralicek, A.V., Hill, T.M., and Dixon, N.E. (2005). Replication termination in Escherichia coli: structure and antihelicase activity of the Tus-Ter complex. Microbiol Mol Biol Rev *69*, 501-526.

Nguyen, V.Q., Co, C., and Li, J.J. (2001). Cyclin-dependent kinases prevent DNA re-replication through multiple mechanisms. Nature *411*, 1068-1073.

Nick McElhinny, S.A., Gordenin, D.A., Stith, C.M., Burgers, P.M., and Kunkel, T.A. (2008). Division of labor at the eukaryotic replication fork. Mol Cell *30*, 137-144.

Nitiss, J.L. (1998). Investigating the biological functions of DNA topoisomerases in eukaryotic cells. Biochim Biophys Acta *1400*, 63-81.

Nudler, E. (2012). RNA polymerase backtracking in gene regulation and genome instability. Cell *149*, 1438-1445.

Olavarrieta, L., Hernandez, P., Krimer, D.B., and Schvartzman, J.B. (2002). DNA knotting caused by head-on collision of transcription and replication. J Mol Biol *322*, 1-6.

Osborn, A.J., and Elledge, S.J. (2003). Mrc1 is a replication fork component whose phosphorylation in response to DNA replication stress activates Rad53. Genes Dev *17*, 1755-1767.

Paciotti, V., Clerici, M., Lucchini, G., and Longhese, M.P. (2000). The checkpoint protein Ddc2, functionally related to S. pombe Rad26, interacts with Mec1 and is regulated by Mec1-dependent phosphorylation in budding yeast. Genes Dev *14*, 2046-2059.

Paciotti, V., Lucchini, G., Plevani, P., and Longhese, M.P. (1998). Mec1p is essential for phosphorylation of the yeast DNA damage checkpoint protein Ddc1p, which physically interacts with Mec3p. Embo J *17*, 4199-4209.

Palakodeti, A., Han, Y., Jiang, Y., and Le Beau, M.M. (2004). The role of late/slow replication of the FRA16D in common fragile site induction. Genes Chromosomes Cancer *39*, 71-76.

Park, J.S., and Roberts, J.W. (2006). Role of DNA bubble rewinding in enzymatic transcription termination. Proc Natl Acad Sci U S A *103*, 4870-4875.

Pasero, P., Braguglia, D., and Gasser, S.M. (1997). ORC-dependent and origin-specific initiation of DNA replication at defined foci in isolated yeast nuclei. Genes Dev *11*, 1504-1518.

Paulovich, A.G., and Hartwell, L.H. (1995). A checkpoint regulates the rate of progression through S phase in S. cerevisiae in response to DNA damage. Cell *82*, 841-847.

Paulovich, A.G., Margulies, R.U., Garvik, B.M., and Hartwell, L.H. (1997). RAD9, RAD17, and RAD24 are required for S phase regulation in Saccharomyces cerevisiae in response to DNA damage. Genetics *145*, 45-62.

Pellicioli, A., Lee, S.E., Lucca, C., Foiani, M., and Haber, J.E. (2001). Regulation of Saccharomyces Rad53 checkpoint kinase during adaptation from DNA damage-induced G2/M arrest. Mol Cell *7*, 293-300.

Pellicioli, A., Lucca, C., Liberi, G., Marini, F., Lopes, M., Plevani, P., Romano, A., Di Fiore, P.P., and Foiani, M. (1999). Activation of Rad53 kinase in response to DNA damage and its effect in modulating phosphorylation of the lagging strand DNA polymerase. Embo J *18*, 6561-6572.

Peter, B.J., Ullsperger, C., Hiasa, H., Marians, K.J., and Cozzarelli, N.R. (1998). The structure of supercoiled intermediates in DNA replication. Cell *94*, 819-827.

Pomerantz, R.T., and O'Donnell, M. (2008). The replisome uses mRNA as a primer after colliding with RNA polymerase. Nature *456*, 762-766.

Pomerantz, R.T., and O'Donnell, M. (2010). Direct restart of a replication fork stalled by a head-on RNA polymerase. Science *327*, 590-592.

Postow, L., Crisona, N.J., Peter, B.J., Hardy, C.D., and Cozzarelli, N.R. (2001). Topological challenges to DNA replication: conformations at the fork. Proc Natl Acad Sci U S A *98*, 8219-8226.

Postow, L., Hardy, C.D., Arsuaga, J., and Cozzarelli, N.R. (2004). Topological domain structure of the Escherichia coli chromosome. Genes Dev *18*, 1766-1779.

Proshkin, S., Rahmouni, A.R., Mironov, A., and Nudler, E. (2010). Cooperation between translating ribosomes and RNA polymerase in transcription elongation. Science *328*, 504-508.

Pursell, Z.F., Isoz, I., Lundstrom, E.B., Johansson, E., and Kunkel, T.A. (2007). Yeast DNA polymerase epsilon participates in leading-strand DNA replication. Science *317*, 127-130.

Raghuraman, M.K., Winzeler, E.A., Collingwood, D., Hunt, S., Wodicka, L., Conway, A., Lockhart, D.J., Davis, R.W., Brewer, B.J., and Fangman, W.L. (2001). Replication dynamics of the yeast genome. Science *294*, 115-121.

Raveendranathan, M., Chattopadhyay, S., Bolon, Y.T., Haworth, J., Clarke, D.J., and Bielinsky, A.K. (2006). Genome-wide replication profiles of S-phase checkpoint mutants reveal fragile sites in yeast. Embo J *25*, 3627-3639.

Reid, G.A., and Schatz, G. (1982). Import of proteins into mitochondria. Yeast cells grown in the presence of carbonyl cyanide m-chlorophenylhydrazone accumulate massive amounts of some mitochondrial precursor polypeptides. J Biol Chem *257*, 13056-13061.

Reyes-Lamothe, R., Possoz, C., Danilova, O., and Sherratt, D.J. (2008). Independent positioning and action of Escherichia coli replisomes in live cells. Cell *133*, 90-102.

Ritchie, K.B., Mallory, J.C., and Petes, T.D. (1999). Interactions of TLC1 (which encodes the RNA subunit of telomerase), TEL1, and MEC1 in regulating telomere length in the yeast Saccharomyces cerevisiae. Mol Cell Biol *19*, 6065-6075.

Rocha, E.P. (2004). The replication-related organization of bacterial genomes. Microbiology *150*, 1609-1627.

Roy, D., Zhang, Z., Lu, Z., Hsieh, C.L., and Lieber, M.R. (2010). Competition between the RNA transcript and the nontemplate DNA strand during R-loop formation in vitro: a nick can serve as a strong R-loop initiation site. Mol Cell Biol *30*, 146-159.

Ruiz-Herrera, A., Garcia, F., Fronicke, L., Ponsa, M., Egozcue, J., Caldes, M.G., and Stanyon, R. (2004). Conservation of aphidicolin-induced fragile sites in Papionini (Primates) species and humans. Chromosome Res *12*, 683-690.

Samadashwily, G.M., Dayn, A., and Mirkin, S.M. (1993). Suicidal nucleotide sequences for DNA polymerization. Embo J *12*, 4975-4983.

Sanchez, Y., Bachant, J., Wang, H., Hu, F., Liu, D., Tetzlaff, M., and Elledge, S.J. (1999). Control of the DNA damage checkpoint by chk1 and rad53 protein kinases through distinct mechanisms. Science *286*, 1166-1171.

Sanchez, Y., Desany, B.A., Jones, W.J., Liu, Q., Wang, B., and Elledge, S.J. (1996). Regulation of RAD53 by the ATM-like kinases MEC1 and TEL1 in yeast cell cycle checkpoint pathways. Science *271*, 357-360.

Santocanale, C., and Diffley, J.F. (1998). A Mec1- and Rad53-dependent checkpoint controls late-firing origins of DNA replication. Nature *395*, 615-618.

Schvartzman, J.B., Martinez-Robles, M.L., Hernandez, P., and Krimer, D.B. (2013). The benefit of DNA supercoiling during replication. Biochem Soc Trans *41*, 646-651.

Schvartzman, J.B., and Stasiak, A. (2004). A topological view of the replicon. EMBO Rep *5*, 256-261.

Schwartz, M., Zlotorynski, E., Goldberg, M., Ozeri, E., Rahat, A., le Sage, C., Chen, B.P., Chen, D.J., Agami, R., and Kerem, B. (2005). Homologous recombination and nonhomologous end-joining repair pathways regulate fragile site stability. Genes Dev *19*, 2715-2726.

Schwartz, M.F., Duong, J.K., Sun, Z., Morrow, J.S., Pradhan, D., and Stern, D.F. (2002). Rad9 phosphorylation sites couple Rad53 to the Saccharomyces cerevisiae DNA damage checkpoint. Mol Cell *9*, 1055-1065.

Segurado, M., de Luis, A., and Antequera, F. (2003). Genome-wide distribution of DNA replication origins at A+T-rich islands in Schizosaccharomyces pombe. EMBO Rep *4*, 1048-1053.

Sequeira-Mendes, J., Diaz-Uriarte, R., Apedaile, A., Huntley, D., Brockdorff, N., and Gomez, M. (2009). Transcription initiation activity sets replication origin efficiency in mammalian cells. PLoS Genet *5*, e1000446.

Shaw, N.N., and Arya, D.P. (2008). Recognition of the unique structure of DNA:RNA hybrids. Biochimie *90*, 1026-1039.

Shinohara, A., Ogawa, H., and Ogawa, T. (1992). Rad51 protein involved in repair and recombination in S. cerevisiae is a RecA-like protein. Cell *69*, 457-470.

Shirahige, K., Hori, Y., Shiraishi, K., Yamashita, M., Takahashi, K., Obuse, C., Tsurimoto, T., and Yoshikawa, H. (1998). Regulation of DNA-replication origins during cell-cycle progression. Nature *395*, 618-621.

Shroff, R., Arbel-Eden, A., Pilch, D., Ira, G., Bonner, W.M., Petrini, J.H., Haber, J.E., and Lichten, M. (2004). Distribution and dynamics of chromatin modification induced by a defined DNA double-strand break. Curr Biol *14*, 1703-1711.

Siede, W., Friedberg, A.S., and Friedberg, E.C. (1993). RAD9-dependent G1 arrest defines a second checkpoint for damaged DNA in the cell cycle of Saccharomyces cerevisiae. Proc Natl Acad Sci U S A *90*, 7985-7989.

Smeets, D.F., and van de Klundert, F.A. (1990). Common fragile sites in man and three closely related primate species. Cytogenet Cell Genet *53*, 8-14.

Sogo, J.M., Lopes, M., and Foiani, M. (2002). Fork reversal and ssDNA accumulation at stalled replication forks owing to checkpoint defects. Science *297*, 599-602.

Spell, R.M., and Holm, C. (1994). Nature and distribution of chromosomal intertwinings in Saccharomyces cerevisiae. Mol Cell Biol *14*, 1465-1476.

Srivatsan, A., Tehranchi, A., MacAlpine, D.M., and Wang, J.D. (2010). Co-orientation of replication and transcription preserves genome integrity. PLoS Genet *6*, e1000810.

Steinmetz, E.J., Conrad, N.K., Brow, D.A., and Corden, J.L. (2001). RNA-binding protein Nrd1 directs poly(A)-independent 3'-end formation of RNA polymerase II transcripts. Nature *413*, 327-331.

Stevenson, J.B., and Gottschling, D.E. (1999). Telomeric chromatin modulates replication timing near chromosome ends. Genes Dev *13*, 146-151.

Stone, D.M., Jacky, P.B., Hancock, D.D., and Prieur, D.J. (1991). Chromosomal fragile site expression in dogs: I. Breed specific differences. Am J Med Genet *40*, 214-222.

Sun, Z., Fay, D.S., Marini, F., Foiani, M., and Stern, D.F. (1996). Spk1/Rad53 is regulated by Mec1-dependent protein phosphorylation in DNA replication and damage checkpoint pathways. Genes Dev *10*, 395-406.

Sun, Z., Hsiao, J., Fay, D.S., and Stern, D.F. (1998). Rad53 FHA domain associated with phosphorylated Rad9 in the DNA damage checkpoint. Science *281*, 272-274.

Sung, P. (1994). Catalysis of ATP-dependent homologous DNA pairing and strand exchange by yeast RAD51 protein. Science *265*, 1241-1243.

Sutherland, G.R., Baker, E., and Richards, R.I. (1998). Fragile sites still breaking. Trends Genet *14*, 501-506.

Takayama, Y., Kamimura, Y., Okawa, M., Muramatsu, S., Sugino, A., and Araki, H. (2003). GINS, a novel multiprotein complex required for chromosomal DNA replication in budding yeast. Genes Dev *17*, 1153-1165.

Tanaka, S., and Diffley, J.F. (2002). Interdependent nuclear accumulation of budding yeast Cdt1 and Mcm2-7 during G1 phase. Nat Cell Biol *4*, 198-207.

Tanaka, T., and Nasmyth, K. (1998). Association of RPA with chromosomal replication origins requires an Mcm protein, and is regulated by Rad53, and cyclin- and Dbf4-dependent kinases. Embo J *17*, 5182-5191.

Tercero, J.A., and Diffley, J.F. (2001). Regulation of DNA replication fork progression through damaged DNA by the Mec1/Rad53 checkpoint. Nature *412*, 553-557.

Thomas, J.O., and Travers, A.A. (2001). HMG1 and 2, and related 'architectural' DNA-binding proteins. Trends Biochem Sci *26*, 167-174.

Torres, J.Z., Schnakenberg, S.L., and Zakian, V.A. (2004). Saccharomyces cerevisiae Rrm3p DNA helicase promotes genome integrity by preventing replication fork stalling: viability of rrm3 cells requires the intra-S-phase checkpoint and fork restart activities. Mol Cell Biol *24*, 3198-3212.

Toulme, F., Mosrin-Huaman, C., Sparkowski, J., Das, A., Leng, M., and Rahmouni, A.R. (2000). GreA and GreB proteins revive backtracked RNA polymerase in vivo by promoting transcript trimming. Embo J *19*, 6853-6859.

Tsurimoto, T., and Stillman, B. (1989). Purification of a cellular replication factor, RF-C, that is required for coordinated synthesis of leading and lagging strands during simian virus 40 DNA replication in vitro. Mol Cell Biol *9*, 609-619.

Tsurimoto, T., and Stillman, B. (1990). Functions of replication factor C and proliferating-cell nuclear antigen: functional similarity of DNA polymerase accessory proteins from human cells and bacteriophage T4. Proc Natl Acad Sci U S A *87*, 1023-1027.

Ursic, D., Himmel, K.L., Gurley, K.A., Webb, F., and Culbertson, M.R. (1997). The yeast SEN1 gene is required for the processing of diverse RNA classes. Nucleic Acids Res *25*, 4778-4785.

Usdin, K., and Woodford, K.J. (1995). CGG repeats associated with DNA instability and chromosome fragility form structures that block DNA synthesis in vitro. Nucleic Acids Res *23*, 4202-4209.

Vasiljeva, L., Kim, M., Mutschler, H., Buratowski, S., and Meinhart, A. (2008). The Nrd1-Nab3-Sen1 termination complex interacts with the Ser5-phosphorylated RNA polymerase II C-terminal domain. Nat Struct Mol Biol *15*, 795-804.

Vialard, J.E., Gilbert, C.S., Green, C.M., and Lowndes, N.F. (1998). The budding yeast Rad9 checkpoint protein is subjected to Mec1/Tel1-dependent hyperphosphorylation and interacts with Rad53 after DNA damage. Embo J *17*, 5679-5688.

Vilette, D., Ehrlich, S.D., and Michel, B. (1995). Transcription-induced deletions in Escherichia coli plasmids. Mol Microbiol *17*, 493-504.

Visintin, C., Tomson, B.N., Rahal, R., Paulson, J., Cohen, M., Taunton, J., Amon, A., and Visintin, R. (2008). APC/C-Cdh1-mediated degradation of the Polo kinase Cdc5 promotes the return of Cdc14 into the nucleolus. Genes Dev *22*, 79-90.

Vogelauer, M., Rubbi, L., Lucas, I., Brewer, B.J., and Grunstein, M. (2002). Histone acetylation regulates the time of replication origin firing. Mol Cell *10*, 1223-1233.

Wakayama, T., Kondo, T., Ando, S., Matsumoto, K., and Sugimoto, K. (2001). Pie1, a protein interacting with Mec1, controls cell growth and checkpoint responses in Saccharomyces cerevisiae. Mol Cell Biol *21*, 755-764.

Walter, J., Sun, L., and Newport, J. (1998). Regulated chromosomal DNA replication in the absence of a nucleus. Mol Cell *1*, 519-529.

Wang, J.C. (1996). DNA topoisomerases. Annu Rev Biochem *65*, 635-692.

Wang, J.C. (2002). Cellular roles of DNA topoisomerases: a molecular perspective. Nat Rev Mol Cell Biol *3*, 430-440.

Weaver, D.T., and DePamphilis, M.L. (1982). Specific sequences in native DNA that arrest synthesis by DNA polymerase alpha. J Biol Chem *257*, 2075-2086.

Weinert, T.A., and Hartwell, L.H. (1988). The RAD9 gene controls the cell cycle response to DNA damage in Saccharomyces cerevisiae. Science *241*, 317-322.

Weinert, T.A., and Hartwell, L.H. (1990). Characterization of RAD9 of Saccharomyces cerevisiae and evidence that its function acts posttranslationally in cell cycle arrest after DNA damage. Mol Cell Biol *10*, 6554-6564.

Weinert, T.A., Kiser, G.L., and Hartwell, L.H. (1994). Mitotic checkpoint genes in budding yeast and the dependence of mitosis on DNA replication and repair. Genes Dev *8*, 652-665.

Weinreich, M., and Stillman, B. (1999). Cdc7p-Dbf4p kinase binds to chromatin during S phase and is regulated by both the APC and the RAD53 checkpoint pathway. Embo J *18*, 5334-5346.

Wellinger, R.E., and Sogo, J.M. (1998). In vivo mapping of nucleosomes using psoralen-DNA crosslinking and primer extension. Nucleic Acids Res *26*, 1544-1545.

Wells, R.D. (2007). Non-B DNA conformations, mutagenesis and disease. Trends Biochem Sci *32*, 271-278.

Westover, K.D., Bushnell, D.A., and Kornberg, R.D. (2004). Structural basis of transcription: separation of RNA from DNA by RNA polymerase II. Science *303*, 1014-1016.

Wiesendanger, B., Lucchini, R., Koller, T., and Sogo, J.M. (1994). Replication fork barriers in the Xenopus rDNA. Nucleic Acids Res *22*, 5038-5046.

Wyrick, J.J., Aparicio, J.G., Chen, T., Barnett, J.D., Jennings, E.G., Young, R.A., Bell, S.P., and Aparicio, O.M. (2001). Genome-wide distribution of ORC and MCM proteins in S. cerevisiae: high-resolution mapping of replication origins. Science *294*, 2357-2360.

Yao, N.Y., Johnson, A., Bowman, G.D., Kuriyan, J., and O'Donnell, M. (2006). Mechanism of proliferating cell nuclear antigen clamp opening by replication factor C. J Biol Chem *281*, 17528-17539.

Zhu, J., Newlon, C.S., and Huberman, J.A. (1992). Localization of a DNA replication origin and termination zone on chromosome III of Saccharomyces cerevisiae. Mol Cell Biol *12*, 4733-4741.

Zou, L., and Elledge, S.J. (2003). Sensing DNA damage through ATRIP recognition of RPA-ssDNA complexes. Science *300*, 1542-1548.

Zou, L., Mitchell, J., and Stillman, B. (1997). CDC45, a novel yeast gene that functions with the origin recognition complex and Mcm proteins in initiation of DNA replication. Mol Cell Biol *17*, 553-563.

Zou, L., and Stillman, B. (1998). Formation of a preinitiation complex by S-phase cyclin CDK-dependent loading of Cdc45p onto chromatin. Science *280*, 593-596.